THE UNIVERSITY OF CHICAGO

THE ESSENTIAL ROLE OF M6A MRNA METHYLATION AND M6A READER PROTEIN YTHDF1 IN MAINTAINING CELL-TYPE SPECIFIC FUNCTIONS IN THE BASAL GANGLIA

A DISSERTATION SUBMITTED TO

THE FACULTY OF THE DIVISION OF THE BIOLOGICAL SCIENCES

AND THE PRITZKER SCHOOL OF MEDICINE

IN CANDIDACY FOR THE DEGREE OF

DOCTOR OF PHILOSOPHY

COMMITTEE ON GENETICS, GENOMICS, AND SYSTEMS BIOLOGY

BY

ZHUOYUE SHI

CHICAGO, ILLINOIS

DECEMBER 2023

To my family and in memory of my grandfather, Longgeng Shi

TABLE OF CONTENTS

LIST OF FIGURES

LIST OF ABBREVIATIONS

3'UTR	3' untranslated regions
AC5	adenylate cyclase 5
AD	Alzheimer's Disease
cAMP	3',5'-cyclic adenosine monophosphate
D1-SPNs	dopamine D1 receptor-expressing medium spiny projection neurons
D2-SPNs	dopamine D2 receptor-expressing medium spiny projection neurons
DA	dopamine
DAT	dopamine transporter
DLS	dorsolateral striatum
DMS	dorsal medial striatum
FTO	m^6A eraser, fat mass and obesity-associated protein
GPe	external globus pallidus
GPi	internal globus pallidus
m^6A	N^6-methyladenosine
METTL14	m^6A writer, Methyltransferase-like 14
NAc	nucleus accumbens core
PD	Parkinson's Disease
PTM	post-translational modification
RBP	RNA binding protein
SNc	substantia nigra pars compacta
STN	subthalamic nucleus
TF	transcription factor
TH	tyrosine hydroxylase
VTA	ventral tegmental area
YTHDF1	m^6A reader, YT521-B homology (YTH) domain containing protein 1

ACKNOWLEDGEMENT

First of all, I want to express my deepest gratitude to my advisor, Dr. Xiaoxi Zhuang, for your enduring patience and trust in me. I still remember it was five and a half years ago, I went to Xiaoxi's office and asked for doing a rotation in his lab. At that time, I had no experience in mouse experiment and no background in neuroscience. Xiaoxi welcomed me and started introducing me to the fundamental aspects of brain and all the ongoing projects in the lab, it was my first time to hear about a brain region called "striatum". After my rotation, I joined the lab, and from that moment, Xiaoxi has been an exceptional mentor and a very nice "gardian", who gives me enough space to learn at my own pace, but still always being able to provide help whenever I ask for. I always admire Xiaoxi for his broad knowledge and how fast he can pick up new information. Yet, he remains humble and willing to listen all the time. Thank you Xiaoxi for teaching me that doing research is not just about pursuiting significant results, but rather in formulating interesting questions to ask and find ways to answer them. Thank you for letting me know that it is perfectly fine for experiments to fail, and the more important thing is to get valuable information from the non-significant results. If in the future I can have my own lab, Xiaoxi is the exact kind of advisor I wish I could become.

I want to thank all my committee members: Dr. Paschalis Kratsios, Dr. Christopher M. Gomez and Dr. Xin He. Your insightful suggestions and comments have been essential in the development of my thesis. My thanks also go to the Genetics, Genomics and System Biology (GGSB) program and all the chairs through these years: Dr. Douglas Bishop, Dr. Yoav Gilad, Dr. Marcelo Nobrega and Dr. Luis Barriero. A special mention to our program's wonderful

administrator: Susan Levison, we always call her “mommy Sue”. Thank you for taking care of all of us.

To my family: my parents, my in-laws, my loving husband, and my soon-to-be born baby boy, Damian, and also my furry companions: Rou Bao, Dou Dou, Da Da and Cai Bao. Without the unconditional love and supports from you, it will be impossible for me to overcome all the difficulties during these years. Damian, thank you for being with mommy during those long nights of thesis writing and thank you for giving me this new role in my life. I wish for you a life filled with healthy and joy, and I promise to stand by you, offering my support whenever you need it.

Finally, my friends, you each hold a special place in my heart. Thank you for bringing me all the joy and happiness in my life.

ABSTRACT

The N^6-methyladenosine (m^6A) methylation, identified in the 1970s, has become increasingly understood with the development of recent high-throughput sequencing techniques. The discovery of its distinct distribution and associated effectors has enabled many functional studies on this reversible modification. m^6A methylation plays an essential role in the post-transcriptional regulation of mRNA, dynamically influencing mRNA metabolism and various cellular functions.

In neurons, precise control of protein synthesis is crucial during the activity-dependent transportation of mRNAs. Thus, post-transcriptional regulation offers a potentially ideal mechanism to dynamically drive local translation in neurons, allowing synaptic plasticity regulation and dendritic remodeling. m^6A level dramatically increases by adulthood, suggesting its unique role in the adult brain, which is a topic just beginning to be systematically studied.

For my thesis, I take advantage of the fact that there are only two prominent neuronal cell types throughout the striatum: the dopamine (DA) D1 and D2 receptor-expressing medium spiny projection neurons (SPNs). Moreover, D1 and D2 SPNs have well-documented opposing functions in motor control, simplifying the molecular studies and allowing comparison of behavioral phenotypes.

In the first part of my thesis, by using transgenic mouse models with selective deletion of *Mettl14* in D1 and D2 SPNs, I found that *Mettl14* deficiency blunted responses to environmental challenges at cellular and behavioral levels in the adult brain.

One of m^6A modification's downstream reader proteins, YTHDF1, has been shown to promote protein synthesis in neurons and regulate synaptic plasticity and learning. However, it is unclear if YTHDF1 is the primary downstream mediator of m^6A function in the brain. In the

second part, I found that *Ythdf1* deletion in D1 and D2 SPNs resembled the behavioral impairments caused by *Mettl14* deletion in a cell type-specific manner, suggesting YTHDF1 as the primary mediator of the functional consequences of m^6A modification in the striatum. Moreover, striatal neurons from *Ythdf1* constitutive knockout mice were incapable of adapting to environmental challenges.

DA affects striatal neuronal activity and regulates corticostriatal plasticity. In the third part, I examined the role of m^6A mRNA methylation in dopaminergic neurons. I found that in all three cell types: D1-SPNs, D2-SPNs, and dopaminergic neurons, *Ythdf1* deletion resembled the behavioral impairments caused by *Mettl14* deletion. Down-regulation of m^6A is found to induce cell apoptosis in the dopaminergic cells *in vitro*. However, I found no significant difference in tyrosine hydroxylase (TH)-positive cell number in the midbrain of *Mettl14* conditional knockout mice. This suggests that m^6A depletion did not cause dopaminergic neuron degeneration in any age group.

The fourth part is our ongoing experiments to examine the role of m^6A modification in maintaining cell identity and normal functions in the adult brain. I found that *Mettl14* deletion in D1-SPNs caused behavioral impairments in an age-dependent manner, suggesting the significance of m^6A increases as the mice age. In the future, we plan to explore the expression profile of the transcription factors (TFs) and track the temporal features of m^6A distribution on these genes in D1 and D2 SPNs.

In summary, my thesis work took advantage of cell type specific deletion of the m^6A "writer" METTL14 and the m^6A "readers" YTHDF1 in mice. I made the following important discoveries:

1. In three different cell types in the adult brain, namely D1 SPNs, D2 SPNs, and DA neurons, *Mettl14* gene deletion and *Ythdf1* gene deletion resulted in almost identical behavioral phenotypes in various behavioral paradigms, suggesting that the functional impact of the m^6A mRNA methylation in the adult brain is likely mediated by YTHDF1. This is in sharp contrast to previous claims that there is redundancy among YTHDF1, YTHDF2 and YTHDF3.
2. Responses at the molecular (*de novo* protein synthesis), cellular (action potentials) and behavioral (learning) levels upon environmental challenges were all blunted under m^6A deficiency condition, suggesting that the m^6A pathway is crucial in cells' ability to adapt to environmental challenges, presumably by rapidly regulating protein synthesis in adult neurons with good spatial and temporal resolution.
3. m^6A deficiency in D1-SPNs and D2-SPNs resulted in opposite behavioral phenotypes. This is not because m^6A deficiency leads to very different functional impairments at the cellular level in these two different cell types. This is simply because D1-SPNs and D2-SPNs have opposing functions in the striatum. To our knowledge, this is the first study in which knocking out the same gene in D1-SPNs vs D2-SPNs resulted in opposite behavioral phenotypes, and a clear demonstration of D1-SPN-dependent learning vs D2-SPN-dependent learning. This is one of the best pieces of *in vivo* evidence supporting the classic basal ganglia direct and indirect pathway model.

CHAPTER 1

INTRODUCTION

1.1 m^6A mRNA methylation overview

Studies devoted to epigenetic regulations, including histone modification, DNA methylation and transcription factor network indicated key mechanisms for gene expression regulation that play an essential role in establishing and maintaining correct neuronal cell identities, connectivities, and functions in the central nervous system (Yao et al., 2016). For example, during cortical development, deletion of the histone methyltransferase, Ezh2, has been shown to cause selective reduction of the upper layer neuron population (Pereira et al., 2010). Precise contribution of the photoreceptor-specific protein, Samd7, through interaction with transcription factors has been demonstrated to establish rod photoreceptor cell identity by silencing non-rod gene expression during retinal cell differentiation (Omori et al., 2017).The significant role of DNA methylation in learning, memory and synaptic plasticity has been studied and suggests a further role of epigenetic regulation in the mature nervous system for normal functions (Feng et al., 2010). Moreover, dysregulation of epigenetic mechanisms has emerged to be crucial in the pathophysiology of neuropsychiatric disorders (Lv et al., 2013). Overall, the aforementioned epigenetic mechanisms have revealed pathways that significantly affect protein expression, regulate cell fate decision and maintain cell identity at the transcriptional level.

Although important, gene expression regulation at the transcriptional level lacks precise spatial or temporal resolution. For neurons that often have thousands of synapses and have to respond to environmental challenges rapidly, precise spatial or temporal resolution in controlling new protein synthesis is especially crucial. From DNA in the nucleus to proteins in the synapse, it

will take hours for RNAs and proteins to be made and transported. Moreover, many synapses of the same neuron may require different proteins during development and in the adult nervous system. An important mechanism in translational control at the post-transcriptional level is epitranscriptomic regulation including mRNA modifications. One of the most abundant and significant type is the reversible m^6A methylation of mRNA. It is widely conserved among eukaryotic species (Yue et al., 2015; Cao et al., 2016). Transcriptome-wide m^6A profiling of the mRNAs shows enrichment of this modification around the stop codon and 3' untranslated regions (3'UTR) (Dominissini et al., 2012; Meyer et al., 2012). m^6A methylation induces changes in RNA secondary structures, alters the accessibilities of RNA binding proteins (RBPs) thus impacts the fate of modified RNAs (Liu et al., 2015; Meyer et al., 2015; Wang et al., 2015). Recent studies have demonstrated the effect of m^6A modification on mRNAs on almost every phase of mRNA metabolism including RNA transport, localization, splicing, stability, and translational efficiency (Wang et al., 2014; Louloupi et al., 2018; Wang et al., 2015). The functional significance of m^6A has been demonstrated in eukaryotic cell apoptosis (Liu et al., 2014), embryonic stem cell differentiation (Meng et al., 2019), tumorigenesis (Cui et al., 2017), hematopoietic stem cell fate decisions, maintaining hematopoietic stem cell identity (Cheng et al., 2019), cortical neurogenesis (Yoon et al., 2017), axon regeneration (Weng et al., 2018), learning and memory (Shi et al., 2018; Koranda et al., 2018).

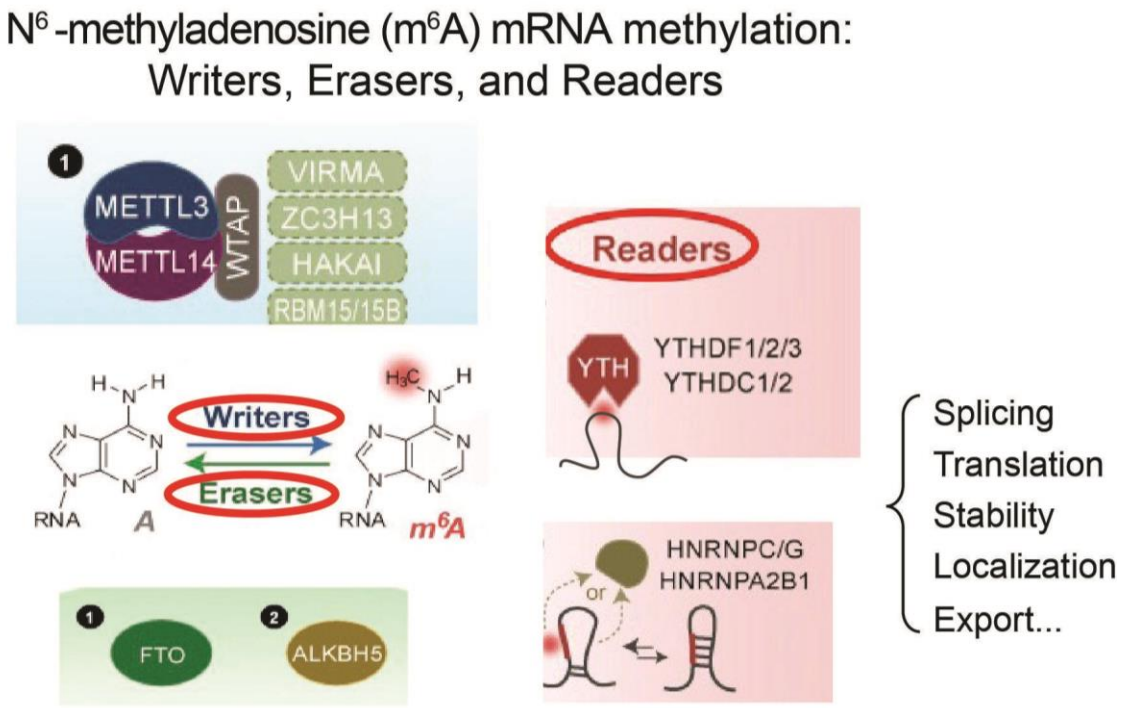

Figure 1.1. N^6-methyladenosine (m^{6}A) mRNA methylation: Writers, Erasers, and Readers. The three effectors of m^{6}A mRNA methylation. Writers: the core writer complex consists of METTL3, METTL14 and other adaptor proteins including: WTAP, VIRMA, AC3H13, HAKAI and RBM15/15B. Erasers: two erasers that have been discovered so far, FTO and ALKBH5, catalyze demethylation and remove the methyl groups on the modified RNA transcripts. Readers: RBPs that recognize and bind to the m^{6}A modified RNA transcripts and regulate the downstream RNA metabolism. (Shi et al., 2019)

1.2 The functional significance of m^{6}A mRNA methylation - Writers, erasers, and readers

Functional studies on m^{6}A RNA methylation have been made possible after the discovery of three groups of proteins in the m^{6}A epitranscriptomic regulation pathway: "writers" (methyltransferases) that install, "erasers" (demethylases) that remove, and "readers" that are RBPs that recognize m^{6}A and determine the cellular fate of the modified RNA (Fu et al., 2014; Liu et al., 2014; Shi et al., 2019) (Figure 1.1).

Writers

The m^{6}A writer protein complex is composed of a core unit formed by Methyltransferase-like 14 (METTL14), the critical structural component that functions in facilitating RNA binding, and Methyltransferase-like 3 (METTL3), the catalytic component that functions in catalyzing the methyl group transfer (Wang et al., 2016; Shi et al., 2019). Further studies revealed additional subunits, including Wilms tumor 1-associating proteins (WTAP), Vir-like m^{6}A methyltransferase associated (VIRMA), Zinc finger CCCH-type containing 13 (ZC3H13), and RNA binding motif protein 15/15B (RBM15/15B), in ensuring the localization and specificity of the complex for optimal deposition of the methyl group (Ping et al., 2014; Yue et al., 2018; Wen et al., 2018; Patil et al., 2016; Knuckle et al., 2018).

The cellular localization of the writer proteins is critical for various biological processes. Under normal conditions, METTL3 and METTL14 form heterodimer and install m^{6}A with a sequence motif RRACH (R = A or G; H = A, C, or U) co-transcriptionally in the nucleus (Ping et al., 2014; Liu et al., 2014; Scholler et al., 2018). Ectopic cytoplasmic expression of the writer proteins is found in several cancer cell lines (Alarcon et al., 2015; Barbieri et al., 2017). For

example, cytoplasmic METTL3 is found in lung cancer cells, functionally promoting translation by interacting with the elongation factor eIF3h of the translation complex (Lin et al., 2016; Choe et al., 2018). Constitutive deletion of *Mettl3* and *Mettl14* are embryonic lethal in mice, suggesting their critical role during development (Geula et al., 2015; Weng et al., 2018; Yoon et al., 2017). Depletion of *Mettl3* in embryonic stem cells shows impairment in cell fate transition, indicating its role in regulating stem cell pluripotency (Batista et al., 2014). METTL3 and METTL14 also dynamically regulate the m^6A sites in response to the local environment. Heat shock triggers METTL3's redistribution to the RNA transcripts ensuring their later clearance (knuckles et al., 2017). Stress such as DNA double-strand breaks caused by UV radiation also recruits METTL3 to the damage site, likely interacting with RNA polymerase II and participating in the DNA damage repair pathway (Xiang et al., 2017).

Recently, more methyltransferases have been discovered but with more specific targets. Methyltransferase-like 16 (METTL16) installs m^6A with a different sequence motif and prefers binding to stem-loop structured RNAs and various noncoding RNAs (Pendleton et al., 2017; Warda et al., 2017; Doxtader et al., 2018). Methyltransferase-like 5 (Mettl5) and CCHC zinc finger-containing protein 4 (ZCCHC4) are also identified as writer proteins that mainly catalyze methylation of ribosomal RNAs (Van Tran et al., 2019; Ma et al., 2019).

Erasers

m^6A mRNA methylation is a reversible process. The methyl group can be removed by demethylases such as the fat mass and obesity-associated protein (FTO) and AlkB homolog 5 (ALKBH5) (Jia et al., 2011; Zheng et al., 2013). Variations in the expression levels of FTO and ALKBH5 across different tissues indicate their roles in diverse biological processes.

FTO was first shown to be associated with body mass and obesity in humans, as its mutations lead to altered body mass index and elevated risk of obesity (Scuteri et al., 2007; Frayling et al., 2007). After the identification of FTO as the first RNA demethylase, research on m^6A biology resurged since its discovery in the 1970s (Wei et al., 1975). In adult mice, FTO has the highest expression in the brain (Gerken et al., 2007). Deletion of *Fto* resulted in postnatal growth retardation manifested as reduced body weight and length in mice (Gao et al., 2010), suggesting its critical role during development. ALKBH5 is the second RNA demethylase discovered, and unlike FTO, ALKBH5 has high expression in mouse testis. In male mice, Alkbh5 knockouts affect spermatogenesis (Zheng et al., 2013).

Readers

In order for m^6A to carry out various post-transcriptional functions, the m^6A modified RNA transcripts need to be recognized by RBPs and directed to designated destinations within the cell. m^6A reader proteins are special types of RBPs that recognize the m^6A-modified RNA transcripts.

Through pull-down assay that probes m^6A and attached proteins, one class of m^6A reader proteins that have been identified is the YT521-B homology (YTH) domain containing protein family, including YTHDF1, 2, and 3 and YTHDC1 and 2 (Dominissini et al., 2012; Luo et al., 2014). The YTHDF sub-family are cytosolic m^6A readers whereas the YTHDC sub-family are nuclear m^6A readers. YTHDF2 is the first m^6A reader protein characterized and has been shown to bind to m^6A RNA transcripts, functionally guide them to the process bodies (P-bodies) in the cytoplasm, and regulate RNA decay (Wang et al., 2014). Studies in zebrafish embryos revealed that deletion of Ythdf2 affects the decay of maternal transcripts and impairs the maternal-to-zygotic transition (Zhao et al., 2017). YTHDF2 has also been shown to regulate progenitor cell

specification during embryogenesis, indicating its critical role during development (Zhang et al., 2017). YTHDF3's function in promoting RNA decay and facilitating translation has also been documented (Shi et al., 2017; Chang et al., 2020). The nuclear reader protein YTHDC1 has been shown to interact with splicing regulators, regulating RNA splicing and the downstream nuclear export of the m^6A mRNA transcripts (Wilkinson et al., 2003; Xiao et al., 2016; Roundtree et al., 2017). Unlike the other YTH-domain containing proteins, YTHDC2's expression is mainly enriched in the testis. Deletion of Ythdc2 leads to spermatogenesis deficits in male mice (Hsu et al., 2017; Bailey et al., 2017). Besides the YTH-domain containing m^6A readers, there are also indirect m^6A reader proteins that do not bind to m^6A directly, but they recognize m^6A through indirect mechanisms (Liu et al., 2015). These include the heterogeneous nuclear ribonucleoprotein A2/B1 (HNRNPA2B1), heterogeneous nuclear ribonucleoprotein C (HNRNPC), and heterogeneous nuclear ribonucleoprotein G (HNRNPG). HNRNPA2B1 has been shown to regulate mRNA maturation and transport, it has also been shown to regulate the metabolism of long noncoding RNAs (Alarcon et al., 2015; Wu et al., 2018). HNRNPC/G has been shown to function in pre-mRNA processing (Liu et al., 2015). Studies also reveal that FMRP prefers to bind to m^6A-containing RNAs through interactions with YTHDF1, and regulates neuronal activity-dependent translation, suggesting that its well-known function in inhibiting *de novo* protein synthesis may be mediated by inhibiting YTHDF1 (Zou et al., 2022).

The main function of YTHDF1 is to promote translation through interaction with the translation initiation factors, and this translation-promoting effect is also stimulus-dependent (Wang et al., 2015). Part of this dissertation is to investigate YTHDF1's function in regulating translational control in the adult brain downstream of m^6A RNA methylation. Neurons are the

most compartmentalized cell type with a unique morphology. In response to neuronal activity, signals are usually received by dendrites; after processing in the soma, they will be transmitted through the axon, establishing long-range synaptic connections with efferent neurons. In order to overcome the distance constraints, direct transportation of selected mRNA transcript rather than proteins to distal neuronal processes will offer spatial and temporal advantages for changes in local protein composition in response to synaptic inputs or other challenges. RNA binding proteins (RBPs) have been shown to play an essential role, both in inhibiting mRNA translation during transport and in activating translation efficiently in response to physiologic events such as synaptic activity (Eom et al., 2003; Zhang et al., 2012; Buxbaum et al., 2014; Lepelletier et al., 2017). Indeed, precise translational control and spatial organization of mRNAs, afforded by various RBPs, are shown to be essential in neuronal and synaptic functions (Martin and Zukin, 2006; Holt and Schuman, 2013; Glock et al., 2017).

The level of m^6A drastically increases in the adult brain, indicating its unique role in adult neurons (Meyer et al., 2012). m^6A allows selected mRNA transcripts to be recognized by m^6A readers and to be transported to specific subcellular space, to be translated efficiently (e.g., via YTHDF1), or to be degraded rapidly (e.g., via YTHDF2). This is potentially one of the most important mechanisms in spatial and temporal control of new protein synthesis in neurons and synapses in response to challenges. Increased translation efficiency and increased degradation seem to have opposing effects on the same m^6A methylated transcript. However, they may work together to offer better temporal control by rapidly turning on and then turning off translation.

YTHDF1, 2, and 3 have been shown to be functionally distinct cytoplasmic reader proteins. YTHDF1 enhances translation by interacting with initiation factors, YTHDF2 promotes mRNA

degradation, and YTHDF3 as the facilitator that ensures the maximized efficiency for translational control by working together with YTHDF1 or YTHDF2 (Wang et al., 2015; Wang et al., 2014; Shi et al., 2017; Chang et al., 2020). Recently, Zaccara et al. proposed another model based on these reader proteins' high sequence identity in RNA binding and effector domains. They found that YTHDF proteins localized to similar cytoplasmic locations with similar interactors and suggested that YTHDF1, 2, and 3 working together in regulating mRNA degradation in a redundant manner and can compensate each other, as the triple knockdown of YTHDF proteins leads to highest mRNA stabilization in cells (Zaccara et al., 2020). However, this redundancy model has not been confirmed *in vivo* yet, it is not clear whether the functions of YTHDF1, 2 and 3 are context and tissue dependent. It is also not clear whether the functional consequences of m^6A are mediated by specific reader proteins in the brain. These questions will be addressed in Chapter 3.

1.3 The role of m^6A mRNA methylation during neurodevelopment

The development of the nervous system involves numerous processes, including neurogenesis, cell migration, axon growth and synaptogenesis etc. During each of these stages, many signaling pathways are turned on and off in different cells at different time (Lutolf et al., 2002; Lupo et al., 2006; Franco and Muller, 2013). Thus, a key mechanism to ensure the proper regulation of these dynamic signaling networks is the precise localization of translational machinery, including mRNA transcripts and RNA-binding proteins (RBPs), to different subcellular regions for local translation to happen at a precise time (Jung et al., 2014; Holt et al., 2019).

Among all cell types, neurons contain a higher level of m^6A, suggesting m^6A's significance in the nervous system (Meyer et al., 2012; Dominissini et al., 2012). m^6A depletion in embryonic

neural stem cells impairs proliferation and leads to premature differentiation (Wang et al., 2018). *Mettl14* and *Mettl3* deletions in the embryonic mouse brain prolong the cell cycle of radial glial cells and extend cortical neurogenesis into postnatal stages (Yoon et al., 2017). Moreover, reader protein YTHDF2 has been identified as an important regulator during cortical neurogenesis, facilitating RNA decay of the genes associated with differentiation (Li et al., 2018). *Mettl3* conditional knockout mice exhibited increased apoptosis of the cerebellar granule cells, leading to underdevelopment of the cerebellum (Wang et al., 2018). *Fto-deficient* mice exhibited decreased brain size, *and Alkbh5* knockout mice also showed smaller cerebellum size and reduced number of neurons (Li et al., 2017; Ma et al., 2018). The reader proteins also play a critical role in cerebellum development, YTHDF1 and YTHDF2 are found as negative regulators for the cerebellar parallel fiber growth (Yu et al., 2021). However, it remains to be determined if m^6A's significant role in neurodevelopment is due to its involvement in local translation.

In other studies, it seems that m^6A's significant role in neurodevelopment is at least partially due to its involvement in local translation. m^6A mRNA methylation also plays a critical role in regulating axon growth. FTO is found to be highly expressed in the dendrites and synapses (Li et al., 2017); by inhibiting FTO activity, the m^6A level is upregulated and leads to inhibited axon elongation and impaired local axonal translation (Yu et al., 2018). In drosophila melanogaster, the YTHDF protein modulates axon growth by regulating the translation of related mRNA transcripts (Worpenberg et al., 2021). In mice, YTHDF1 and 2 are found to work synergistically regulating local translation on the Wnt5a signaling pathway (Yu et al., 2021).

Overall, these studies highlight the critical role of m^6A in the formation and function of the nervous system. Reader proteins are especially important in recognizing and binding to

neurodevelopmental-related m^{6}A modified mRNAs, precisely regulating translation and ensuring proper development of the nervous system.

1.4 The role of m^{6}A mRNA methylation in the adult brain

The level of m^{6}A drastically increases in the adult brain, indicating its unique role (Meyer et al., 2012). Although the significance of RNA methylation in the matured nervous system has not been systematically studied yet, multiple studies have suggested that m^{6}A is essential for synaptic plasticity, learning, memory formation, and stress response regulation in adult mice (Engel et al., 2018; Shi et al., 2018; Koranda et al., 2018; Zhang et al., 2018).

Brain-wide region specific m^{6}A profiling reveals high expressions of m^{6}A modified transcripts encoding the synaptic proteins (Chang et al., 2017). Mice with FTO deletion in the dopaminergic neurons alter the dopaminergic midbrain circuitry, leading to increased cocaine-induced locomotor activity and reduced response to quinpirole (Hess et al., 2013). In another study, the other essential subunit of the m^{6}A methyltransferase complex, METTL3, has been found to regulate the efficacy of hippocampus-dependent memory consolidation by promoting the translation of immediate early genes during memory formation (Zhang et al., 2018). YTHDF1, 2, and 3 are found at the dendrites in the mouse hippocampus, and loss of the YTHDF proteins results in dysfunction of synaptic transmission (Merkurjev et al., 2018). In *Drosophila*, YTHDF reader proteins are also critical to memory formation (Kan et al., 2021). YTHDF1 plays an essential role in promoting synaptic protein synthesis (e.g., CaMKIIα) in neurons and synapses in response to stimuli, in synaptic plasticity, and in learning (Shi et al., 2018). These data suggest that the m^{6}A-modified mRNA can potentially be recognized and transported to dendrites and axons for local translation, regulating synaptic plasticity and behavior through m^{6}A readers (e.g., YTHDF1).

Interestingly, the m^{6}A profile in the brain alters after exposure to stress, suggesting its role in adaptations to environmental challenges. Deletion of *Mettl3* or *Fto* in the adult neurons increases fear memory in mice and alters m^{6}A localization and expression response to fear (Engel et al., 2018). Loss of YTHDF1 has been shown to globally attenuate injury-induced protein synthesis and axon regeneration in the adult brain (Weng et al., 2018).

However, it's not clear if the role of m^{6}A in adult neurons is mainly mediated by YTHDF1. It's not clear either if *in vivo* neuronal activity in response to environmental challenges is impaired in mice with m^{6}A deficiency. Finally, it's not clear if m^{6}A has similar functions at the cellular level in different neurons, but m^{6}A deficiency may be manifested in different behavioral level phenotypes due to functional differences of these different neurons. My dissertation work took advantage of the only two prominent neuronal cell types throughout the striatum: the dopamine (DA) D1 receptor-expressing medium spiny projection neurons (SPNs), and the dopamine D2 receptor-expressing SPNs. These two cell types are known to have opposing roles in motor control. By selectively deleting *Mettl14* and *Ythdf1* in D1 or D2 SPNs, I will address the above questions.

1.5 The intrinsic excitability and plasticity of D1 and D2 SPNs in the striatum and their role in movement control

In this dissertation, I will take advantage of the anatomical and functional features of the striatum and the available genetic tools to investigate the role of m^{6}A mRNA methylation in dopaminergic neurons, D1-SPNs, and D2-SPNs in the adult brain.

The basal ganglia are a group of subcortical nuclei that are essential for movement control, response selection, value-based decisions, and motor learning (Graybiel et al., 1994; Gerfen and Wilson, 2004; Balleine et al., 2009). The input stage of the basal ganglia, the striatum, receives

inputs mainly from the cortex and thalamus, as well as receives innervation from midbrain DA neurons. Both types of SPNs in the striatum influence motor cortical neurons through the cortico-striato-thalamo-cortical feedback loops (Bolam et al., 2000; Gerfen and Surmeier, 2011). In general, the striatum can be subdivided into the two regions: dorsal and ventral. The dorsal striatum can be divided into dorsolateral striatum (DLS), which receive inputs from the sensorimotor cortex, plays an important role in the execution of habitual behavior (Yin et al., 2004; Devan et al., 2011), and dorsomedial striatum (DMS), which receives inputs from the associative frontal cortex, is more important in goal-directed actions (Hintiryan et al., 2016; Yin et al., 2005). The ventral striatum, with the nucleus accumbens (NAc) core and shell as its main components, integrates inputs from many brain areas, including the ventral midbrain, amygdala, hippocampus, thalamus and prelimbic and prefrontal cortex (Fallon and Moore, 1978; Kelly and Griffiths, 1982; Phillipson and Griffiths, 1985). It has been established that NAc plays an essential role in reward and motivation (Carlezon and Thomas, 2009; Day et al., 2011). Dysfunction in the basal ganglia can lead to various movement and psychiatric disorders such as Parkinson's disease, schizophrenia and addiction.

The majority of neurons in the striatum (90%-95%) are GABAergic medium spiny projection neurons (SPNs) (Gerfen et al., 1990), which simplifies biochemical studies. The SPNs can be dichotomized based on their gene expression, axonal projections, and function (Albin et al., 1989). The striatonigral pathway, so called direct pathway, goes through the dopamine D1 receptor expressing SPNs, projects directly to the internal globus pallidus (GPi) and substantia nigra pars reticulata (SNr), promotes motor behavior. In contrast, the striatopallidal pathway, so called indirect pathway, goes through the dopamine D2 receptor expressing SPNs, projects to the external

globus pallidus (GPe). GABAergic neurons from the GPe then project to the subthalamic nucleus (STN), which send excitatory glutamatergic signals to GPi/SNr, ultimately reduce cortical premotor drive, and inhibit movement (Gerfen et al.,1990; Smith et al., 1998; Gerfen and Surmeier, 2011) (Figure 1.2).

DA modulates the striatal signaling via G-protein coupled receptors (GPCRs) in the SPNs. The D1-like receptors from the direct pathway are coupled to Gαs/olf, which stimulate adenylate cyclase 5 (AC5), leading to an increase in intracellular 3',5'-cyclic adenosine monophosphate (cAMP) and the activation of protein kinase A (PKA) (Zhuang et al., 2000). In contrast, D2-like receptors from the indirect pathway are coupled to Gαi/o, which inhibit AC5 and PKA (Missale et al., 1998). PKA then acts on various intracellular targets including sodium and potassium inward rectifying channels, L-type calcium channels. This action ultimately affects synaptic plasticity as well as intrinsic excitability of the SPNs (Surmeier et al., 1995; Nisenbaum et al., 1998; Neve et al., 2004). For example, the combination of cortical inputs and lack of DA can induce LTP in corticostriatal synapses that connect motor cortical neurons and D2 receptor expressing SPNs (Shen et al., 2008; Augustin et al., 2014). The strengthening of these synapses can cause stronger inhibition of motor cortical neurons through the indirect pathway of the cortico-striato-thalamo-cortical feedback loops. At the behavioral level, such synaptic strength change is reflected in "inhibitory motor learning", a phenomenon in which lack of DA in combination with motor task experience causes experience dependent and task specific motor inhibition that gradually worsens with more experience in the same motor task (Beeler et al., 2010; Beeler et al., 2012; Koranda et al., 2016; Cheung et al., 2023).

However, as I will discuss in Chapter 2, the view that the indirect pathway is inhibitory is not accurate. The action potential firing activity of D2 receptor expressing SPNs is almost always positively correlated with movement speed. How do they inhibit movement is a question that I will address in Chapter 2.

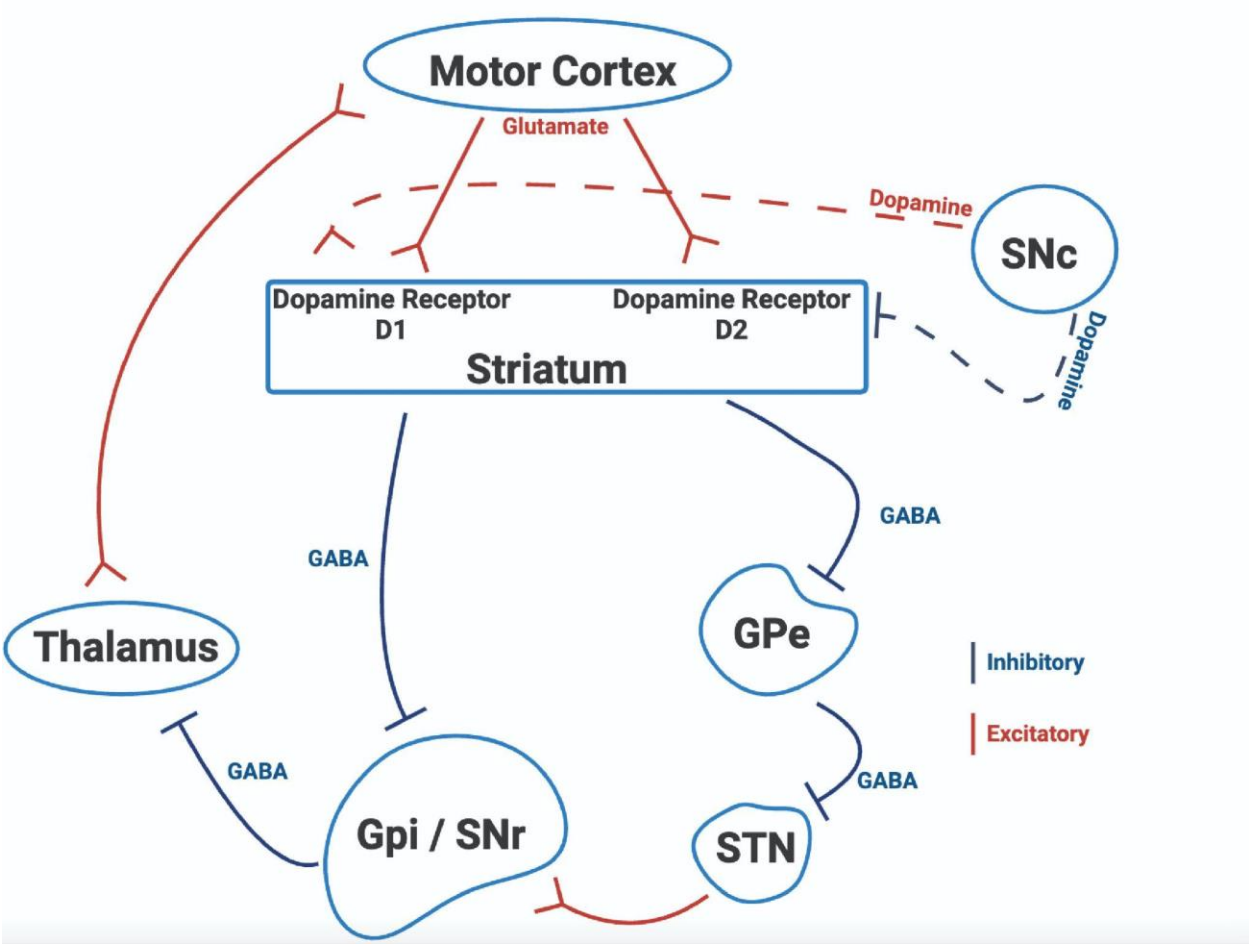

Figure 1.2. The direct and indirect pathway in the striatum. GABA (blue) is inhibitory while glutamate (red) is excitatory. In the direct pathway, the D1 receptor binds DA, which causes activation of these GABAergic neurons project to SNr. This negative signal, when acting on another population of GABAergic neurons that send an inhibitory signal to the thalamus, causes a disinhibition of the pathway. This ultimate positive activity in the thalamus results in promoting movement. When D2 SPNs are activated, they require an extra step of projection to the GPe. GABAergic neurons of GPe then project to the STN, which then send excitatory glutamatergic signals to SNr. The overall signal coming into the SNr is positive, which causes the opposite effect of the direct pathway on movement, resulting in the inhibition of movement.

1.6 METTL14 is essential in maintaining normal striatal function in adult mice

In a previous study published from our lab (Koranda et al., 2018), the necessity of m^6A mRNA methylation in adult striatal neurons was investigated. Conditional knockout mice were generated with *Mettl14*, an important component from the core writer protein complex, deleted in the two prominent mouse neuronal populations in the striatum: D1-SPNs and D2-SPNs. The functional consequences of m^6A depletion in these neurons were examined.

To characterize the behavior phenotypes of mice with *Mettl14* deletion in D1-SPNs and D2-SPNs, the performance during striatum dependent sensorimotor learning was assessed using accelerating rotarod. Sensorimotor learning was severely impaired in mice with *Mettl14* deletion in D1-SPNs. Sensorimotor learning was significantly impaired in mice with *Mettl14* deletion in D2-SPNs as well although less severe. These data suggest that *Mettl14* deletion impairs striatal dependent learning in the adult mice (Figure 1.3).

To characterize the intrinsic physiological properties of D1-SPNs with *Mettl14* deletion, whole-cell recordings were performed. *Mettl14* deletion significantly reduced the threshold for D1 neurons to generate action potentials, suggesting an increased excitability. However, the number of spikes in response to current injections was reduced after *Mettl14* deletion, indicating the role of m^6A in maintaining neurons' ability in spike frequency adaptation in response to excitation (Figure 1.4). Without m^6A, such adaptation is significantly impaired, and it's compensated by increased firing in response to subthreshold stimulation.

In order to examine the molecular level changes in D1-SPNs and D2-SPNs caused by *Mettl14* deletion, m^6A mRNA sequencing was performed in *Mettl14*-deleted striatum. There was

downregulation of similar striatal mRNAs encoding neuron- and synapse-specific proteins in both neuronal types. However, D1-SPNs and D2-SPNs specific identity genes were uniquely downregulated in manipulations targeting D1-SPNs and D2-SPNs respectively. *Mettl14* deletion in D1-SPNs showed reduced expression of dynorphin (Pdyn) and the precursor of substance-P (Tac1), whereas *Mettl14* deletion in D2-SPNs showed reduced expression of D2R (Drd2) and enkephalin precursor (Penk) (Figure 1.5).

In summary, by using electrophysiological, behavioral, and molecular approaches, our previous study offered the first direct evidence that loss of m^6A mRNA methylation in specific neurons of the adult brain impairs learning. This effect is likely due to altered intrinsic excitabilities, impaired adaptation, potentially resulting from neurons' inability to maintain their identities post-maturation.

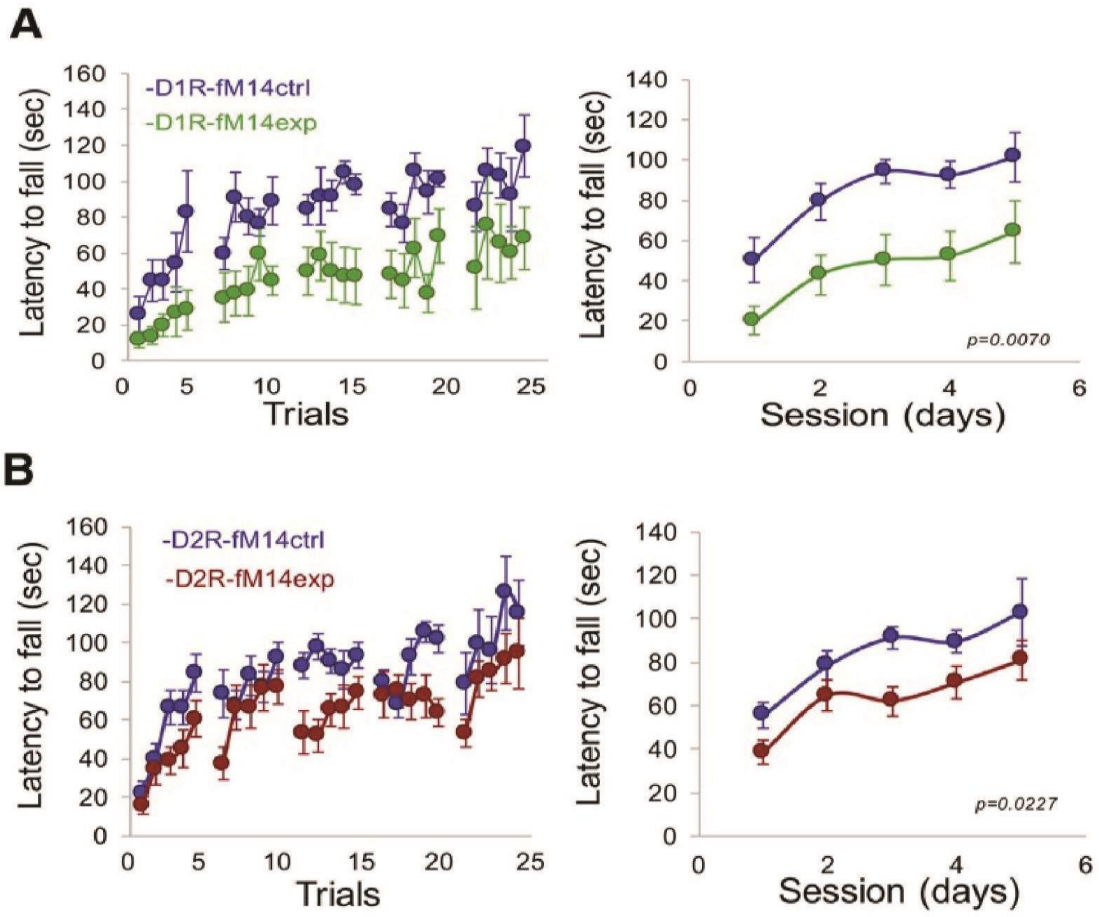

Figure 1.3. *Mettl14* deletion in D1-SPNs and D2-SPNs impaired striatal-dependent behavior. (A) Latency to fall recorded from the accelerating rotarod in mice with *Mettl14* gene deletion in D1-SPNs (green, n=8), and their control littermates (blue, n=7), p = 0.0070, repeated measurement ANOVA. (B) Latency to fall recorded from the accelerating rotarod in mice with Mettl14 deletion in D2-SPNs (red, n=14), and their control littermates (blue, n=17), p = 0.0227, repeated measurement ANOVA (Koranda et al. 2018).

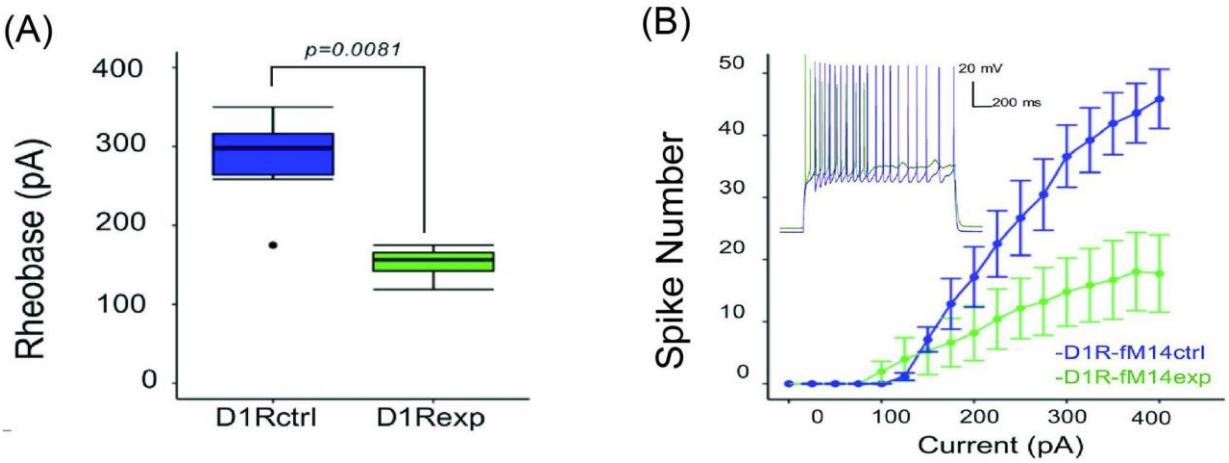

Figure 1.4. Physiological analysis of D1-SPNs with *Mettl14* gene deletion. (A) Rheobase (pA), the minimal current to induce action potential, in the conditional knockout mice (green, 4 mice, 15 cells recorded) and their control littermates (blue, 6 mice, 23 cells recorded), p = 0.0081, Student's t-test. (B) Average spike number produced at given current injections of D1 neurons with *Mettl14* gene deletion (green, 4 mice, 11 cells recorded), and the control group (blue, 6 mice, 15 cells recorded), p = 0.0254, repeated measurement ANOVA (Korenda et al., 2018).

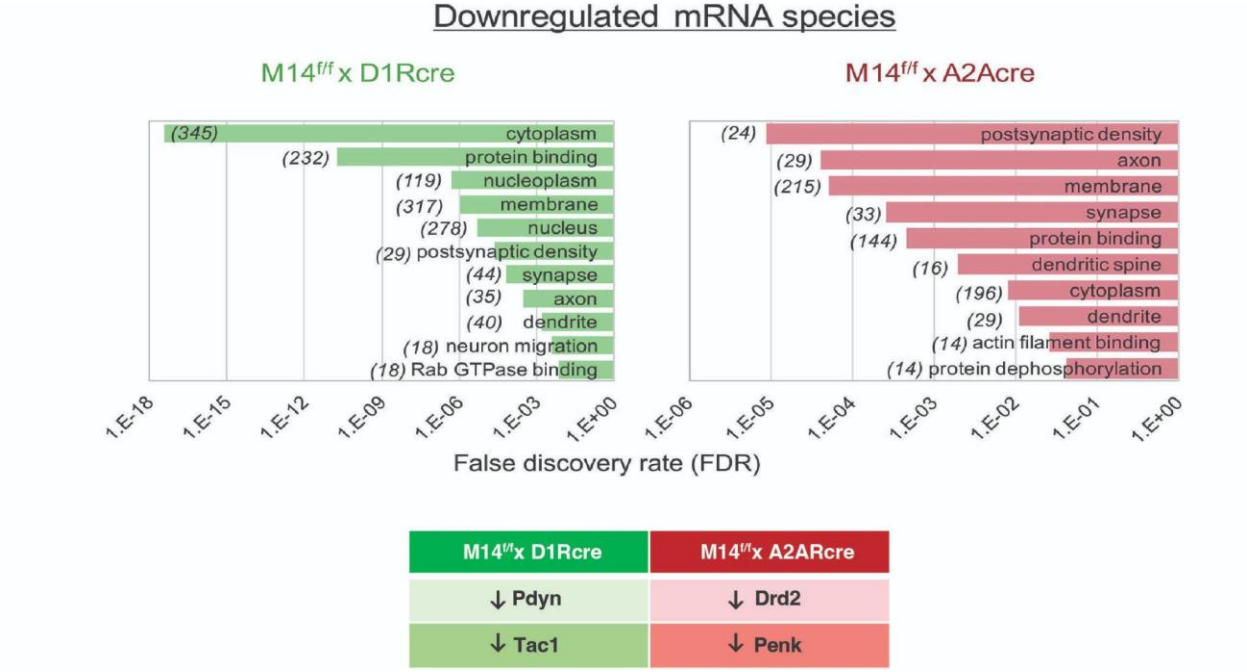

Figure 1.5. ***Mettl14*** **gene deletion in D1-SPNs and D2-SPNs caused downregulation of neuron-related mRNAs as well as downregulation in cell-type specific identity genes.** Upper: GO analysis of the downregulated mRNA species in D1-SPNs (green) and D2-SPNs (red) caused by *Mettl14* deletion. Number of genes in each GO category are shown in parentheses. Lower: Downregulation of D1-SPNs identity genes encoding dynorphin (Pdyn, p = 0.0061) and the precursor of substance-P (Tac1, p = 0.0190) in mice with *Mettl14* deletion in D1-SPNs. Downregulation of D2-SPNs identity genes encoding D2R (Drd2, p = 0.02805) and enkephalin precursor (Penk, p = 0.0029) in mice with *Mettl14* deletion in D2-SPNs. (Koranda et al. 2018)

1.7 Dissertation overview

Previous work in our lab has demonstrated the significance of m^6A in maintaining normal function in the adult striatum in mice. Furthermore, YTHDF1 has been shown to promote protein synthesis in neurons, and *Ythdf1* constitutive knock mice have impaired synaptic plasticity in the hippocampus and impaired learning (Shi et al., 2019). However, m^6A deficiency may involve many proteins and affect many cellular functions, it is not clear whether the functional consequences of m^6A are mediated by specific reader proteins in the adult brain, or, according to the redundancy model, YTHDF1, 2 and 3 work together in regulating mRNA degradation in the brain in response to neuronal events. It's not clear either if m^6A mRNA methylation affects the *in vivo* neuronal activity in response to environmental challenges. Finally, it's not clear if the impaired learning we observed in the YTHDF1 constitutive knockout mice has cell-type specificity. The m^6A deficiency caused by *Mettl14* gene deletion affects many downstream transcripts and proteins, thus, for my thesis, I aim to further investigate the downstream impact of m^6A and m^6A reader proteins in the adult brain.

In this dissertation, I first determined the effects of *Mettl14* gene deletion on *in vivo* neuronal response during either D1 or D2 SPNs dependent learning paradigms (Chapter 2). Subsequently, I explored how the downstream reader protein, YTHDF1, impacts translational control in response to behavioral adaptations (Chapter 3) and if impaired learning in cell type specific *Mettl14* knockout mice is mainly mediated by YTHDF1 in the adult brain. Given that the striatum constantly receives DA modulation to regulate neuronal excitability and plasticity, in chapter 4, I examined the role of m^6A mRNA methylation and YTHDF1 in dopaminergic neurons. DA not only acutely modulates the intrinsic excitability of SPNs but also affects corticostriatal

plasticity, which indicates its essential role in both striatum-dependent learning and performance. Finally, in both humans and mice, m^6A's expression level increases as animals age, suggesting its unique role in the matured post-mitotic neurons (Shafik et al., 2021). I therefore performed a preliminary study on the behavioral phenotypes of *Mettl14* and *YThdf1* gene deletion in mice across different age groups in order to rule out any developmental defects and to confirm the essential role of m^6A mRNA methylation in maintaining normal neuronal functions in the adult brain. These data will be discussed in the last chapter: future directions.

CHAPTER 2

IMPACTS OF *METTL14* GENE DELETION ON NEURONAL RESPONSE AND LEARNING REVEAL STRIATAL D1 AND D2 SPNS PLAY OPPOSING AND COOPERATIVE ROLES

2.1 Abstract

Animals adapt to environmental challenges with long-term changes at the behavioral, circuit, cellular, and synaptic levels. Changes in gene expression in neurons are essential in this regard. The discovery of reversible m^6A modifications of mRNA has revealed an important layer of post-transcriptional regulation which affects almost every phase of mRNA metabolism and function. Many *in vitro* and *in vivo* studies have demonstrated the significant role of m^6A in cell differentiation and survival, but its role in adult neurons is understudied. We used cell-type specific deletion of *Mettl14,* which encodes one of the subunits of the m^6A methyltransferase, in dopamine D1 receptor expressing and D2 receptor expressing neurons. We found that *Mettl14* deficiency blunted responses to environmental challenges at cellular and behavioral levels. In three different behavioral paradigms, we found that gene deletion of *Mettl14* in D1 neurons impaired D1-dependent learning, whereas gene deletion of *Mettl14* in D2 neurons impaired D2-dependent learning. Modulation of D1 and D2 neuron firing in response to changes in environments were blunted in all three behavioral paradigms as well.

2.2 Introduction

The discovery of reversible m^6A mRNA methylation (m^6A-tagging) has revealed an important layer of post-transcriptional gene regulation (Meyer and Jaffrey, 2014; Zhao et al., 2017).

m^6A is the most abundant internal mRNA modification in the mammalian cells and widely conserved among eukaryotic species (Yue et al., 2015; Cao et al., 2016). Studies have demonstrated the effect of m^6A modification on RNAs on almost every phase of mRNA metabolism including RNA transport, localization, splicing, stability and translational efficiency (Wang et al., 2014; Louloupi et al., 2018; Wang et al., 2015; Liu et al., 2014).

Among other cell types, the brain contains higher level of m^6A (Meyer and Jaffrey, 2014). m^6A levels in mouse brain tissue are relatively low through embryogenesis but drastically increase by adulthood (Meyers et al., 2012), suggesting that m^6A-tagging plays a unique role in the adult brain which has just begun to be systematically studied. Multiple studies have shown that m^6A is essential for stress response regulation, synaptic plasticity, learning and memory formation in adult mice (Engel et al., 2018; Shi et al., 2018; Koranda et al., 2018; Zhang et al., 2018).

m^6A modification is catalyzed by the m^6A methyltransferase heterodimer METTL14 and METTL3. In our earlier work, we used cell-type specific deletion of *Mettl14* in the striatum and demonstrated that striatal m^6A deficiency impaired synaptic gene expression, neuronal activity, and striatum-dependent learning (Koranda et al. 2018). However, the full scope of m^6A's *in vivo* influences on neuronal responses to environmental changes remains to be elucidated. It is also not clear whether m^6A deficiency impacts real-time neuronal activity in behaving animals.

Striatum, as the input stage of the basal ganglia, has been long recognized as the key structure in movement control, behavior selection, and motor skill learning (Graybiel et al., 1994; Gerfen and Wilson, 2004; Balleine et al., 2009). We take advantage of the fact that there are only two prominent neuronal cell types throughout the striatum: the dopamine D1 receptor-expressing GABAergic medium spiny projection neurons (SPNs) in the direct pathway, and the dopamine D2

receptor-expressing SPNs in the indirect pathway (Gerfen et al., 1990, Albin et al., 1989, Smith et al., 1998; Gerfen and Surmeier, 2011). We used three different behavioral paradigms to specifically target D1 and D2- dependent learning, and by simultaneously performing cell-type specific *in vivo* recording, we aim to dissect the influences of *Mettl14* on these distinct neuronal pathways. We showed that *Mettl14* deficiency reduced the baseline neuronal activity and blunted the responses to environmental challenges at cellular and behavioral levels in adult mice.

2.3 Results

2.3.1 Mettl14 gene deletion in D1 and D2 SPNs blunted cellular responses to cocaine in both cell types but led to opposite behavioral phenotypes

Both D1 and D2 SPNs are involved in animals' responses to cocaine. However, they may play different roles. Our previous in vitro data suggest that *Mettl14* deletion alters spike frequency adaptation in D1 neurons (Koranda et al., 2018). In order to examine cell-type specific functional role of m^6A *in vivo*, we generated mice with conditional deletion of *Mettl14* in D1 and D2 expressing neurons respectively (D1-Cre; $Mettl14^{f/f}$ and A2A-Cre; $Mettl14^{f/f}$ mice). We examined cocaine's locomotor sensitization effect in open field boxes in mutants and their respective control littermates (Figure 2.1A). Mice with *Mettl14* deletion in D1 neurons exhibited both impaired acute locomotor response to cocaine and sensitization compared to controls (genotype main effect, $p=0.0037$; genotype x time interaction, $p=0.0057$) (Figure 2.1C). In contrast, mice with *Mettl14* deletion in D2 neurons displayed enhanced acute locomotor response to cocaine and sensitization compared to controls (genotype main effect, $p=0.0006$; genotype x time interaction, $p=0.0144$) (Figure 2.1D).

In order to characterize the *in vivo* activity of D1 and D2 SPNs and their responses to cocaine, we performed fiber photometry recordings in the dorsal striatum. Cre-dependent GCaMP6m AAV were injected into the dorsal striatum of D1-Cre; Mettl14$^{f/f}$ and A2A-Cre; Mettl14$^{f/f}$ mice as well as their littermate controls to selectively label D1 and D2 neurons. Ca^{2+} transients were recorded in freely moving mice after saline and cocaine intraperitoneal (IP) injections (Figure 2.1B). Under baseline conditions, D2 neurons exhibited stronger intrinsic Ca^{2+} transients than D1 neurons, as reflected in higher mean GCamP6m fluorescence (Figure 2.1E, F). Cocaine acutely increased the Ca^{2+} transients in D1 neurons and inhibited the Ca^{2+} transients in D2 neurons in the control mice (Figure 2.1E, F). This is in agreement with the literature that the D1 receptor is positively coupled to the cAMP pathway whereas the D2 receptor is negatively coupled to the cAMP pathway; and that cocaine elevates DA level in the synapse and causes more activation of both receptors. *Mettl14* deletion significantly reduced the baseline Ca^{2+} transients in both D1 and D2 neurons (Figure 2.1E, F). *Mettl14* deletion also significantly blunted the increased firing in D1 neurons after acute cocaine and decreased firing in D2 neurons after acute cocaine (Figure 2.1E, F).

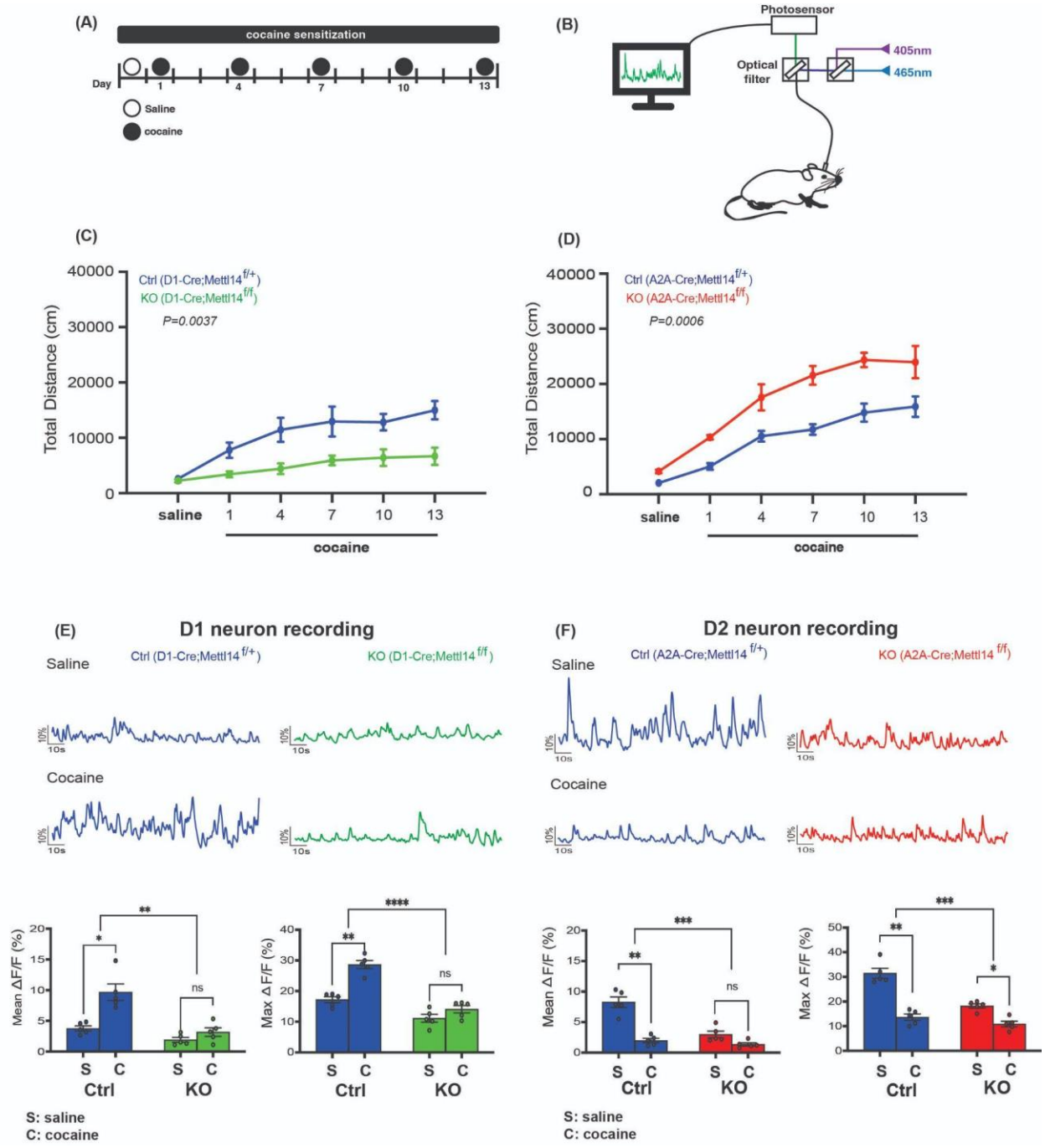

Figure 2.1. *Mettl14* gene deletion in D1 and D2 SPNs blunted cellular responses to cocaine in both cell types but led to opposite behavioral phenotypes.

cont. Figure 2.1. *Mettl14* gene deletion in D1 and D2 SPNs blunted cellular responses to cocaine in both cell types but led to opposite behavioral phenotypes. (A) Schematic diagram of the timeline to examine cocaine's sensitization effect in the open field box. (B) Schematic diagram of fiber photometry set up and recording after cocaine treatment. (C, D) Cocaine-induced locomotor sensitization. C, D1-Cre;Mettl14$^{f/+}$ (Ctrl, blue) and D1-Cre;Mettl14$^{f/f}$ (KO, green), n=7. D, A2A-Cre;Mettl14$^{f/+}$ (Ctrl, blue) and A2A-Cre;Mettl14$^{f/f}$ (KO, red), n=7. Locomotor activity is recorded for 60 min after saline/cocaine injection. Total distance traveled is recorded. (E) Upper left: representative Ca^{2+} traces of D1-Cre;Mettl14$^{f/+}$ (Ctrl, blue) after saline injection using fiber photometry. Upper Right: representative Ca^{2+} traces of D1-Cre;Mettl14$^{f/f}$ (KO, green) after saline injection using fiber photometry. Lower left: representative Ca^{2+} traces of D1-Cre;Mettl14$^{f/+}$ (Ctrl, blue) after cocaine injection using fiber photometry. Lower Right: representative Ca^{2+} traces of D1-Cre;Mettl14$^{f/f}$ (KO, green) after cocaine injection using fiber photometry. Left bar graph: Mean Ca^{2+} activity of D1-Cre;Mettl14$^{f/+}$ (Ctrl, blue) and D1-Cre;Mettl14$^{f/f}$ (KO, green) from 15 min fiber photometry recording after saline (S) and cocaine (C) injection. * P=0.0163, paired T-test, ns. P=0.0702, paired T-test, ** P=0.0010, 2-way ANOVA. Right bar graph: Peak Ca^{2+} transients level comparison. ** P=0.0029, paired T-test, ns. P=0.1250, paired T-test. **** P<0.0001, 2-way ANOVA, n=5. (F) Upper left: representative Ca^{2+} traces of A2A-Cre;Mettl14$^{f/+}$ (Ctrl, blue) after saline injection using fiber photometry. Upper Right: representative Ca^{2+} traces of A2A-Cre;Mettl14$^{f/f}$ (KO, red) after saline injection using fiber photometry. Lower left: representative Ca^{2+} traces of A2A-Cre;Mettl14$^{f/+}$ (Ctrl, blue) after cocaine injection using fiber photometry. Lower Right: representative Ca^{2+} traces of A2A-Cre;Mettl14$^{f/f}$ (KO, red) after cocaine injection using fiber photometry. Left bar graph: Mean Ca^{2+} activity of A2A-Cre;Mettl14$^{f/+}$ (Ctrl, blue) and A2A-Cre;Mettl14$^{f/f}$ (KO, red) from 15 min fiber photometry recording after saline (S) and cocaine (C) injection. ** P=0.0020, paired T-test, ns. P=0.0690, paired T-test, *** P=0.0007, 2-way ANOVA. Right bar graph: Peak Ca^{2+} transients level comparison. ** P=0.0011, paired T-test, * P=0.0150, paired T-test. *** P=0.0007, 2-way ANOVA, n=5. All data expressed as mean ± SEM.

2.3.2 Mettl14 gene deletion in D1 SPNs blunted changes in D1 neuron activity during rotarod motor skill learning and impaired rotarod motor skill learning

The above data suggest that m^6A's role at the cellular level could be similar in different neurons, however, the behavioral consequences could be very different depending on the specific cells and circuits impaired. It is also one of the best demonstrations that the D1 (direct) and D2 (indirect) pathways have opposing functions: deletion of the exact same gene in D1 versus D2 SPNs leads to the exact opposite behavioral phenotype.

Although D1 and D2 SPNs often work together for any motor tasks, there are examples in which a particular motor learning can be mostly D1-dependent or D2-dependent. For example, the rotarod motor skill learning is mostly D1-dependent whereas sensitization of haloperidol-induced catalepsy is mostly D2-dependent.

To examine closely the contribution of m^6A to each type of learning, we recorded from D1 SPNs from D1-Cre; Mettl14$^{f/f}$ mice and their littermate controls while they learn to run on the accelerating rotarod (Figure 2.2A). Similar to what we reported in our earlier studies, *Mettl14* deletion in D1 neurons severely impaired motor skill learning (Figure 2.2C and 2.2G). Throughout training, the mean Ca^{2+} transients in D1 neurons reduced as performance improved in control mice (Figure 2.2B-D). In contrast, the mean Ca^{2+} transients in D1 neurons slightly increased in the D1-Cre; Mettl14$^{f/f}$ conditional gene deletion mice throughout training (Figure 2.2E-2F).

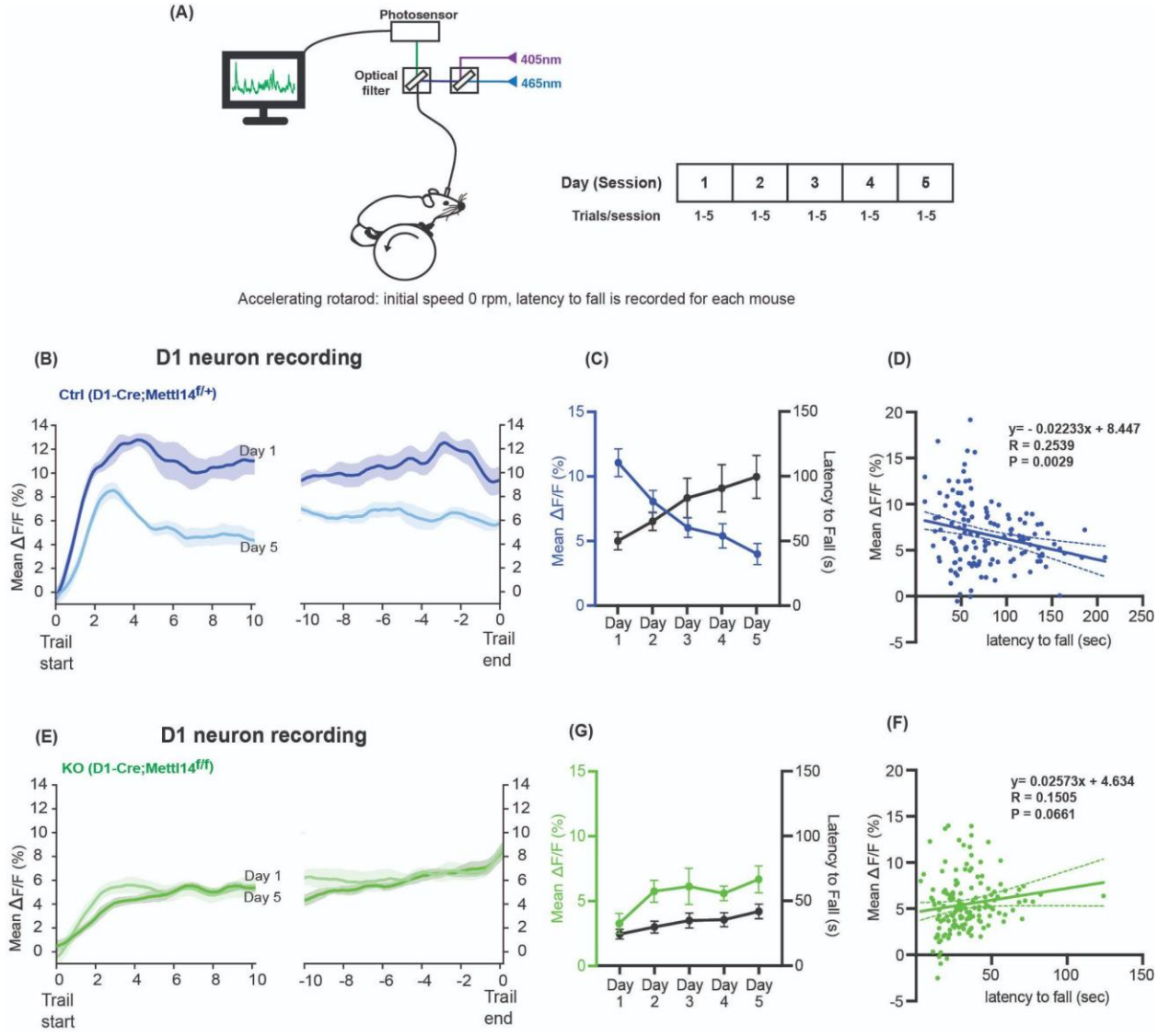

Figure 2.2. *Mettl14* gene deletion in D1 SPNs blunted changes in D1 neuron activity during rotarod motor skill learning and impaired rotarod motor skill learning.

cont. Figure 2.2. *Mettl14* gene deletion in D1 SPNs blunted changes in D1 neuron activity during rotarod motor skill learning and impaired rotarod motor skill learning. (A) Schematic diagram and timeline of rotarod motor learning training paradigm combining with fiber photometry recording. (B) Left: Comparison of the mean Ca^{2+} traces of D1-Cre;Mettl14$^{f/+}$ (Ctrl, blue) during the first 10s of training between Day 1 and Day 5. Right: Comparison of the mean Ca^{2+} traces of D1-Cre;Mettl14$^{f/+}$ (Ctrl, blue) during the last 10s of training between Day 1 and Day 5. Shaded area represents SEM. (C) The daily average performance (s) and the mean Ca^{2+} activity in D1-Cre;Mettl14$^{f/+}$ (Ctrl, blue) are plotted together. (D) Negative correlation between motor learning performance and mean D1 Ca^{2+} activity. Each point represents the mean D1 Ca^{2+} activity and performance of one trial, p=0.0029.. (E) Left: Comparison of the mean Ca^{2+} traces of D1-Cre;Mettl14$^{f/f}$ (KO, green) during the first 10s of training between Day 1 and Day 5. Right: Comparison of the mean Ca^{2+} traces of D1-Cre;Mettl14$^{f/f}$ (KO, green) during the last 10s of training between Day 1 and Day 5. Shaded area represents SEM. (F) The daily average performance (s) and the mean Ca^{2+} activity in D1-Cre;Mettl14$^{f/f}$ (KO, green) are plotted together. (G) Correlation between motor learning performance and mean D1 Ca^{2+} activity in D1-Cre;Mettl14$^{f/f}$ (KO, green). Each point represents the mean D1 Ca^{2+} activity and performance of one trial, p=0.0661. All data expressed as mean ± SEM, n=5.

2.3.3 Mettl14 gene deletion in D2 SPNs blunted changes in D2 neuron activity during haloperidol-induced catalepsy and diminished haloperidol-induced catalepsy

To probe the D2 (indirect) pathway specific learning, we used an established paradigm that is known to be dependent on the D2 pathway plasticity: sensitization of haloperidol-induced catalepsy. Mice treated with D2 antagonist haloperidol initially showed akinesia and rigidity (i.e., catalepsy). With repeated daily treatment, more severe catalepsy was observed (sensitization). We recorded from D2 SPNs in A2A-Cre; Mettl14$^{f/f}$ conditional KO mice and their control littermates (Figure 2.3A). Significant reduced cataleptic and sensitization were observed in the conditional knockout mice (genotype main effect, p=0.0003; time, p=0.0007) (Figure 2.3C). We analyzed the *in vivo* activity of D2 neurons during haloperidol-induced catalepsy (Figure 2.3B). During the catalepsy response, D2 neurons were quiescent, evident Ca^{2+} activity was followed immediately after movement initiation (Figure 2.3D). Sensitization was presented as the quiescent time prolonged in D2 neurons, more severe catalepsy responses exhibited after repeated treatment (Figure 2.5). *Mettl14* deletion in D2 neurons significantly impaired changes in D2 neuron firing in the conditional knockout mice in this paradigm (Figure 2.3E-F). Whereas in mice with D1 neuron deletion of *Mettl14*, normal catalepsy and sensitization response were observed (Figure 2.4, 2.5).

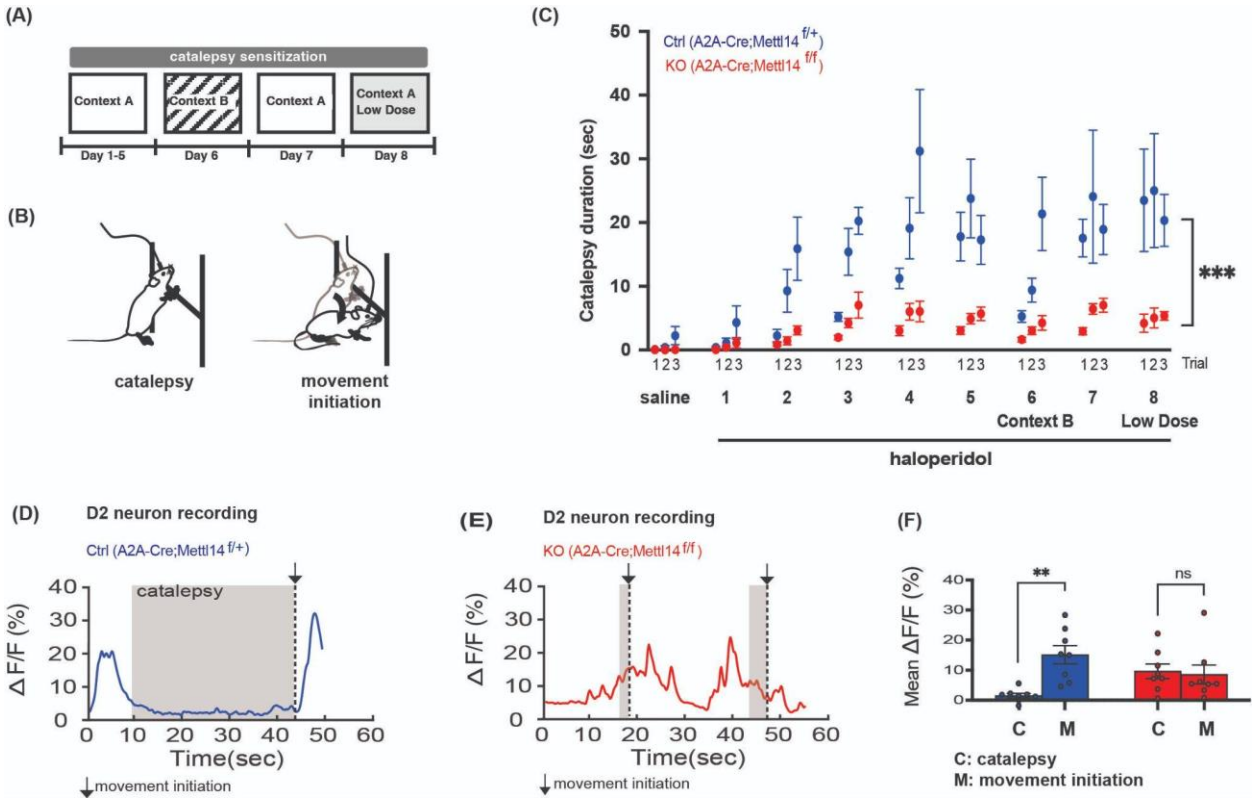

Figure 2.3. *Mettl14* gene deletion in D2 SPNs blunted changes in D2 neuron activity during haloperidol-induced catalepsy and diminished haloperidol-induced catalepsy. (A) Schematic timeline for testing the haloperidol-induced catalepsy sensitization. (B) Schematic diagram represents the fiber photometry recording paradigm: during catalepsy and after movement initiation. (C) The haloperidol-induced catalepsy sensitization response in A2A-Cre;Mettl14$^{f/+}$ (Ctrl, blue) and A2A-Cre;Mettl14$^{f/f}$ (KO, red). Catalepsy duration is recorded (s). *** P=0.0003, 2-way ANOVA, n=8. (D) Representative Ca^{2+} trace of A2A-Cre;Mettl14$^{f/+}$ (Ctrl, blue), catalepsy response and the time point of movement initiation are depicted. (E) Representative Ca^{2+} trace of A2A-Cre;Mettl14$^{f/f}$ (Ctrl, red), reduced catalepsy response and the time points of movement initiation are depicted. (F) The mean Ca^{2+} activity in A2A-Cre;Mettl14$^{f/+}$ (Ctrl, blue) and A2A-Cre;Mettl14$^{f/f}$ (KO, red) during catalepsy response and after movement initiation, each data point represents a mouse. ** P=0.0018, paired t -test, ns. P=0.8184. All data expressed as mean ± SEM, n=8.

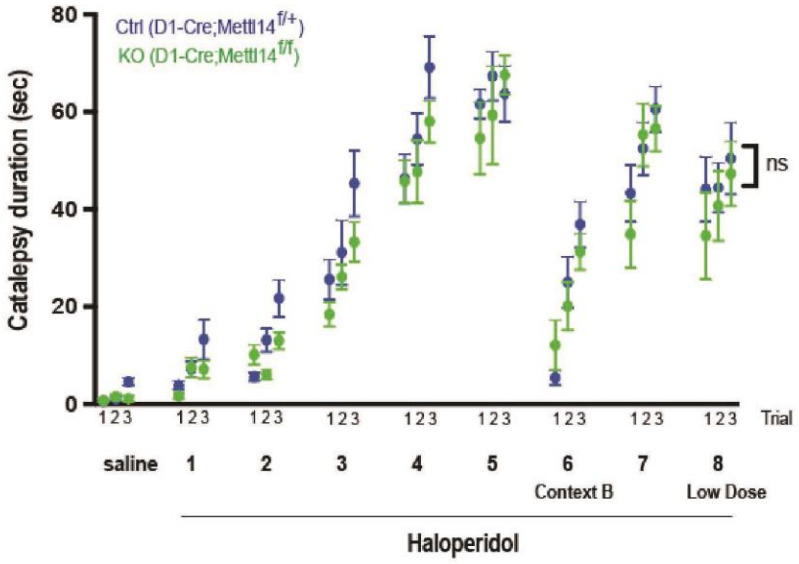

Figure 2.4. Catalepsy sensitization response was normal in mice with *Mettl14* gene deletion in D1-SPNs. The haloperidol-induced catalepsy sensitization response in D1-Cre;Mettl14$^{f/+}$ (Ctrl, blue) and D1-Cre;Mettl14$^{f/f}$ (KO, green). Catalepsy duration is recorded (s). ns. P=0.9218, 2-way ANOVA, n=7. All data expressed as mean ± SEM.

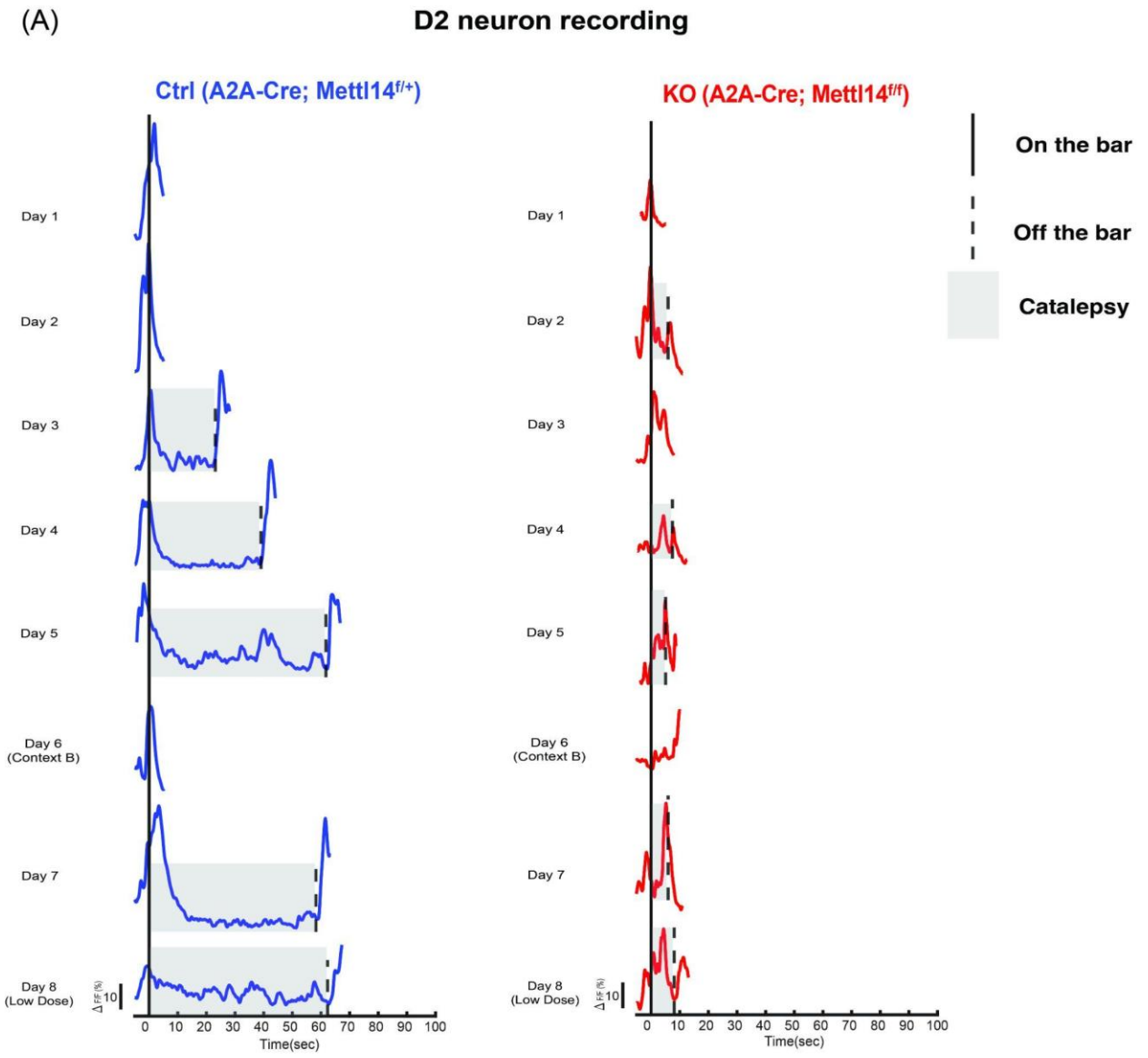

Figure 2.5. Representative traces of D1 and D2 SPNs during the haloperidol-induced catalepsy sensitization response. (A) Representative traces of 8-days recording in A2A-Cre;Mettl14$^{f/+}$ (Ctrl, blue, left) and A2A-Cre;Mettl14$^{f/f}$ (KO, green, right). (B) Representative traces of 8-days recording in D1-Cre;Mettl14$^{f/+}$ (Ctrl, blue, left) and D1-Cre;Mettl14$^{f/f}$ (KO, green, right).

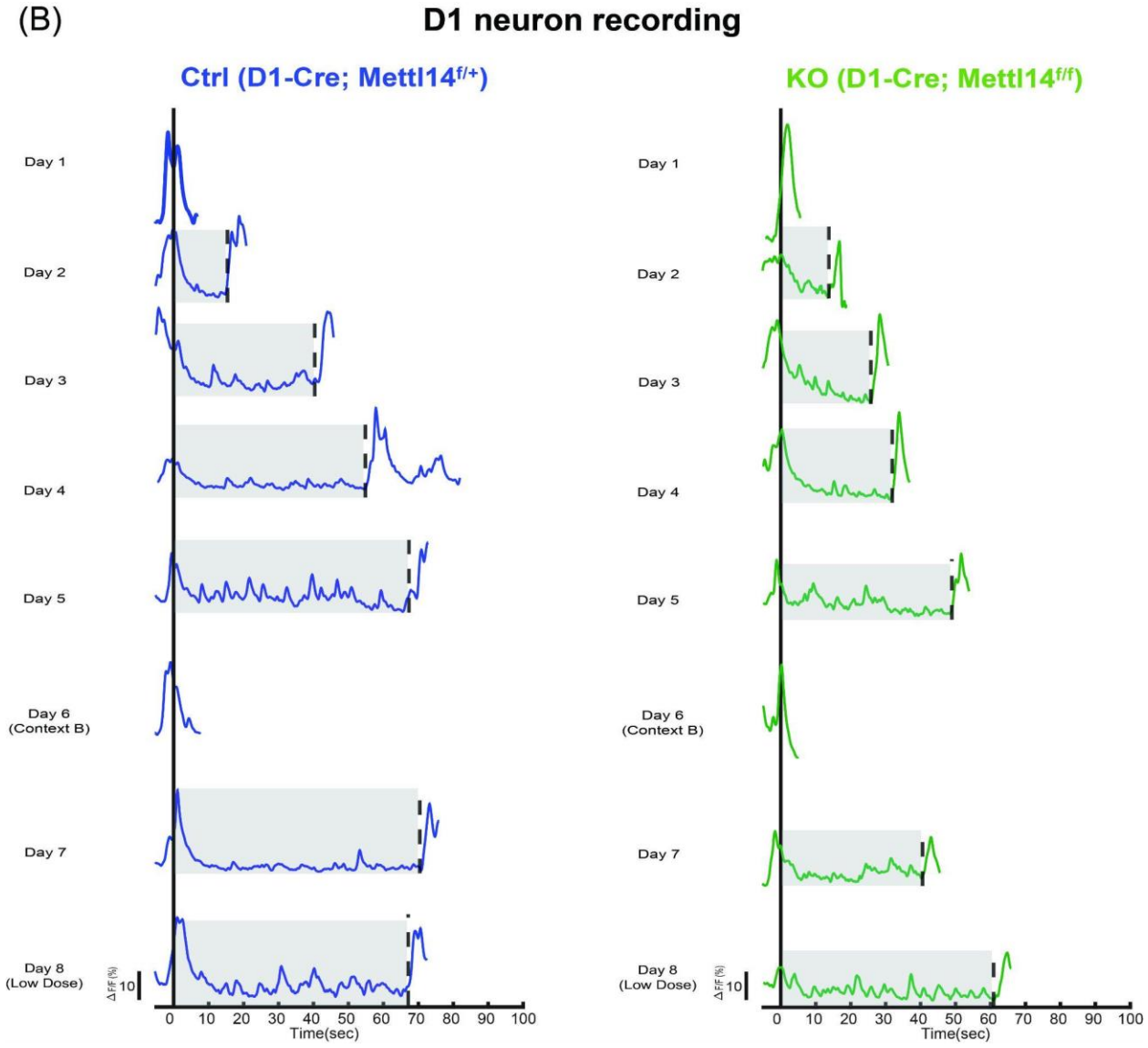

cont. Figure 2.5. Representative traces of D1 and D2 SPNs during the haloperidol-induced catalepsy sensitization response.

2.3.4 D2 SPN firing was positively correlated with movement speed. Haloperidol increased D2 SPN firing and inhibited movement. Mettl14 gene deletion blunted both types of modulation

The classic model of D2 (indirect) pathway characterizes it as inhibitory, suggesting that increased D2 SPN activity leads to motor inhibition. This "No Go" pathway concept is supported by our D2 recording data in Figure 2.1, where cocaine treatment resulted in reduced D2 neuron firing and increased locomotion in the littermate controls. However, in Figure 2.3, we also observed that D2 neuron firing positively correlated with movement, and there was almost no D2 neuron firing when there was no movement (i.e., during catalepsy). This seems to be contradictory to the classic model of the D2 pathway's role in movement inhibition.

In order to take a closer look at D2 neuron firing during behavior to resolve these paradoxical observations, we then recorded from D2 SPNs and simultaneously recorded the open field locomotor activity continuously from both A2A-Cre; Mettl14$^{f/f}$ conditional knockout mice and their littermate controls under haloperidol or saline treatment (Figure 2.6). This would allow us to correlate D2 neuron firing with locomotor activity while dissociating drug effects and genotype effects.

In the littermate controls, individual regression analyses of D2 activity and locomotor speed indicate that D2 neuron firing positively correlated with speed (Figure 2.6 D). However, the comparison between the haloperidol group and saline group suggests a negative correlation between locomoter speed and D2 neuron firing. Haloperidol reduced the total locomotion as it induced catalepsy responses (Figure 2.6 A). Haloperidol also increased the firing of D2 neurons, as it caused an upward shift in the regression line (Figure 2.6 C, E), as well as the increase in the

mean calcium activity of D2 neurons (Figure 2.6 B). This is in agreement with D2 antagonist's effect on elevating cAMP levels in D2 SPNs since the D2 receptor is negatively coupled to the cAMP pathway.

With *Mettl14* deletion, both the above correlations were blunted. *Mettl14* deletion caused a downward shift in the regression line when compared D2 firing to locomotor speed (Figure 2.6 F). Haloperidol did not cause a significant change in total locomotion (Figure 2.6 A). Haloperidol did not increase the firing of D2 neurons, as it did not cause significant changes in the regression line (Figure 2.6 C, G), and no significant changes in the mean calcium activity of D2 neurons either (Figure 2.6 B).

We also subdivided the locomotor activities based on movement: movements with a velocity less than 0.8 cm/s were classified as "not moving". We found that D2 neurons in the conditional KO mice and their littermate controls exhibited quiescence in this state. This feature is drug-independent since no significant changes in the mean Ca^{2+} transients were observed after haloperidol treatment in all mice (Figure 2.6B).

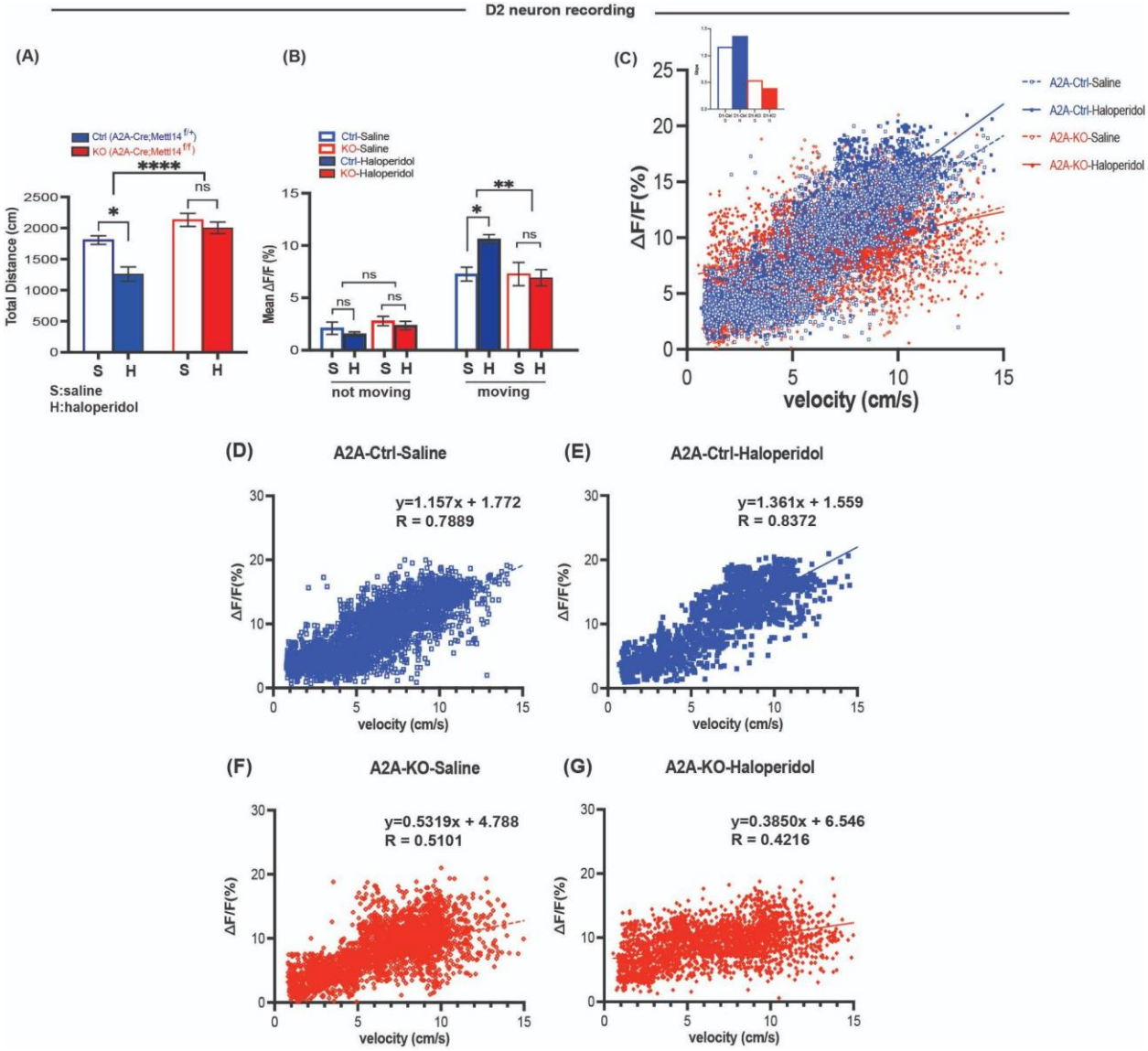

Figure 2.6. D2-SPN firing was positively correlated with movement speed. Haloperidol increased D2 SPN firing and inhibited movement. *Mettl14* gene deletion blunted both types of modulation.

cont. Figure 2.6. D2-SPN firing was positively correlated with movement speed. Haloperidol increased D2 SPN firing and inhibited movement. *Mettl14* gene deletion blunted both types of modulation. (A) Open field locomotor activity in A2A-Cre;Mettl14$^{f/+}$ (Ctrl, blue) and A2A-Cre;Mettl14$^{f/f}$ (KO, red) after saline (S) and haloperidol (H) treatment. Total distance traveled is recorded (cm). * P=0.0490, paired T-test, ns P=0.5632, paired T-test, **** P<0.0001, 2-way ANOVA, n=4. (B) The mean Ca^{2+} activity of A2A-Cre;Mettl14$^{f/+}$ (Ctrl, blue) and A2A-Cre;Mettl14$^{f/f}$ (KO, red) after saline (S) and haloperidol (H) treatment that are separately plotted according to speed. Not moving: speed < 0.8cm/s, Ctrl (blue), S vs. H, ns. P = 0.4608, paired T-test. KO (red), S vs. H: ns. P = 0.0996, paired-T-test, Ctrl vs. KO, ns. P =0.2494, 2-way ANOVA. Moving: speed > 0.8cm/s, Ctrl (blue), S vs. H, * P = 0.0410, paired T-test. KO (red), S vs. H: ns. P = 0.8501, paired-T-test, Ctrl vs. KO, ** P = 0.0029, 2-way ANOVA. All data expressed as mean ± SEM. (C) Scatter plot of Ca^{2+} activity and speed (cm/s). Hollow blue circle, dashed blue line: A2A-Cre;Mettl14$^{f/+}$ (Ctrl) after saline treatment; filled blue circle, solid blue line: A2A-Cre;Mettl14$^{f/+}$ (Ctrl) after haloperidol treatment; hollow red triangle, dashed red line: A2A-Cre;Mettl14$^{f/f}$ (KO) after saline treatment; filled red triangle, solid red line: A2A-Cre;Mettl14$^{f/f}$ (KO) after cocaine treatment, inset bar graph compares the slopes of four regression lines. (D-G) Individual regression analysis of the four conditions depicted in C.

2.4 Discussion

In three different behavioral paradigms, we showed that gene deletion of *Mettl14* in D1-SPNs impaired D1-dependent learning, whereas gene deletion of either *Mettl14* or *Ythdf1* in D2 neurons impaired D2 dependent learning. The *in vivo* neuronal responses to changes in the environment during the learning paradigm are also impaired with the same cell type specificity. Moreover, the modulation of D1 and D2 neuron firing in response to changes in environments were blunted in all three behavioral paradigms as well.

The D1 (direct) pathway is known to be the excitatory, or "Go", pathway, i.e., increased activity of D1 SPNs will increase motor output. In contrast, the D2 (indirect) pathway is known to be the inhibitory, or "NoGo", pathway, i.e., increased activity of D2 SPNs will cause more motor inhibition. Our recording data in Figure 2.1 also support this "classic rate model": cocaine increased D1 firing and reduced D2 neuron firing which are correlated with increased locomotion. Moreover, gene deletion of *Mettl14* in D1 neurons impaired cocaine-induced hyperlocomotion and sensitization, whereas gene deletion of *Mettl14* in D2 neurons enhanced cocaine-induced hyperlocomotion. Finally, gene deletion of *Mettl14* in D2 neurons diminished haloperidol-induced catalepsy which is characterized by movement inhibition. All these data fit well with the classic rate model of basal ganglia's "Go" versus "NoGo" pathways described above.

However, in Figure 2.3, D2 SPN neuron firing was clearly correlated with movement positively, and also, there was almost no D2 neuron firing during catalepsy response (i.e., no movement). These data seem to contradict the classic rate model but are in agreement with other published studies that correlate D2 SPN firing with movement (Cui et al., 2013; Tecuapetla et al., 2016; Parker et al., 2018). To take a closer look at D2 neuron firing during behavior, we recorded

from D2 SPNs and simultaneously recorded open field locomotor activity continuously. This allowed us to correlate D2 neuron firing with locomotor activity while dissociating drug effects and genotype effects (Figure 2.4). In this analysis, D2 neuron firing is clearly correlated with locomotor speed positively. However, haloperidol treatment reduced locomotor activity and at the same time increased D2 neuron firing as it caused an upward shift in the regression line in the control mice (but not in the conditional knockout mice).

One explanation that could reconcile the seemingly contradictory data is that the positive correlation between D2 SPN firing and motor activity is an indication that D2 neurons and its function in inhibiting the motor cortex is always needed in any motor acts. It's also understandable that D2 SPNs receive direct inputs from motor cortical neurons like D1 SPNs do. It will be surprising if D2 SPNs do not increase firing when they receive more excitation from motor cortical neurons. On the other hand, when D2 neuron themselves were stimulated or inhibited independent of cortical inputs, it will result in decreased or increased motor outputs respectively as shown in our haloperidol data as well as many published papers using D2 selective pharmacological, optogenetic, or chemogenetic manipulations (Kravitz et al., 2010).

Striatum-dependent motor learning is mediated by corticostriatal synaptic plasticity in the dorsal striatum (Yin and Knowlton., 2006). Interestingly, our recording data showed that the corticostriatal activity of D1-SPNs during rotarod training also decreased over the course of training (Figure 2.2). This also seems to contradict some earlier reports of increased DLS activity after training (Yin et al., 2009; Hawes et al., 2015). One possible explanation is that motor learning involves the fine-tuning of presynaptic cortical inputs and the postsynaptic potentiation in the dorsal striatum, a concept known as "engram selection". Engram neurons are a population of

neurons that are reactivated in a task specific manner. During motor learning, only the motor engram neuron output is selectively strengthened and projects onto DLS SPNs (Hwang et al., 2022). Further validation of this hypothesis requires *in vivo* recording at single-cell resolution, such as calcium imaging, to track individual SPN activity over the course of training.

2.5 Methods

2.5.1 General Animal Information

All experiments were conducted with male and female C57BL/J mice aged 6-8 months. All the mice were housed under a 12-hour light/dark cycle in a temperature and humidity controlled barrier facility, with *ad libitum* access to standard food and water at the University Chicago. All the behavioral experiments and procedures were conducted during the light cycle in accordance with guidelines approved by the Institutional Animal Care and Use Committee at the University of Chicago.

2.5.2 Conditional Mettl14 deletion

The conditional KO mice with *Mettl14* deletion in D1 and D2 MSNs we used were described in the previous study (Koranda et al. 2018). Mice carrying a conditional removable *Mettl14* allele (Mettl14$^{f/f}$) were crossed to a D1 receptor promoter-driven Cre recombinase (D1-Cre) transgenic line (B6.FVB(Cg)-Tg(Drd1-cre)EY262Gsat/Mmucd, RRID: MMRRC-030989-UCD) or an adenosine 2A receptor promoter-driven Cre recombinase (A2A-Cre) transgenics line (B6.FVB(Cg)-Tg(Adora2a-cre)KG139Gsat/Mmucd, RRID: MMRRC_036158-UCD) to selectively delete *Mettl14* in D1 or D2 MSNs. All experiments were performed in both double transgenic mice (D1-Cre;Mettl14$^{f/f}$, A2A-Cre;Mettl14$^{f/f}$), and the respective control littermates (D1-Cre;Mettl14$^{f/+}$, A2A-Cre;Mettl14$^{f/+}$).

2.5.3 Drugs

Cocaine (Sigma Life Science, Lot SLBR5044V) and haloperidol (Sigma, Lot 101K1176) were used in the behavioral studies. All drugs were dissolved in 0.9% sterile saline, and all injections were intraperitoneal (i.p.).

2.5.4 Cocaine sensitization behavior

Mice were injected with cocaine (0.01mg/g of body weight) and the locomotor activity was recorded in an open field box (43.2 x 43.2 cm, Med Associates, St. Albns, VT, USA) with infrared beams at the bottom to record the distance traveled (cm) for 60 min immediately after treatment. Each open field box was paired with lighting at 21 lux and surrounded by black curtains to obscure the views beyond the box. The sensitization response was measured with one injection every three days, for a total of five injections. Locomotor activity was recorded after each injection. A saline injection was administered before the first day of experiment for baseline measurement vehicle control.

2.5.5 Haloperidol induced catalepsy sensitization behavior

An elevated bar was positioned within an open field box with consistent placement across sessions. Mice were injected with haloperidol (0.5mg/kg of body weight) about one hour before testing. Mice were then positioned on the bar by lifting them by the tail, prompted them to reach out and grasped the bar with their hind feets touching the table. Catalepsy response was scored as the mice remained standing on the bar. Scoring was conducted 3 trials each day, separated by 30 seconds. A trial concluded when the mice made intentional moves, such as paw retraction and head movement. The time to the first intentional move was recorded. The typical sensitization response timeline followed the sequence: Days 1-5, sensitization training with the same set up of elevated

bar and open field (context A); Day 6, tested the context-dependence by setting the elevated bar to a completely different environment (context B). Day 7, reinstatement observation back to context A. Day 8, subthreshold sensitization test in context A with a lower dosage of haloperidol (0.5mg/kg of body weight). A saline injection was administered before the first day of experiment for baseline measurement vehicle control.

2.5.6 Accelerating Rotarod

The accelerating rotarod we used to measure the striatum-dependent sensorimotor learning was described in previous studies (Beeler et al. 2012, Koranda et al. 2016). A computer-controlled rotarod apparatus with infrared beam detectors ((Rotamex-5, Columbus Instruments, Columbus, OH, USA) and a rat rod (7cm diameter) was set to accelerate from 0 to 40 revolutions per minute (rpm) over 300s, and the latency to fall was recorded. Mice received five trials per session with 30s intertrial intervals (ITI), one session per day for four or five consecutive days.

2.5.7 Stereotaxic injections and fiber implantation

All surgical procedures used mice aged ~16 weeks under sterile conditions. Mice were anesthetized using 2% isoflurane and placed in a stereotaxic frame. Skull was exposed and bregma - lambda was identified, hole was drilled above dorsal striatum (AP +0.7, ML +2.25), a guide needle was lowered 2.7mm DV, 400nL of AAV virus with Cre recombinase (AAV.Syn.Flex.GCaMP6s.WPRE.SV40) was delivered at a speed of 100nL/min, and allow for 7min to diffuse post injection before needle retraction. An optic cannula (MFC_400/430-0.66_5mm_MF1.25_FLT, Doric) was inserted into the injection site, 100um above the viral delivery site. The cannula was then secured using dental cement.

2.5.8 Fiber Photometry

TDT-Doric system was used for fiber photometry studies, TDT RZ5P for signal driving and demodulation. This system was adept at delivering light at wavelengths of 405 nm and 465 nm, while monitoring at 525 nm through a specialized Doric minicube (FMC5_IE(400- 410)_E(460-490)_F(500-540)_O(580-680)_S, Doric). The received light was processed by a femtowatt photodetector (Newport Model 2151), which then channeled the signals to the RZ5P. We used distinct modulation frequencies to monitor signals based on calcium dependence. The 465 nm excitation light was calcium-responsive and modulated at 331Hz, while the 405 nm, an isosbestic calcium-independent control, was modulated at 211 Hz using LEDs and LED driver (Doric). Mice were tethered to a patch cord (0.48NA, 400 μm core diameter, Doric) with freely rotary joint and gimbal holder (Doric) for maximum freedom during movement. The TDT Synapse software was employed to interact with the RZ5P system, facilitating data logging, event timestamping via TTL loggers, and LED control.

All data were analyzed in MATLAB or Python. Briefly, first 5s recording was removed for opto-electro artifacts that might significantly affect the fitting parameters in the subsequent step. The calcium-independent signal was subtracted from the calcium-dependent signal to reduce movement or hemodynamic artifacts, a smoothed 405nm signal was fitted to the 465nm signal using linear regression to obtain fitting coefficients. Using the coefficients, we calculated the fitted 405nm and calculated normalized $\Delta F/F$ = (F 465 - F fitted405) / F fitted405.

CHAPTER 3

DYNAMIC REGULATION OF RNA TRANSCRIPTS, TRANSLATIONAL CONTROL AND BEHAVIORAL ADAPTATIONS IN THE STRIATUM BY YTHDF1

3.1 Abstract

Memory formation and environmental adaptation requires dynamic regulation in gene expression in neurons. While gene expression regulation at the transcriptional level has been well characterized, post-transcriptional regulation of de novo protein synthesis could enable better spatial and temporal control, thus more suitable for neurons. The discovery of reversible m^6A mRNA methylation provides a new layer of post-transcriptional mRNA regulation. Here, we used cell-type specific deletion of *Ythdf1*, which encodes one of the cytoplasmic m^6A reader proteins, in dopamine D1 receptor expressing or D2 receptor expressing neurons. We showed that *Ythdf1* deletion resembles impairment caused by *Mettl14* deletion in a cell type specific manner, suggesting YTHDF1 is the main mediator of the functional consequences of m^6A mRNA methylation in the striatum. Boosting DA release by cocaine drastically increased YTHDF1 binding to many mRNA targets in the striatum, especially those encoding structural proteins, suggesting the initiation of long-term neuronal and/or synaptic structural changes. While striatal neurons in control mice responded to elevated cAMP by increasing *de novo* protein synthesis rate, striatal neurons in *Ythdf1* knockout mice didn't.

3.2 Introduction

Changes in gene expression in neurons are essential for animals to form new memories and adapt to an ever-changing environment. In particular, *de novo* protein synthesis of synaptic proteins is required for long-term changes in synaptic strength (Kandel, 2001; Kandel, 2012; Hernandez et al., 2002; Jedynak et al., 2016; Scheyer et al., 2014). Mechanisms that affect gene expression at transcriptional level and their significance have been extensively studied (Yao et al., 2016; Pereira et al., 2010; Omori et al., 2017; Feng et al., 2010; Lv et al., 2013). However, regulation at the transcriptional level sometimes cannot meet the temporal and spatial challenges that a neuron faces. One neuron could have thousands of synapses, and plasticity is often synapse specific. Moreover, the distance between synapses and the nucleus makes transcriptional control of *de novo* protein synthesis less suitable for mechanisms that require fast temporal control.

It is known that *de novo* protein synthesis can also be regulated at the post-transcription level. Some mRNA transcripts are selectively localized to dendrites, suggesting mechanisms that control their distribution and translation. The key regulators include those that control the temporal and spatial regulation of RNA transport, localization, translation, and degradation (Martin and Zukin, 2006; Holt and Schuman, 2013; Glock et al., 2017).

With the development of advanced sequencing techniques, identification of the reversible m^6A mRNA methylation has unveiled a new layer of post-transcriptional mRNA regulation. The functional significance of m^6A RNA methylation is exerted by three groups of proteins: “writers” (methyltransferases) that install, “erasers” (demethylases) that remove, and “readers” that recognize m^6A and determine the cellular fate of the modified RNA (Fu et al., 2014; Zhu et al., 2015; Liu et al., 2013; Wang et al., 2014; Wang et al., 2015; Theler et al., 2014). m^6A “readers" are special RNA binding proteins (RBPs) that recognize m^6A. YTHDF1, one of the YT521-B

homology (YTH) domain-containing proteins, has been demonstrated to interact with initiation factors and facilitate translation initiation (Wang et al., 2015). Using YTHDF1 constitutive knockout mice, our earlier work has demonstrated that YTHDF1 plays an important role in promoting protein synthesis in neurons, in synaptic plasticity and learning.

However, m^6A deficiency affects many proteins and cellular functions, the exact mechanisms by which these effects manifested in adult brain function remain elusive. An important question is whether the functional consequences of m^6A are mediated by a specific reader protein in the adult brain, or, as the recent model suggests, YTHDF1, 2 and 3 act in concert to regulate mRNA degradation in the brain in response to neuronal events. It is also not clear if the impaired learning we observed in the YTHDF1 constitutive knockout mice has cell-type specificity.

The depletion of m^6A by *Mettl14* gene deletion affects many downstream transcripts and proteins. Here we report that *Ythdf1* gene deletion resembles impairment caused by *Mettl14* gene deletion in a cell type specific manner. At the molecular level, boosting DA release by cocaine drastically increased YTHDF1 binding to its targets in the striatum. Importantly, in *Ythdf1* knockout, striatal neurons have a much higher baseline *de novo* protein synthesis rate. While striatal neurons in control mice respond to elevated cAMP by increasing *de novo* protein synthesis rate, striatal neurons in *Ythdf1* knockout mice don't.

3.3 Results

3.3.1 D1 and D2 SPN Ythdf1 gene deletion produced behavioral phenotypes that resembled those of Mettl14 gene deletion in all three behavioral paradigms

Our previous data in conditional *Mettl14* knockout mice suggest that lack of m^6A blunted responses to environmental challenges at both the cellular and behavioral levels (Chapter 2). What is the downstream m^6A reader protein responsible for such profound effects? We generated mice with conditional deletion of *Ythdf1* in either D1 (D1-Cre; $Ythdf1^{f/f}$) or D2 (A2A-Cre;$Ythdf1^{f/f}$) SPNs. Both types of mutant mice and their littermate controls were subjected to all three behavioral paradigms described above.

In locomotor sensitization by cocaine, D1-Cre;$Ythdf1^{f/f}$ mice showed reduced acute response and sensitization (genotype main effect , p=0.0015, genotype x time interaction, p=0.0153) (Figure 3.1A). In contrast, A2A-Cre;$Ythdf1^{f/f}$ mice showed increased acute response and sensitization (genotype main effect, p=0.0175, genotype x time interaction, p=0.0065) (Figure 3.1B).

In rotarod motor skill learning, D1-Cre;$Ythdf1^{f/f}$ mice showed impaired learning (genotype main effect, p= 0.0005， genotype x time interaction, p=0.5413) (Figure 3.1C). In contrast, A2A-Cre;$Ythdf1^{f/f}$ mice were not impaired (genotype main effect, p=0.5989, genotype x time interaction, p=0.0799) (Figure 3.1D).

In haloperidol induced catalepsy and sensitization, A2A-Cre;$Ythdf1^{f/f}$ mice showed diminished acute response and sensitization (Figure 3.1E).

Overall, in all three paradigms, the behavioral phenotypes of *Ythdf1* conditional knockout mice closely resemble those of *Mettl14* conditional knockout mice with cell type specificity (Figure 1.3 A,B; Figure 2.1 C,D; Figure 2.3 C). These data suggest that YTHDF1 is potentially the main downstream reader protein that mediates m^6A's neuronal functions in the adult brain.

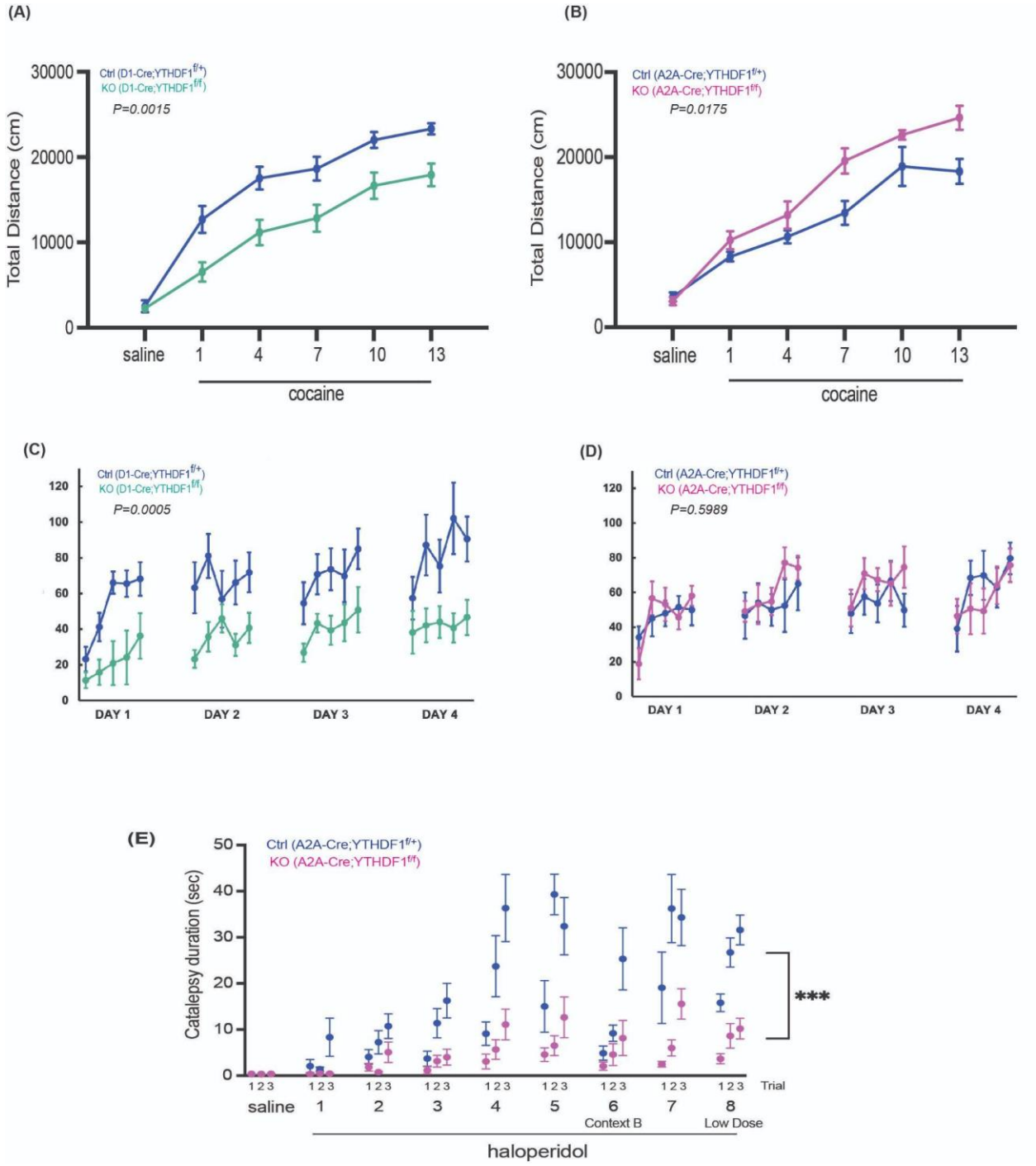

Figure 3.1. D1 and D2 SPN *Ythdf1* gene deletion produced phenotypes that resembled those of *Mettl14* gene deletion in all three behavioral paradigms.

cont. Figure 3.1. D1 and D2 SPN *Ythdf1* gene deletion produced phenotypes that resembled those of *Mettl14* gene deletion in all three behavioral paradigms. (A) Cocaine-induced locomotor sensitization in D1-Cre;Ythdf1$^{f/+}$ (Ctrl, blue) and D1-Cre;Ythdf1$^{f/f}$ (KO, cyan). Locomotor activity is recorded for 60 min after saline/cocaine injection. Total distance traveled is recorded (cm), n=8. (B) Cocaine-induced locomotor sensitization in A2A-Cre;Ythdf1$^{f/+}$ (Ctrl, blue) and A2A-Cre;Ythdf1$^{f/f}$ (KO, magenta). Locomotor activity is recorded for 60 min after saline/cocaine injection. Total distance traveled is recorded (cm), n=8. (C) The rotarod motor learning in D1-Cre;Ythdf1$^{f/+}$ (Ctrl, blue) and D1-Cre;Ythdf1$^{f/f}$ (KO, cyan). Performance is recorded as latency to fall (s), n=5. (D) The rotarod motor learning in A2A-Cre;Ythdf1$^{f/+}$ (Ctrl, blue) and A2A-Cre;Ythdf1$^{f/f}$ (KO, magenta). Performance is recorded as latency to fall (s), N=5. (E) The sensitization of haloperidol-induced catalepsy response of A2A-Cre;Ythdf114$^{f/+}$ (Ctrl, blue) and A2A-Cre;Ythdf1$^{f/f}$ (KO, magenta). Catalepsy duration is recorded (s). *** P=0.0003, 2-way ANOVA, n=7. All data expressed as mean ± SEM.

3.3.2 Cocaine treatment quickly increased RNA transcripts targeted by YTHDF1

m^6A "readers" are special RNA binding proteins that recognize m^6A and impact the fate of the modified mRNA. YTHDF1 has been demonstrated to interact with initiation factors and facilitate translation initiation. What are the targets of YTHDF1? Does YTHDF1 bind to different targets in response to neuronal activities?

We performed Crosslinking and immunoprecipitation (CLIP-seq) to study the RNA targets of YTHDF1 after saline or cocaine treatment of wild-type mice (Figure 3.2A). We found that cocaine treatment caused a significant increase in YTHDF1 RNA target numbers while most original targets were retained (Figure 3.2B). It is possible that the increased number of RNA targets was due to the increased total m^6A level after cocaine treatment, however, mass spectrometry analysis only showed small changes in the total m^6A level (Figure 3.2D). Using gene ontology enrichment analysis, we found that most of the upregulated RNA transcripts encode structural proteins, especially those associated with cilium and microtubule (Figure 3.2C), suggesting that cocaine may be able to quickly cause changes in YTHDF1 protein (e.g., post-translational modification) and its RNA targets, potentially cause rapid synthesis of many structural proteins in neurons and synapses.

To understand how YTHDF1 is able to respond to cocaine treatment rapidly, we directly profiled YTHDF1 post-translational modifications (PTMs) but did not observe any significant changes in a few of the known sites (Figure 3.2E). Since FMRP phosphorylation is known to be a critical regulator of YTHDF1 and together they affect *de novo* protein synthesis (Zou et al., 2022), we thus examined FMRP phosphorylation and found elevated FMRP phosphorylation in striatal

tissues after cocaine treatment, suggesting reduced FMRP activity may contribute to increased *de novo* protein synthesis (Figure 3.2F).

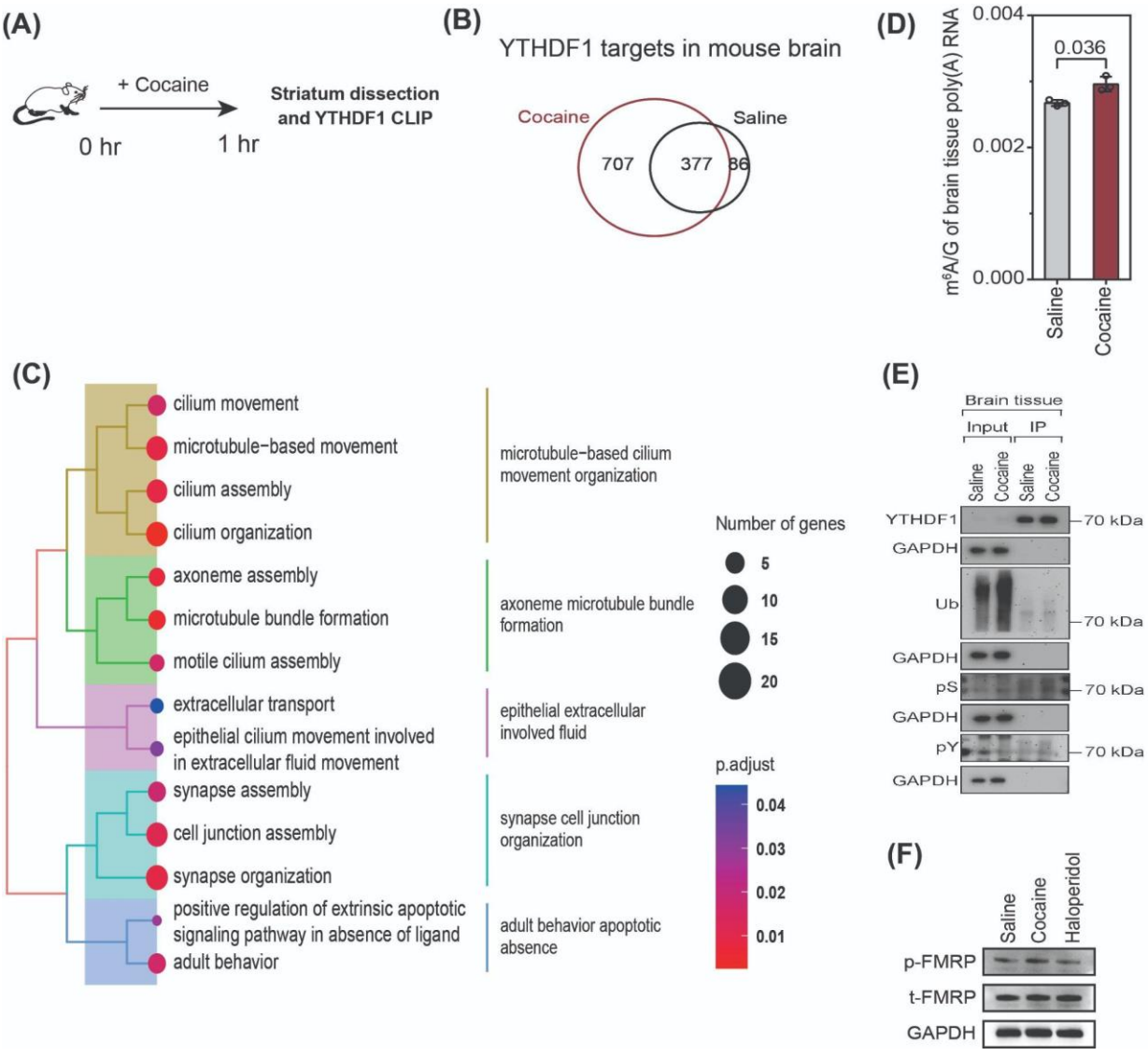

Figure 3.2. Cocaine treatment drastically increased YTHDF1's binding to its RNA targets. Schematic diagram of the YTHDF1 CLIP-seq experiment. (B) Venn diagram depicts the number of YTHDF1 targets after saline and cocaine treatment. (C) Gene ontology (GO) analysis of the upregulated YTHDF1 transcripts after cocaine treatment. (D) UHPLC-MS/MS analysis of m^6A level in the striatum after saline and cocaine treatment. (E) YTHDF1 post-translational PTMs assay using the striatum brain tissue after saline and cocaine treatment.

3.3.3 Striatal neurons from Ythdf1 knockout mice had high baseline de novo protein synthesis rate but did not respond to elevated cAMP

We next examined whether YTHDF1 regulates *de novo* protein synthesis in response to stimulation. We measured the protein synthesis rate using click chemistry in striatal primary neuron cultures from wild type (control) and *Ythdf1* constitutive knockout mice. The methionine analog HPG was incorporated into the newly synthesized polypeptide chain during translation and could be visualized to assess protein synthesis rate in neurons upon stimulation. In wild type striatal neurons, the D1 selective full agonist SKF-81297 significantly increased the HPG incorporation into newly synthesized proteins (Figure 3.3). Striatal neurons from *Ythdf1* constitutive knockout mice had a significantly higher baseline translation rate compared to wild type neurons, but SKF-81297 did not induce changes in protein synthesis rate (Figure 3.3).

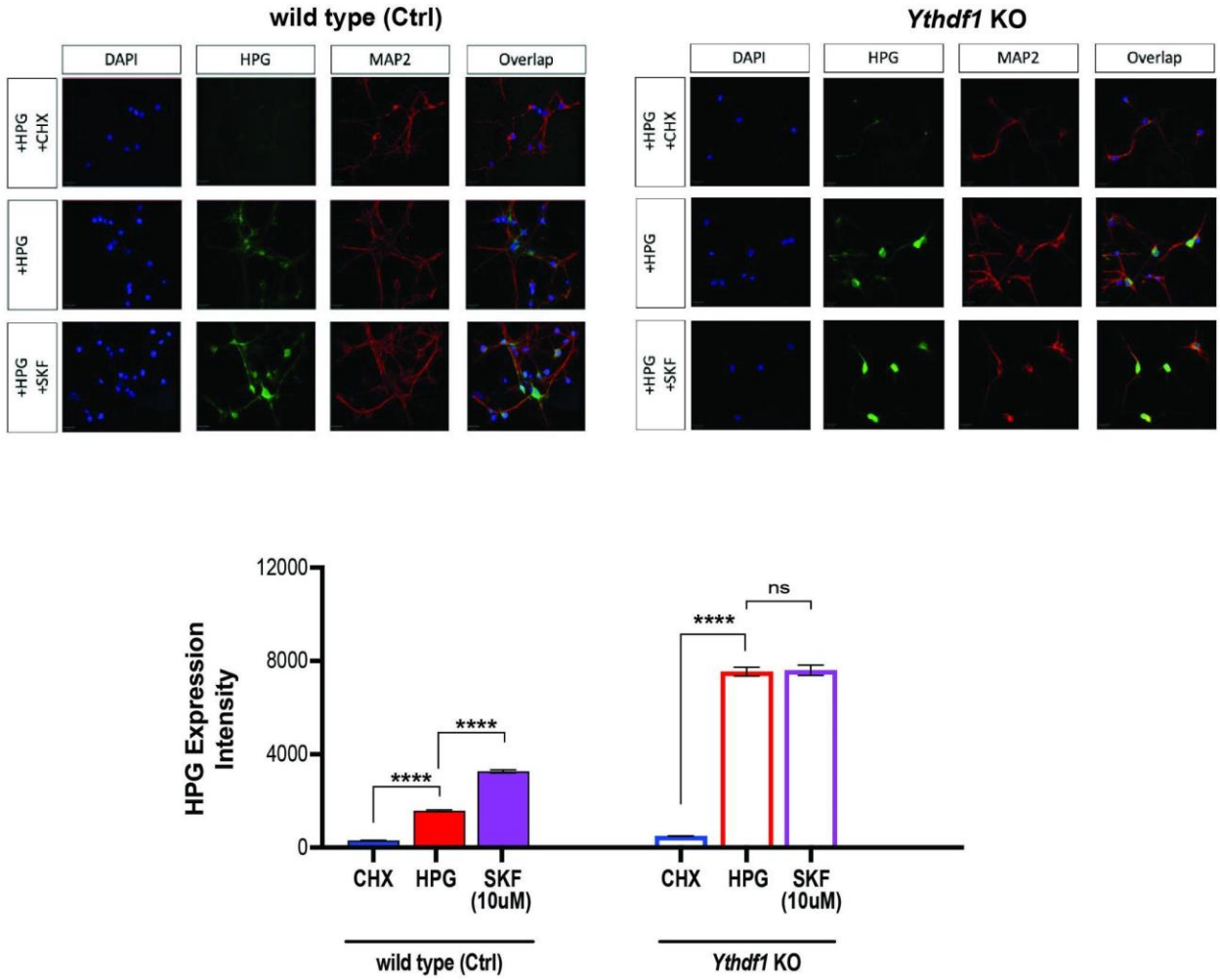

Figure 3.3. Striatal neurons from *Ythdf1* knockout mice had high baseline *de novo* protein synthesis rate but didn't respond to elevated cAMP. Upper left: *De novo* protein synthesis rate assay in the striatal neurons from wild type P1 mice. Three experimental conditions were compared: HPG+CHX group as negative control, HPG group as baseline condition and HPG+SKF group to test the response after cAMP elevation. Immunostaining was performed and stained for DAPI, HPG and MAP2 signals. Upper right: *De novo* protein synthesis rate assay in the striatal neurons from *Ythdf1* KO P1 mice. Three experimental conditions were compared: HPG+CHX group as negative control, HPG group as baseline condition and HPG+SKF group to test the response after cAMP elevation. Immunostaining was performed and stained for DAPI, HPG and MAP2 signals. Lower: Bar graph of the HPG expression intensity in CHX, HPG and SKF group in wild type (Ctrl) and *Ythdf1* KO striatal neurons. Wild type (Ctrl): CHX vs. HPG, **** P<0.0001, paired T-test, HPG vs. SKF (10uM), **** P<0.0001, paired T-test. *Ythdf1* KO: CHX vs. HPG, **** P<0.0001, paired T-test, HPG vs. SKF (10uM), ns P=0.8390, paired T-test.

3.4 Discussion

m^6A readers are special RNA binding proteins that recognize m^6A and impact the fate of the modified mRNA. The almost identical behavioral phenotypes in *Mettl14* and *Ythdf1* knockout mice in all three behavioral paradigms in a cell type specific manner suggest that impaired learning due to m^6A deficiency is mainly mediated by YTHDF1. While YTHDF1, YTHDF2 and YTHDF3 redundancy has been suggested in the literature (Zaccara and Jaffrey, 2020), in the mouse adult striatum, such redundancy is not significant based on our data.

At the molecular level, boosting DA release by cocaine drastically increased YTHDF1 binding to many mRNA targets in the striatum, especially those encode structural proteins, suggesting long-term neuronal and/or synaptic structural changes is likely facilitated by YTHDF1 upon environmental challenges.

In *Ythdf1* knockout, striatal neurons have a much higher baseline *de novo* protein synthesis rate. Correspondingly, our previous work on m^6A mRNA sequencing in *Mettl14*-deleted striatum also showed increased expression of genes linked to metabolism, ribosomal machinery, and translation, which are not exclusive to neuronal functions. These data suggest that a possible cellular response under m^6A deficiency is the compensation by enhancing baseline protein synthesis in order to preserve the essential functions necessary for the cell at the cost of blunted elevation of protein synthesis rate in response to challenges. While striatal neurons in the control mice responded to elevated cAMP by increasing the *de novo* protein synthesis rate, striatal neurons in *Ythdf1* knockout mice didn't. These data underscore the essential role of YTHDF1 in environmental adaptation, which is further corroborated by our published intracellular recording data from D1-neuron specific *Mettl14* knockout striatal slices. Those cells had a higher baseline

firing rate than control cells under *in vitro* conditions that had little cortical or thalamic inputs, yet the firing frequency of the mutant cells did not adapt to increased current injections like control cells did.

We speculate that YTHDF1 PTMs rather than increased m^6A-modified transcripts are the potential mechanism that involved in such a quick increase in YTHDF1 targets upon cocaine challenge. However, it is important to point out that although we didn't observe a significant increase in total m^6A level by mass spectrometry, there is a possibility that the distribution m^6A changes across transcripts could be uneven after cocaine treatment, as m^6A modifications could be upregulated in some genes but downregulated in others. Therefore, we cannot completely rule out the possibility that YTHDF1's increased mRNA target number after cocaine treatment is due to the increased m^6A level on a subset of transcripts. However, the modifications like PTMs that happened directly on proteins still provide faster temporal resolution for immediate responses to environmental stimuli, compared to changes on mRNA modifications. We hypothesize that the significant function of YTHDF1 is to quickly change its PTMs and therefore conformation upon changes in synaptic inputs, and that, in turn, changes YTHDF1's mRNA targets, facilitates *de novo* protein synthesis encoded by these targets, and eventually causes neuronal and/or synaptic structural changes.

Here, by analyzing the few known PTM sites of YTHDF1, we did not detect any significant changes after cocaine treatment, but this does not rule out other PTMs that we don't have the tool to test yet. Alternatively, changes in one of YTHDF1's binding partners (e.g., FMRP) may also explain such a quick response (Zou et al., 2022).

The discovery of reversible m^6A mRNA methylation (m^6A-tagging) has revealed an important layer of post-transcriptional gene regulation. Our data suggest that it plays a critical role for cells and the organism to adapt to environmental challenges. Because this level of post-transcriptional regulation can respond quickly (without going through gene transcription) and locally (e.g., in the synapse), it provides much better temporal and spatial resolution in cells' responses to challenges. Because one m^6A reader protein (e.g., YTHDF1) can quickly affect hundreds of transcripts and facilitate their translation into newly synthesized proteins, with many as structural proteins, it's also a type of regulation that can have broad and long-lasting impacts on the relevant cells.

3.5 Methods

3.5.1 Conditional Ythdf1 deletion

Mice carrying a conditional removable *Ythdf1* allele ($Ythdf1^{f/f}$) were crossed to a D1 receptor promoter-driven Cre recombinase (D1-Cre) transgenic line (B6.FVB(Cg)-Tg(Drd1-cre)EY262Gsat/Mmucd, RRID: MMRRC-030989-UCD) or an adenosine 2A receptor promoter-driven Cre recombinase (A2A-Cre) transgenics line (B6.FVB(Cg)-Tg(Adora2a-cre)KG139Gsat/Mmucd, RRID: MMRRC_036158-UCD) to selectively delete *Ythdf1* in D1 or D2 MSNs. All experiments were performed in both double transgenic mice (D1-Cre;$Ythdf1^{f/f}$, A2A-Cre;$Ythdf1^{f/f}$), and the respective control littermates (D1-Cre;$Ythdf1^{f/+}$, A2A-Cre;$Ythdf1^{f/+}$).

3.5.2 Crosslinking and Immunoprecipitation (CLIP)

Harvested mouse brain tissues were UV crosslinked at 254 nm with a stratalinker (Stratagene) for two times to achieve a 4,500 J/m2 UV flux and flash-frozen in liquid nitrogen. Pellets were thawed on ice and resuspended in 3 volume of ice-cold CLIP lysis buffer (50 mM HEPES pH 7.5, 150

mM KCl, 2 mM EDTA, 0.5% (v/v) NP-40, 0.5 mM DTT, 1 × Halt™ Protease and Phosphatase Inhibitor Cocktail (Thermo Scientific, 78442), 1 × RNaseOUT Recombinant Ribonuclease Inhibitor (Invitrogen, 10777019)). Pellets were lysed by rotating at 4 °C for 15 minutes after passing through a 26 G needle (BD Biosciences). Embryo suspensions were sonicated on a bioruptor (Diagenode) with 30 s on/30 s off for 5 cycles. Lysates were cleared by centrifugation at 21,000 g for 15 minutes at 4 °C on a benchtop centrifuge. Supernatants were applied to Flag antibody (Abcam, ab205606) conjugated protein A beads (Invitrogen, 1001D) and left overnight at 4 °C on an end-to-end rotor. Beads were washed extensively with 1 ml wash buffer (50 mM HEPES pH 7.5, 300 mM KCl, 0.05% (v/v) NP-40, 1 × Halt™ Protease and Phosphatase Inhibitor Cocktail, 1 × RNaseOUT Recombinant Ribonuclease Inhibitor) at 4 °C for 5 times. Protein-RNA complex conjugated to the beads were treated by 8 U/μL RNase T1 (Thermo Scientific, EN0541) at 22 °C for 10 minutes with shaking. Input samples are digested in parallel. Then input and IP samples were separated on an SDS-PAGE gel and gel slices at corresponding size ranges were treated by proteinase K (Invitrogen, 25530049) elution. RNA was recovered with TRIZol reagent (Invitrogen, 15596026). Then T4 PNK (Thermo Scientific, EK0031) end repair was performed with purified RNA before library construction with NEBNext® Small RNA Library Prep Set for Illumina® (NEB, E7330S). Libraries were pooled and sequenced on a NovaSeq 6000 sequencer.

3.5.3 Western blot

Proteins were extracted from respective samples using lysis in RIPA buffer (Thermo Scientific, 89900) containing 1 × Halt™ Protease and Phosphatase Inhibitor Cocktail (Thermo Scientific 78441). The concentration was measured by NanoDrop 8000 Spectrophotometer (Thermo Scientific). Equal amount of total protein lysate was heated at 90 °C in loading buffer (Bio-Rad,

1610747) for 10 minutes. Denatured protein was then loaded into 4-12% NuPAGE Bis-Tris gels (Invitrogen, NP0335BOX) and transferred to PVDF membranes (Thermo Scientific, 88585). Blocking was done using Tris-Buffered Saline, 0.1% Tween® 20 (TBST) with 3% BSA (MilliporeSigma, A7030) for 30 minutes at room temperature, then incubation in diluted primary antibody solution at 4 °C overnight, followed by secondary antibody conjugated to HRP for 1 hour at room temperature. Protein bands were examined using SuperSignal West Dura Extended Duration Substrate kit (ThermoFisher, 34075) with a FluroChem R (Proteinsimple). Blot intensities were quantified with Fiji (ImageJ) Analyze-Gel module.

3.5.4 Quantitative analysis of m^6A levels via UHPLC-MS/MS

75 ng poly(A)+ RNA was digested by nuclease P1 (MilliporeSigma, N8630) in 20 μL buffer containing 20 mM ammonium acetate (NH4OAc) at pH 5.3 for 2 hours at 42 °C. Then, 1 unit of FastAP Thermosensitive Alkaline Phosphatase (Thermo Scientific, EF0651) was added to the reaction and FastAP buffer was added to a 1× final concentration before incubation for 2 hours at 37 °C. The samples were diluted and filtered (0.22 μm, Millipore) and injected into a C18 reverse-phase column coupled online to Agilent 6460 LC-MS/MS spectrometer in positive electrospray ionization mode. The nucleosides were quantified using retention time and the nucleoside to base ion mass transitions (268 to 136 for A; 284 to 152 for G; and 282 to 136 for m^6A). Quantification was performed by comparing with the standard curve obtained from pure nucleoside standards running with the same batch of samples.

3.5.5 Mouse Striatal primary neuron culture

8 chambered coverglass systems (Cellvis C8-1.5H-N) were first prepared by coating them with 0.1 mg/mL poly-D-lysine (Sigma-Aldrich, P6407) solution, followed by incubation at 37°C

overnight. After two washes with 1x Dulbecco's Phosphate-Buffered Saline (DPBS, Fisher Scientific, Catalog NO. 14-190-250), the plates were left to air dry for over 1 hour in a sterile hood. Dissection was conducted under a stereoscope, using cold 1x PBS (Fisher Scientific, Catalog NO. 70011069) for tissue handling. The dissection procedure involved the meticulous removal of the pia membrane after skull exposure, followed by the dissection of the dorsal cortex to expose the striatum structure. The entire striatum was then extracted from both sides and transferred to cold 1x DPBS on ice. Tissue processing included pelleting the collected striatum tissues via centrifugation (160 RCF for 4 minutes at 25°C, consistent conditions throughout), followed by the addition of prewarmed Papain solution (containing DNase, Worthington Biochemical, LK003150) at a ratio of 1 ml per every 3 brains for enzymatic digestion. The striatum tissue was gently chopped with the tip of a 1-ml pipette, followed by incubation in a 37°C incubator for 40 minutes with gentle shaking to resuspend every 10 minutes. Afterward, the tissue was pipetted up and down 20 times in the papain solution. Subsequently, the digested tissue was centrifuged to remove the supernatant. For cell plating, cells were resuspended in plating media and plated at a density of 0.04 million cells per well. After two hours, the media was switched to Neuromaintaining media. Medium maintenance included the replacement of half of the medium four days post-plating and the addition of AraC (Cytosine arabinoside, Sigma-Aldrich, C1768) to reach a final concentration of 2 nM to suppress gliogenesis. Following this, half of the medium was regularly replaced with fresh media every three days to support cell growth and maintenance. The plating media consisted of DMEM medium (Thermo Scientific, Catalog NO. 10313039) containing 1% L-Glutamine, 1% penicillin–streptomycin, 0.8% Glucose, and 10% fetal bovine serum (Thermo Fisher Scientific, catalog number: 26140079), while the Neuromaintaining media was prepared using Neurobasal

medium with 1x B-27 supplement (Thermo Scientific, A3582801), 1x N2 supplement (Fisher Scientific, Catalog NO. 17502048), 1% L-Glutamine, and 1% penicillin–streptomycin.

CHAPTER 4

THE ROLE OF M^{6}A MRNA METHYLATION IN DOPAMINERGIC NEURONS

4.1 Abstract

In this chapter, the role of *Mettl14* and *Ythdf1* in dopaminergic neurons were examined. I found that either *Mettl14* or *Ythdf1* gene deletion in dopaminergic neurons enhanced cocaine induced locomotor hyperactivity. This behavioral phenotype is similar to published studies in which *Fto* gene deletion enhanced cocaine induced locomotor hyperactivity, suggesting that the m^{6}A mRNA methylation pathway in dopaminergic neurons loses the ability to adapt to cocaine challenges when either the methyltransferase or the demethylase is missing. It has been reported that m^{6}A level is decreased in Parkinson's disease (PD) cellular models, and that m^{6}A methylation inhibitor resulted in oxidative stress and cell apoptosis. In my study, I found that *Mettl14* gene deletion did not cause dopaminergic neuron degeneration in either young or old mice.

4.2 Introduction

By selectively impairing the m^{6}A mRNA methylation pathway in D1-SPNs and D2-SPNs in the striatum, the earlier chapters revealed the cooperating and opposing activities of D1-SPNs and D2-SPNs. Using a similar approach, this chapter will focus on a third cell type: dopaminergic neurons, which mainly target D1-SPNs and D2-SPNs. DA projection neurons are mostly localized in the substantia nigra pars compacta (SNc) and ventral tegmental area (VTA) of the ventral midbrain (Björklund and Dunnett, 2007). DA has long been known as an essential neurotransmitter in modulating SPN function in both the dorsal and ventral striata that underlie voluntary movement,

sensorimotor learning, motivation, and reinforcement learning (Wise, 2004; Berke and Hyman, 2000).

DA release and clearance are largely controlled by the dopamine transporter (DAT), which reuptakes and recycles DA from the synaptic cleft into dopaminergic neurons (Graefe and Bonish, 1988). At the cellular level, activation of DA receptors on SPNs modulates gating of ion channels and, therefore, acutely alters the intrinsic excitability of these neurons. Activation of D1 receptors increases the excitability of SPNs in the direct pathway, whereas activation of D2 receptors decreases the excitability of SPNs in the indirect pathway (Gerfen et al., 1990). Both mechanisms increase motor output when DA release is increased (Cui et al., 2013). Conversely, a reduction in DA favors the inhibitory indirect pathway, which reduces motor output (Gerfen et al., 1990; Calabresi et al., 2014; Shen et al., 2008). DA can, therefore, differentially modulate the excitability of SPNs in both the direct and indirect pathways, with a net effect of facilitating movement (Tecuapetla et al., 2014; Panigrahi et al., 2015). Moreover, DA also modulates glutamate release by corticostriatal terminals via D2 receptors localized on the terminal (Tecuapetla et al., 2010; Tritsch et al., 2012).

In addition to modulating the intrinsic excitability of SPNs acutely, DA also influences corticostriatal plasticity and, thereby, produces cumulative and long-lasting changes in corticostriatal throughput (Wang et al., 2006; Calabresi et al., 2007). The temporal relationship between dopaminergic and glutamatergic input to SPNs of the striatum and DA-dependent plasticity at corticostriatal synapses have provided the basis for models of reinforcement learning (Adcock et al., 2006; Pennartz et al., 2009; Witten et al., 2011; Steinberg et al., 2014; Wang et al., 2015). Corticostriatal plasticity can enhance or diminish the responsiveness of direct and indirect

pathways to cortical input (Wang et al., 2006; Costa et al., 2006). Therefore, the central role of DA in modulating the excitability of SPNs and in corticostriatal plasticity suggests that DA is important for both striatum-dependent learning and performance.

DA neuron-specific *Fto* knockout mice have been reported to develop impaired D2 autoreceptor-mediated autoinhibition resulting in attenuated quinpirole-mediated reduction of locomotion and an enhanced sensitivity to the locomotor- and reward-stimulatory actions of cocaine (Hess et al., 2013). Another study reported that m^6A level is decreased in PD cellular models. Overexpression of the m^6A demethylase and m^6A methylation inhibitor both resulted in downregulation of m^6A, elevated Ca^{2+} influx, and oxidative stress, which ultimately induced cell apoptosis (Chen et al., 2019).

Given that DA not only acutely modulates the intrinsic excitability of SPNs but also affects corticostriatal plasticity that can enhance or reduce the reactivity of the direct and indirect pathway in response to cortical inputs. The focus of this chapter is to investigate the behavioral phenotypes caused by m^6A deficiency in the dopaminergic neurons. Moreover, we also assessed the potential impact of m^6A on dopaminergic neuron survival across different stages, as recent studies found downregulation of m^6A in PD models lead to cell death. Here we report that *Ythdf1* gene deletion in the dopaminergic neurons resembles the behavioral phenotypes caused by *Mettl14* gene deletion, consistent with my findings in D1-SPNs and D2-SPNs. Both genetic manipulations increased cocaine induced locomotor response. To examine whether *Mettl14* deletion induces cell death in DA neurons, I performed immunohistochemistry, stained and counted tyrosine hydroxylase (TH)-positive cells in the ventral midbrain of mice with *Mettl14* deletion and controls. I did not observe DA neuron loss in any age groups.

4.3 Results and discussion

4.3.1 Dopaminergic neurons with Ythdf1 gene deletion produced behavioral phenotypes that resembled those with Mettl14 gene deletion

In order to examine the *in vivo* functional role of m^{6}A mRNA methylation in DA neurons, mice with floxed *Mettl14* allele (Mettl14$^{f/f}$) or *Ythdf1* allele (Ythdf1$^{f/f}$) were crossed to a DAT promoter-driven Cre recombinase transgenic line. We examined cocaine's locomotor sensitization effect in open field boxes in mutants and their respective control littermates. DAT-Cre;Mettl14$^{f/f}$ mice showed increased acute response and sensitization (genotype main effect , p=0.0132, genotype x time interaction, p=0.0209) (Figure 4.1A). DAT-Cre;Ythdf1$^{f/f}$ mice also showed increased acute response and sensitization (genotype main effect, p=0.0118, genotype x time interaction, p=0.0294) (Figure 4.1B).

Therefore, *Ythdf1* gene deletion mimics *Mettl14* gene deletion in all three cell types: DA neurons, D1-SPNs and D2-SPNs in the striatum, suggesting that the functional impact of m^{6}A mRNA methylation in the adult brain is mostly mediated by the m^{6}A reader protein YTHDF1.

It is surprising that both *Mettl14* gene deletion and *Fto* gene deletion in DA neurons enhanced cocaine induced locomotor hyperactivity (Hess et al., 2013), even though METTL14 increases while FTO decreases m^{6}A levels in the affected cells. One possible interpretation is that cocaine induced locomotor hyperactivity is mostly mediated by the striatum, whereas DA neurons develop tolerance to cocaine (Siciliano et al., 2015). The fact that *Mettl14 or Ythdf1* gene deletion in D1-SPNs impaired cocaine induced locomotor hyperactivity supports the idea that cocaine induced locomotor hyperactivity is mostly mediated by the striatum. D1-SPNs are known to promote motor outputs. In contrast, *Mettl14 or Ythdf1* gene deletion in D2-SPNs enhanced cocaine

induced locomotor hyperactivity. This observation also supports the idea that cocaine induced locomotor hyperactivity is mostly mediated by the striatum since D2-SPNs are known to inhibit motor outputs. It is possible that either lack of METTL14 or FTO impairs DA neuron's ability to adapt to the challenge and develop cocaine tolerance, therefore leads to enhanced cocaine induced locomotor hyperactivity.

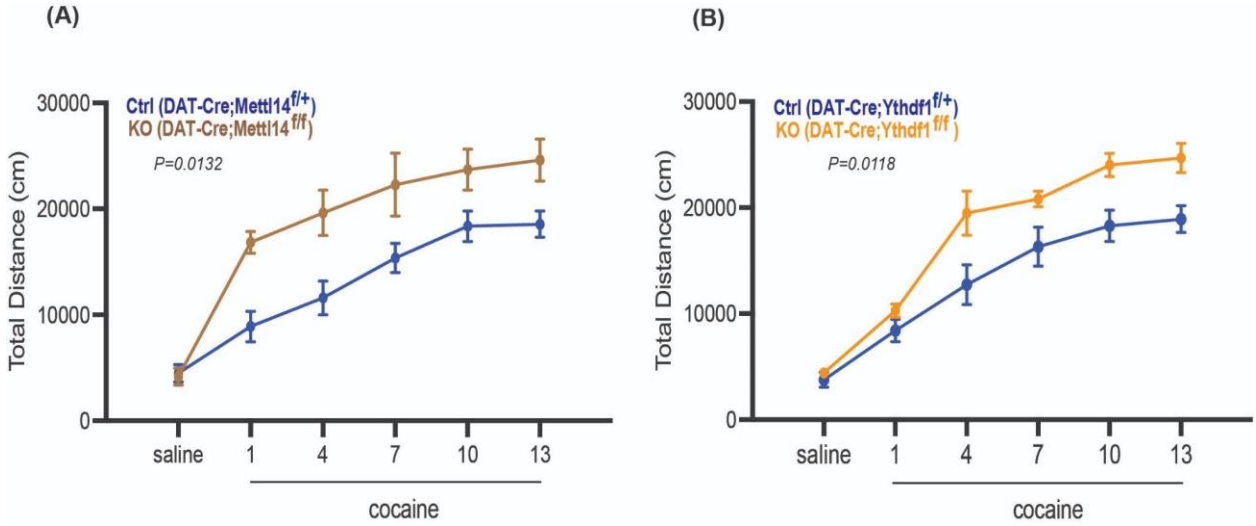

Figure 4.1. Dopaminergic neurons with *Ythdf1* gene deletion produced phenotypes that resembled those with *Mettl14* gene deletion in cocaine-induced locomotor sensitization. Locomotor activity is recorded for 60 min after saline/cocaine injection. Total distance traveled in the open field box is recorded (cm). A: Cocaine-induced locomotor sensitization in DAT-Cre;Mettl14$^{f/+}$ (Ctrl, blue) and DAT-Cre;Mettl14$^{f/f}$ (KO, brown), n=6, genotype main effect, p = 0.0132; genotype x time, p = 0.0209, 2-way ANOVA. B: Cocaine-induced locomotor sensitization in DAT-Cre;Ythdf1$^{f/+}$ (Ctrl, blue) and DAT-Cre;Ythdf1$^{f/f}$ (KO, orange), n=5, genotype main effect, p = 0.0118; genotype x time, p = 0.0294, 2-way ANOVA. All data expressed as mean ± SEM.

4.3.2 Mettl14 gene deletion didn't cause significant difference in tyrosine hydroxylase (TH)-positive neuron number across different ages

To examine whether *Mettl14* deletion induces cell death in DA neurons. Mice from different age groups (postnatal day 1, 3 weeks, 6 weeks, 9 weeks, 13 weeks as well as 18 weeks old) were used. Both DAT-Cre; Mettl14$^{f/f}$ conditional knockout mice and their control littermates were perfused with 4% paraformaldehyde (PFA), and then fixed brains were serial sectioned to 10-micron coronal slices. After immunostaining with TH antibody and DAPI, the TH positive cells in the SNc and VTA regions were counted separately (Figure 4.2 A, B). There was no significant difference in DA cell number between DAT-Cre; Mettl14$^{f/f}$ conditional knockout mice and their control littermates in any age groups (Figure 4.2 C).

It has been reported that m^{6}A level is decreased in PD cellular models. Overexpression of the m^{6}A demethylase and m^{6}A methylation inhibitor both resulted in downregulation of m^{6}A, elevated Ca^{2+} influx, and oxidative stress, which ultimately induced cell apoptosis (Chen et al., 2019). However, in my *in vivo* model, I did not observe DA neuron degeneration even in old mice. There are many differences between cell culture and animal models. In cell culture models, the cells are never truly DA neurons. In addition, there are many protective mechanisms in whole animals such as glial cells.

In the striatum, loss of METTL14 in either D1 or D2 SPNs can eventually lead to lethal phenotype and shrinkage of the striatum. Why DA neurons are different in vulnerability to m^{6}A deficiency is worth further investigation. DA neuron degeneration is found in PD whereas striatum degeneration is found in Huntington's disease (HD). It's an unsolved problem that different cell types show differential vulnerability in different diseases even though the mutated genes in causing

the respective disease are usually expressed in all cell types. What adaptive and protective mechanisms are involved in combating cellular stress in each cell type, and whether the m^6A pathway is involved need to be investigated further.

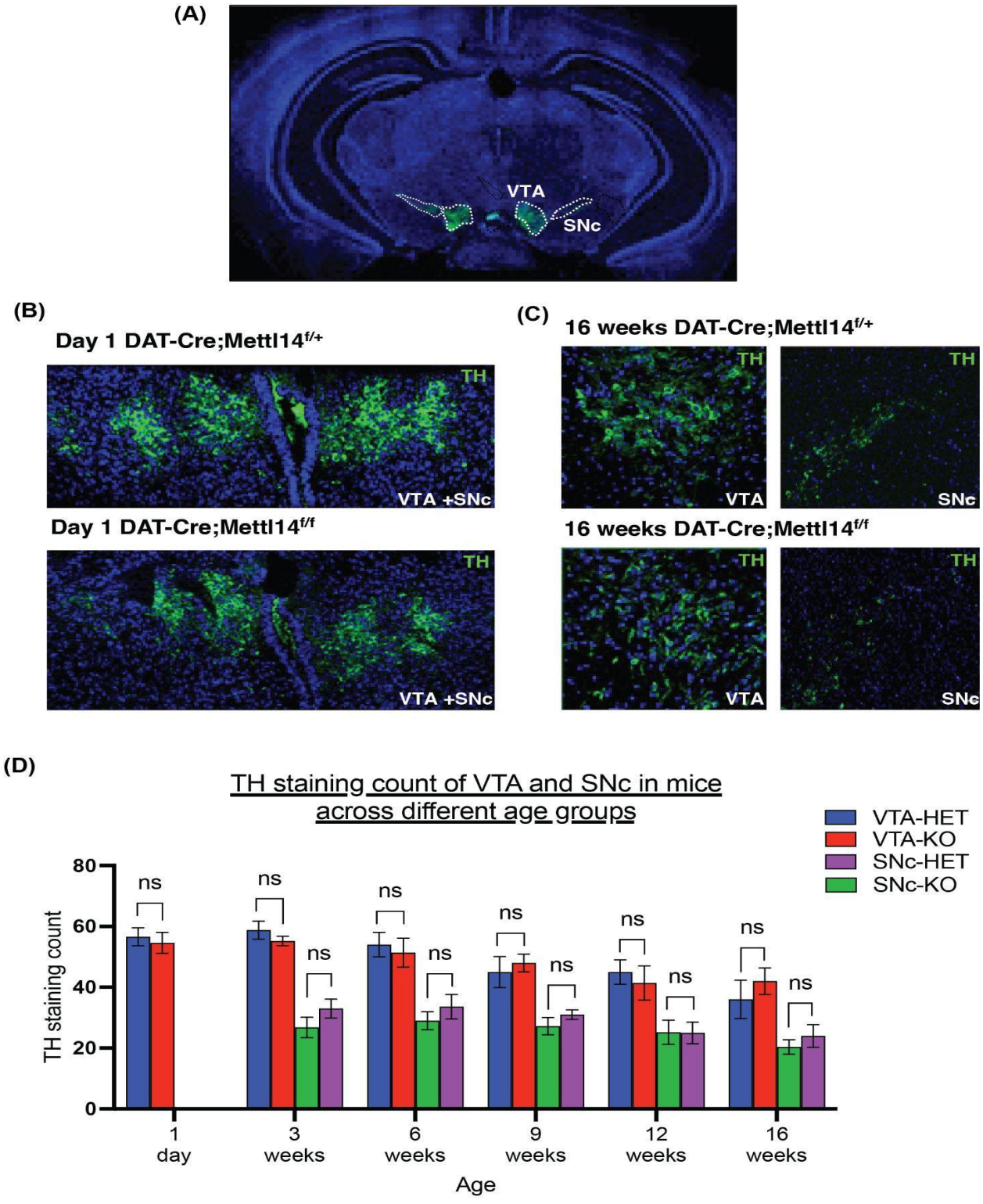

Figure 4.2. TH staining of VTA and SNc in mice with *Mettl14* gene deletion in dopaminergic neurons.

cont. Figure 4.2. TH staining of VTA and SNc in mice with *Mettl14* gene deletion in dopaminergic neurons. (A) Whole brain coronal section with DAPI (blue) and TH (green) staining of VTA and SNc regions marked out. (B) Upper: Coronal section with DAPI (blue) and TH (green) staining of VTA and SNc in postnatal day 1 DAT-Cre; $Mettl14^{f/+}$ mice. Lower: Coronal section with DAPI (blue) and TH (green) staining of VTA and SNc in postnatal day 1 DAT-Cre; $Mettl14^{f/f}$ mice. (C) Upper : Coronal section with DAPI (blue) and TH (green) staining of VTA and SNc in 16 weeks DAT-Cre; $Mettl14^{f/+}$ mice. Lower : Coronal section with DAPI (blue) and TH (green) staining of VTA and SNc in 16 weeks DAT-Cre; $Mettl14^{f/f}$ mice. (D) TH staining count in DAT-Cre; $Mettl14^{f/f}$ conditional knockout mice and DAT-Cre; $Mettl14^{f/+}$ control littermates across different age groups. 1 day: VTA (SNc), HET vs. KO, ns, $p = 0.6728$; 3 weeks: VTA, HET vs. KO, ns, $p = 0.3130$; SNc, HET vs. KO, ns, $p = 0.2135$. 6 weeks: VTA, HET vs. KO, ns, $p = 0.6868$; SNc, HET vs. KO, ns, $p = 0.3832$. 9 weeks: VTA, HET vs KO, ns, $p = 6218$; SNc, HET vs. KO, ns, $p = 0.2755$. 12 weeks: VTA, HET vs. KO, ns, $p = 0.6169$; SNc, HET vs. KO, ns, $p = 0.9708$. 16 weeks, HET vs. KO, ns, $p = 0.4554$; SNc, HET vs. KO, ns, $p = 0.4392$. Paired t-test. HET: DAT-Cre; $Mettl14^{f/+}$; KO: DAT-Cre; $Mettl14^{f/f}$.

4.4 Methods

4.4.1 Conditional Mettl14 deletion

Mice carrying a conditional removable *Mettl14* allele (Mettl14$^{f/f}$) were crossed to a DAT "knock-in" line that has a nuclear-localized Cre recombinase inserted upstream of the first coding ATG of *Dat* (Slc6a3tm1(cre)Xz/J, RRID: IMSR_JAX:020080) to selectively delete *Mettl14* in dopaminergic neurons. All experiments were performed in both double transgenic mice (DAT-Cre;Mettl14$^{f/f}$), and the respective control littermates (DAT-Cre;Mettl14$^{f/+}$).

4.4.2 Conditional Ythdf1 deletion

Mice carrying a conditional removable *Ythdf1* allele (Ythdf1$^{f/f}$) were crossed to a DA transporter (DAT) "knock-in" line that has a nuclear-localized Cre recombinase inserted upstream of the first coding ATG of *Dat* (Slc6a3tm1(cre)Xz/J, RRID: IMSR_JAX:020080) to selectively delete *Ythdf1* in dopaminergic neurons. All experiments were performed in both double transgenic mice (DAT-Cre;Ythdf1$^{f/f}$), and the respective control littermates (DAT-Cre;Ythdf1$^{f/+}$).

4.4.3 Immunohistochemistry

Mice were euthanized with overdose isoflurane prior to perfusion. Fixed whole brains were then transferred to 4% formaldehyde (PFA) overnight then switched into 30% sucrose for 24 - 48 hours, until fully dehydrated. Brain samples were then fast frozen at -80°C for at least overnight.

10 µm coronal serial brain sections were made using a cryostat (Leica Instruments). Sections were incubated in blocking buffer (PBS containing 5% normal donkey serum with 0.3% Triton X-100) for 1 hour at room temperature before overnight incubation in primary antibody mixed in blocking buffer at 4°C. Antibodies used: mouse monoclonal anti-TH (1:500, BD Transduction), secondary antibody donkey anti-mouse Alexa Fluor 488 (Invitrogen A21202). For imaging, a confocal

microscope (Marianas 3i spinning disk confocal) was used and slices visualization was done under 20x or 40x objective.

CHAPTER 5

CONCLUSIONS AND FUTURE DIRECTIONS

Modifications on the mRNA was initially discovery in the 1970s, with m^6A being found to be the most abundant internal modification (Desrosiers et al., 1974, Perry and Kelley, 1974). However, for a long time, their significance was not recognized and there were not much functional studies due to limited analysis or manipulation approaches. In the past decade, however, there is an explosion of functional studies and the significance of mRNA modifications, especially m^6A, has been found in stem cell biology, cancer biology, immunology, and neurobiology among others (Frye et al., 2018; Geula et al., 2015; Batista et al; 2014; Alarcon et al., 2015; Barbieri et al., 2017; Yoon et al., 2017; Koranda et al., 2018; Shi et al., 2018). This is largely due to 1) the development of advanced profiling techniques such as immunoprecipitation sequencing, which enables global mapping of mRNA modifications (Meyer et al., 2012; Dominissini et al., 2012).; and 2) the discovery of specific enzymes that install these modifications ("writers") and enzymes that remove these modifications ("erasers"), as well as RBPs that recognize such modifications ("readers") and cause many downstream functional consequences such as mRNA transportation, degradation and translation ((Fu et al., 2014; Liu et al., 2014; Shi et al., 2019). Biochemical studies using these proteins as well as genetic studies via mutating genes encoding these proteins have revealed some of the details in how m^6A methylation and demethylation is regulated and how different readers carry out specific downstream functions (Wang et al., 2016; Lin et al., 2016; Choe et al., 2018; Wang et al., 2014; Shi et al., 2017; Chang et al., 2020; Wilkinson et al., 2003; Xiao et al., 2016; Roundtree et al., 2017).

My thesis work took advantage of cell type specific deletion of the m^{6}A "writer" METTL14 and the m^{6}A "readers" YTHDF1 in mice. I made the following important discoveries:

1. In three different cell types in the adult brain, namely D1 SPNs, D2 SPNs, and DA neurons, *Mettl14* gene deletion and *Ythdf1* gene deletion resulted in almost identical behavioral phenotypes in various behavioral paradigms. Suggesting that the functional impact of the m^{6}A mRNA methylation in the adult brain is likely mediated by YTHDF1. This is in sharp contrast to previous claims that there is redundancy among YTHDF1, YTHDF2 and YTHDF3 (Zaccara and Jaffery, 2020).
2. Responses at the molecular (*de novo* protein synthesis), cellular (action potentials) and behavioral (learning) level upon environmental challenges were all blunted under m^{6}A deficiency condition, suggesting that the m^{6}A pathway is crucial in cell's ability to adapt to environmental challenges, presumably by rapidly regulating protein synthesis in adult neurons with good spatial and temporal resolution.
3. Although m^{6}A deficiency in D1-SPNs and D2-SPNs resulted in opposite behavioral phenotypes, it does not mean that m^{6}A has very different functions in different cells. On the contrary, it means that m^{6}A has very similar functions in different cells. Because D1-SPNs and D2-SPNs are known to have opposing functions, promoting versus inhibiting motor outputs respectively, m^{6}A deficiency in D1-SPNs and D2-SPNs is expected to result in opposite behavioral phenotypes if the cellular level functional impairments are the same. Given the opposing functions of D1 and D2 pathways in movement control, it is also reasonable to argue that a deficiency in any critical protein required for D1 and D2-SPN development or function could lead to similar functional outcomes, by specifically

disturbing the movement promoting or inhibiting function of D1 and D2 SPNs respectively, resulting in opposite behavioral phenotypes. Here we want to emphasize our discovery of a specific gene, by maintaining the normal neuronal activities, regulating learning and environmental adaptation in a cell type specific manner. The cell type specific YTHDF1 knockout mice are healthy and do not have baseline motor impairments. To our knowledge, this is the first study in which knocking out the same gene in D1-SPNs vs D2-SPNs resulted in opposite behavioral phenotypes, and also clearly demonstrated D1-SPNs-dependent learning vs D2-SPNs-dependent learning. This is probably one of the best *in vivo* evidence supporting the classic basal ganglia direct and indirect pathway model.

4. In most studies, it is often difficult to dissociate learning impairment from performance impairment. Learning impairment will surely lead to performance impairment. Performance impairment can significantly reduce the opportunity to learn and will therefore lead to learning impairment. In the catalepsy paradigm, because catalepsy sensitization is a type of "inhibitory" learning in which learning causes more severe catalepsy whereas impaired learning leads to reduced catalepsy and better motor function. In this paradigm, I was able to unambiguously confirm learning impairment caused by *Mettl14* or *Ythdf1* gene deletion in D2-SPNs.

In addition to the above, there are three important details worth discussing, and hopefully they will inspire future studies.

1. My data have clearly demonstrated that m^6A deficiency in D1-SPNs and D2-SPNs result in opposite behavioral phenotypes, and that D1-SPNs-dependent learning (normal acquisition) are very different from D2-SPNs-dependent learning (inhibitory learning), supporting the

classic basal ganglia direct (Go) and indirect (NoGo) pathway model. However, the D2 neuron firing data was clearly correlated with locomotor speed positively. Also, there was almost no D2 neuron firing during catalepsy response. These data seem to contradict the classic model in which the indirect pathway inhibits motor output (Albin et al., 1989; DeLong, 1990; Shen et al., 2008). Therefore, I took a closer look at D2 neuron firing during open field behavior. I was able to correlate D2 neuron firing with locomotor activity while dissociate drug effects and genotype effects. In this analysis, D2 neuron firing is clearly correlated with locomotor speed positively. However, haloperidol treatment reduced locomotor activity and at the same time increased D2 neuron firing. Therefore, in the same dataset, I was able to observe both positive correlation between D2 neuron firing and locomotor speed (overall data) as well as negative correlation between D2 neuron firing and locomotor speed (comparing haloperidol treatment to vehicle treatment). My interpretation is that when D2 neuron firing is driven by cortical inputs, then there's a positive correlation between D2 neuron firing and locomotor speed. However, when D2 neuron firing is altered directly by drugs, optogenetics, chemogenetics etc., then there's a negative correlation between D2 neuron firing and locomotor speed. This model implies that the same cortical neurons usually project to both D1 and D2 neurons. In any motor acts, both D1 and D2 neurons are activated by cortical inputs. However, D1 and D2 neurons play different roles, with D1 neurons promote whereas D2 neurons inhibit motor outputs. It also implies that although the indirect pathway and D2 neurons inhibit motor outputs, their activation is necessary in any motor acts. Both anatomical and *in vivo* recording experiments are needed in the future to test such a model directly.

2. At the molecular level, I found a dramatic increase in YTHDF1's binding to its RNA targets, many encode structural proteins, in response to increased DA in the striatum. I also found that striatal neurons in *Ythdf1* knockout mice are incapable of regulating *de novo* protein synthesis in response to elevated cAMP. Interestingly, striatal neurons in *Ythdf1* knockout mice also exhibit significantly higher baseline protein synthesis rate. These observations are consistent with our previously published data on m^6A sequencing in *Mettl14*-deleted striatum. We found downregulation of mRNA species functionally associated with neuronal and synaptic activities and upregulation of mRNA species functionally associated with metabolism, ribosomal machinery and translation, which are not neuronal-specific (Koranda et al., 2018). Together, these data suggest that the m^6A pathway is crucial in cell's ability to adapt to environmental challenges, presumably by rapidly regulating protein synthesis in adult neurons in response to environmental challenges with good spatial and temporal resolution. In cells with m^6A deficiency, there are likely compensations to upregulate baseline protein synthesis in order to preserve the essential functions necessary for the cell. However, without translational regulation via YTHDF1, cells are impaired to rapidly and dynamically regulate *de novo* protein synthesis in response to environmental stimuli. Neurons rely on quick *de novo* protein synthesis, thereby dynamically adapting to environmental changes, this mechanism is essential for regulating synaptic plasticity and stress response. Depletion of YTHDF1/3 in cells has been reported to impair stress granule formation and attenuate the recruitment of mRNA to stress granules (Fu et al. 2020). What are the mechanisms that enable the cell to rapidly regulate protein synthesis in adult neurons with good spatial and temporal resolution? One possibility is post-translational

modifications of YTHDF1, which in turn can change YTHDF1 conformation and its mRNA binding targets, then their translation. Compared to regulatory mechanisms at the transcriptional level, post-translational modifications of YTHDF1 can facilitate local protein synthesis rapidly in axons, dendrites, and synapses. It can dynamically regulate synthesis of many proteins at once in response to stimuli (Walsh et al. 2005). We tested a few known sites of YTHDF1 post-translational modifications, but no significant changes were detected in response to increased DA in the striatum. However, we found that FMRP phosphorylation is increased in the striatum in response to increased DA. FMRP phosphorylation, a known regulator of YTHDF1, is found to affect protein synthesis (Zou et al. 2022), suggesting reduced FMRP activity, and reduced inhibition of YTHDF1 by FMRP in response to increased DA in the striatum. However, we only examined a few known post-translational modification sites on YTHDF1 here, including ubiquitylation, serine phosphorylation, and tyrosine phosphorylation. Future studies are needed to take an unbiased approach to examine additional post-translational modification sites, such as acetylation, O-linked β-N-acetylglucosamine (O-GlcNAc), SUMOylation etc. Overall, a comprehensive screen of the post-translational modification changes on YTHDF1 in response to stimuli would unveil another layer of protein expression regulation in the brain. Future studies are also needed to investigate exactly how YTHDF1 responds to synaptic inputs, changes in neuronal activities, Ca^{2+} or cAMP levels etc. Additional studies are also needed to investigate how increased de novo protein synthesis affect synaptic plasticity and/or structural changes in neurons, axons, dendrites, and synapse.

3. m^6A mRNA methylation has been shown to exhibit developmental changes during postnatal brain development as well as in aging (Meyer et al., 2012; Chen et al., 2019). The overall m^6A level increases with age (Shafik et al., 2021). Recently, a surge of studies has been dedicated to exploring m^6A's role in regulating the physiological processes during aging and their implications in degenerative disorders (Li et al., 2018; Wu et al., 2020; Liu et al., 2021; Zhu et al., 2021; Sun et al., 2022). For instance, deletion of *Mettl3*, which leads to m^6A depletion, has been linked to accelerated aging in human bone marrow stem cells, likely due to disruption in the binding of the reader protein to the cell cycle regulator MISI2, which impairs cell stability (Wu et al., 2020). In Alzheimer's disease (AD) mouse models, an elevated expression of FTO is found in the brain; depletion of FTO induces Tau phosphorylation in neurons (Li et al., 2018). We previously found downregulation of cell-type identity genes in D1 and D2 SPNs in the striatum of adult mice with *Mettl14* deletion (Koranda et al., 2018), suggesting the underlying molecular mechanism for reduced neuronal activities in the *Mettl14* knockout mice could be the altered protein expression that makes D1 neurons less "D1-like" and D2 neurons less "D2-like", or even makes neurons less "neuron-like". This disturbance of the maintenance of normal cell identity could potentially explain the blunted responses at the molecular (*de novo* protein synthesis), cellular (action potentials) and behavioral (learning) level upon environmental challenges under m^6A deficiency condition.

In order to determine the necessity of m^6A mRNA methylation's role in maintaining normal neuronal functions in the adult mice and at the same time rule out the developmental effects in our cell type specific *Mettl14* and *Ythdf1* knockout mice, I examined and compared the

behavioral phenotypes in mice with either *Mettl14* or *Ythdf1* gene deletion in D1-SPNs across different age groups. I found that 6-8 weeks D1-Cre;Mettl14$^{f/f}$ mice showed normal acute response and sensitization to cocaine (genotype main effect , p=0.7389, genotype x time interaction, p=0.9827) compared to their control littermates (Figure 5.1 B). Similarly, 6-8 weeks D1-Cre;Ythdf1$^{f/f}$ mice also exhibited normal acute response and sensitization to cocaine (genotype main effect, p=0.3746 genotype x time interaction, p=0.8589) compared to their control littermates (Figure 5.1 D). However, in aged mice with either *Mettl14* or *Ythdf1* gene deletion in D1-SPNs , we observed blunted sensitization responses (Figure 5.1 A, C). This age-dependent behavioral phenotype indicates that m^{6}A mRNA methylation is essential for maintaining normal neuronal functions in adults. This is in agreement with our previous published data showing that *Mettl14* deletion did not result in morphological deficits such as dendritic branching, spine number, and volume in D1-SPNs (Koranda et al., 2018). Overall, we conclude that the behavioral phenotypes that we observed throughout my thesis work are unlikely due to developmental effects of gene knockout.

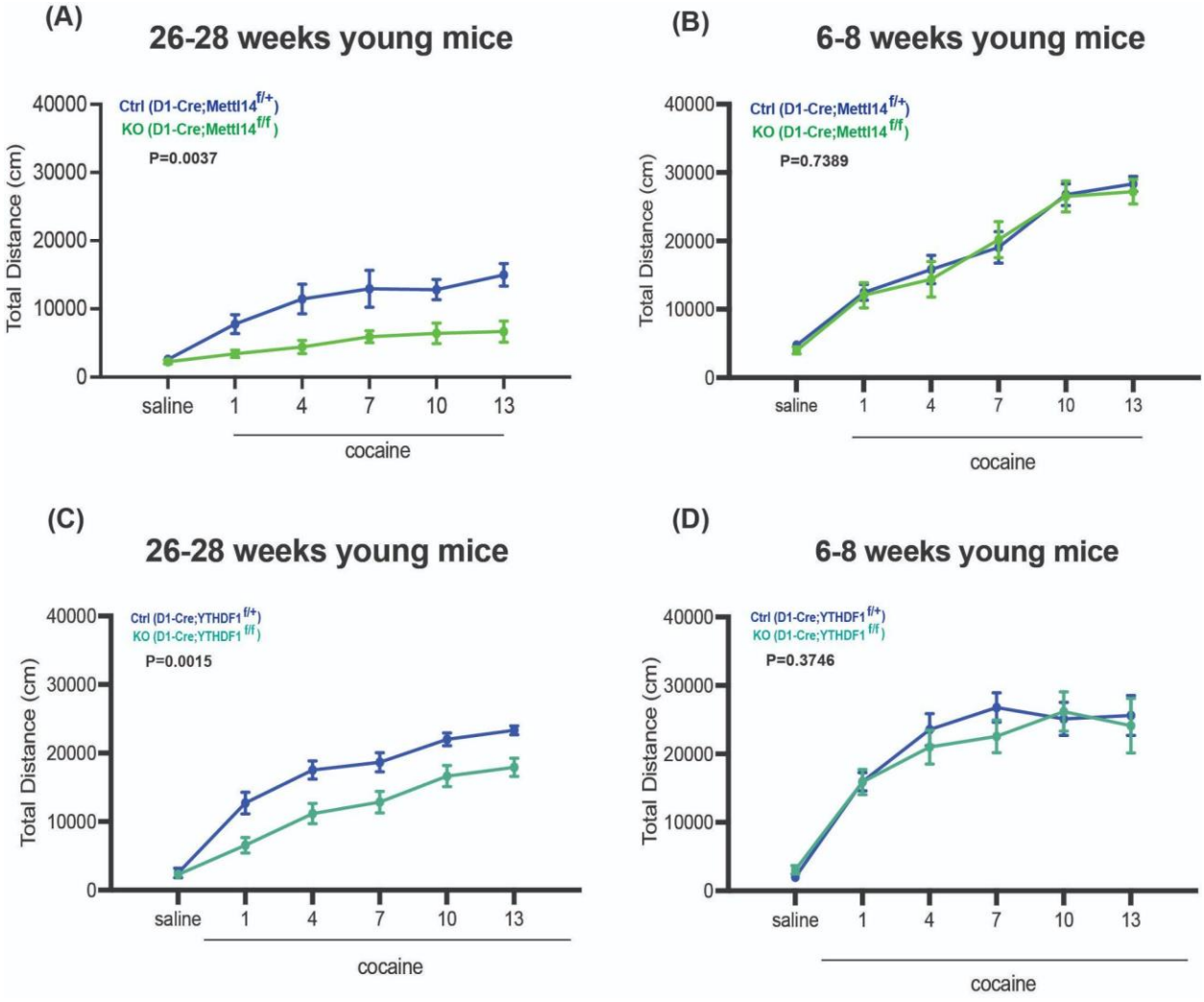

Figure 5.1. ***Mettl14*** **gene deletion and** ***Ythdf1*** **gene deletion produced age-dependent behavioral phenotypes.** (A, B) Cocaine-induced locomotor sensitization in D1-Cre;Mettl14$^{f/+}$ (Ctrl, blue) and D1-Cre;Mettl14$^{f/f}$ (KO, green). Locomotor activity is recorded for 60 min after saline/cocaine injection. Total distance traveled in the open field box is recorded (cm). A: 26-28 weeks aged mice, n=7, genotype main effect, p=0.0037, genotype x time interaction, p=0.0057, 2-way ANOVA. B: 6-8 weeks young mice, n=6, genotype main effect, p=0.7389, genotype x time interaction, p=0.9827, 2-way ANOVA. (C, D) Cocaine-induced locomotor sensitization in D1-Cre;Ythdf1$^{f/+}$ (Ctrl, blue) and D1-Cre;Ythdf1$^{f/f}$ (KO, cyan). Locomotor activity is recorded for 60 min after saline/cocaine injection. Total distance traveled in the open field box is recorded (cm). C: 26-28 weeks aged mice, n=8, genotype main effect, p=0.0015, genotype x time interaction, p=0.0153, 2-way ANOVA. B: 6-8 weeks young mice, n=7, genotype main effect, p=0.3746, genotype x time interaction, p=0.8589, 2-way ANOVA. All data expressed as mean ± SEM.

My data suggest a potential role of m^6A mRNA methylation in maintaining cell identities and normal neuronal functions in post-mitotic neurons in the adult brain.

Although the exact gene regulatory programs required for maintaining cell identities in the striatum have not been studied yet, studies in invertebrates have revealed that certain terminal selector transcription factors (TFs) that initially expressed during the specification and differentiation of neuronal cells continue to function throughout the terminal stage to maintain cell identities (Holmberg and Perlmann., 2012; Kratsios and Hobrt, 2018; Hobert and Kratsios, 2019). The continued expression of these terminal selector TFs is maintained through direct autoregulation; a similar regulatory mechanism has been revealed in vertebrates as well (Evan and Oliver, 2014). Since m^6A mRNA methylation is the most abundant internal modification that takes a critical role in post-transcriptional regulation, we hypothesized that the dynamic changes on m^6A modifications and reader proteins is critical for maintaining cell identities and normal neuronal functions in the adult brain.

Striatal development starts around embryonic day E14-15 in mice (Dunnett and Bjorklund, 2000). Many of the maker genes are TFs such as DLX1/2, ASCL1, EBF1, FOX1/2; while others are related to specific neurotransmitters or receptors differentially expressed in D1 and D2 SPNs such as TAC1 (tachykinin 1), DRD1, PENK (Enkephalin) and DRD2. These markers are expressed during differentiation of D1 and D2 neurons and at different stages of development (Marija et al. 2015).

Our previous sequencing data was derived from the entire striatum, which did not offer specificity at the cellular level. In order to achieve cell-type specific sequencing for D1 and D2-SPNs, we developed a FACs protocol to isolate D1 and D2 SPNs with fluorescent tags from the

adult brain (Figure 6). D1-tdtomato and D2-GFP BAC transgenic mice were decapitated and the whole brain were extracted immediately. 250-micron coronal sections were sliced using a vibratome and digested using Pronase. The striatum was then dissected and manually triturated to achieve a single-cell suspension. Neurons were subsequently separated through the OptiPrep gradient. I then sent the samples to the Cytometry and Antibody Core Facility at the University of Chicago for sorting with FACSAria III, D1 and D2-SPNs were isolated based on their fluorescence.

In the future, it will be interesting to explore the expression profile of the TFs and to track the temporal features of m^6A distribution on these genes in D1 and D2 SPNs through various developmental stages, from postnatal period to late adulthood. Currently, we are in the process of breeding D1-Cre;Mettl14$^{f/f}$;D1-tdTomato and A2A-Cre;Mettl14$^{f/f}$;D2-GFP triple transgenic mice. This will allow us to investigate the effects of m^6A depletion in the gene regulatory landscape of adult striatal neurons with cell-type specific resolution. We will test our hypothesis that m^6A deficiency impairs the maintenance of normal neuronal cell types, leading to reduced neuronal activity and even cell death. Collectively, these experiments will provide more insights to the contribution of m^6A in maintaining postmitotic neuronal cell identities and sustaining normal neuronal activities.

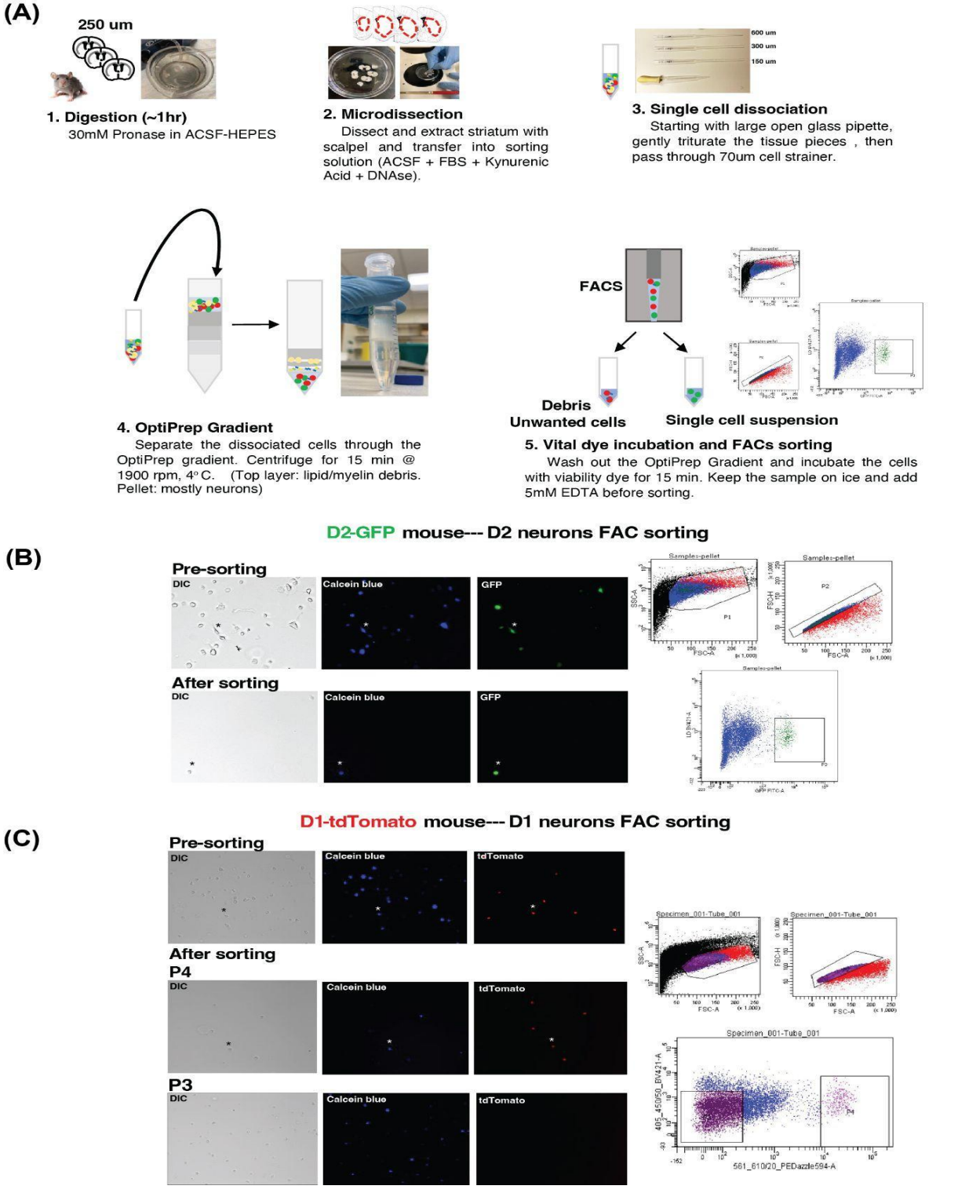

Figure 5.2. Purification of striatal neurons from adult mouse brain through FAC-sorting.

cont. Figure 5.2. Purification of striatal neurons from adult mouse brain through FAC-sorting. (A) 1-5: Brief description of the FACs protocol to purify D1 and D2 SPNs from the adult brain. (B) Imaging of isolated D1 SPNs with Tdtomato tags (red) and D2 SPNs with GFP tags (green). DIC: openfield imaging, Calcein blue: cell dye for identification of alive cells, *: isolated D1-SPN or D2-SPN.

REFERENCES

Adcock, R. A., Thangavel, A., Whitfield-Gabrieli, S., Knutson, B. and Gabrieli, J. D. (2006). Reward-motivated learning: mesolimbic activation precedes memory formation. Neuron *50*, 507–517.

Alarcón, C.R., Goodarzi, H., Lee, H., Liu, X., Tavazoie, S. and Tavazoie, S.F. (2015). HNRNPA2B1 Is a Mediator of m(6)A-Dependent Nuclear RNA Processing Events. Cell. *162*, 1299-1308.

Alarcón, C.R., Lee, H., Goodarzi, H., Halberg, N. and Tavazoie, S.F. (2015). N6-methyladenosine marks primary microRNAs for processing. Nature, *519*, 482-485.

Albin, R. L., Young, A. B. & Penney, J. B. (1989). The functional anatomy of basal ganglia disorders. Trends Neurosci. *12*, 366–375.

Augustin, S.M., Beeler, J.A., McGehee, D.S. and Zhuang X.X. (2014). Cyclic AMP and afferent activity govern bidirectional synaptic plasticity in striatopallidal neurons. J Neurosci. *34,* 6692-9.

Bailey, A. S. et al. (2017). The conserved RNA helicase YTHDC2 regulates the transition from proliferation to differentiation in the germline. eLife *6*, e26116.

Balleine, B.W., Liljeholm, M. and Ostlund, S.B. (2009). The integrative function of the basal ganglia in instrumental conditioning. Behavioral Brain Research *199*, 43–52.

Barbieri, I., Tzelepis, K., Pandolfini, L., Shi, J., Millán-Zambrano, G., Robson, S.C., Aspris, D., Migliori, V., Bannister, A.J. and Han N et al. (2017). Promoter-bound METTL3 maintains myeloid leukaemia by m^6A-dependent translation control. Nature *552*, 126-131.

Batista, P.J., Molinie, B., Wang, J., Qu, K., Zhang, J et al. (2014). m^6A RNA modification controls cell fate transition in mammalian embryonic stem cells. Cell Stem Cell *15*, 707–719.

Beeler, J.A., Cao, Z.F.H., Kheirbek, M.A., Ding, Y.M., Koranda, J.L. et al. (2010). Dopamine-dependent motor learning: insight into levodopa's long-duration response. Ann Neurol. *67*, 639-47.

Beeler, J.A., Frank, M.J., McDaid, J., Alexander, E., Turkson, S. et al. (2012). A role for dopamine-mediated learning in the pathophysiology and treatment of Parkinson's disease. Cell Rep. *2*, 1747-61.

Berke, J.D. and Hyman, S.E. (2000). Addiction, dopamine, and the molecular mechanisms of memory. Neuron *25*, 515-32.

Björklund, A. and Dunnett, S. B. (2007). Dopamine neuron systems in the brain: an update. Trends in Neurosciences. *30*, 194-202.

Bolam, J. P., Hanley, J. J., Booth, P. A. C. and Bevan, M. D. (2000). Synaptic organization of the basal ganglia. The Journal of Anatomy. *196*, 527-542.

Buxbaum, A. R., Wu, B. and Singer, R. H. (2014). Single beta-actin mRNA detection in neurons reveals a mechanism for regulating its translatability. Science. *343*, 419–422.

Calabresi, P., Picconi, B., Tozzi, A. and Di Filippo, M. (2007). Dopamine-mediated regulation of corticostriatal synaptic plasticity. Trends Neurosci. *30*, 211–219.

Calabresi, P., Picconi, B., Tozzi, A., Ghiglieri, V. and Filippo, M. (2014). Direct and indirect pathways of basal ganglia: a critical reappraisal. Nat Neurosci. *17*, 1022–30.

Cao, G., Li, H.-B., Yin, Z. and Flavell, R. A. (2016). Recent advances in dynamic m^6A A RNA modification. Open Biol *6*, 160003.

Carlezon, W.A. and Thomas, M.J. (2009). Biological substrates of reward and aversion: a nucleus accumbens activity hypothesis. Neuropharmacology *56*, 122-32.

Chang, G., Shi, L., Ye, Y., Shi, H., Zeng, L., Tiwary, S. et al. (2020). YTHDF3 induces the translation of mA-enriched gene transcripts to promote breast cancer brain metastasis. Cancer Cell *38*, 857–871.e7.

Chang, M., Lv, H., Zhang, W. et al. (2017). Region-specific RNA m(6)a methylation represents a new layer of control in the gene regulatory network in the mouse brain. Open Biol. *7*, 170166.

Chen, J., Zhang, Y.-C., Huang, C., Shen, H., Sun, B. et al. (2019). m^6A regulates neurogenesis and neuronal development by modulating histone methyltransferase Ezh2. Genom. Proteom. Bioinform. 17, 154–168.

Chen, X.C., Yu, C., Guo, M.J., Zheng, X.T., Ali, S. et al. (2019). Down-Regulation of m^6A mRNA Methylation Is Involved in Dopaminergic Neuronal Death. ACS Chem. Neurosci. *5*, 2355-2363.

Cheng, Y., Luo, H., Izzo, F., Pickering, B. F., Nguyen, D et al. (2019). m^6A RNA methylation maintains hematopoietic stem cell identity and symmetric commitment. Cell reports *28*, 1703-1716.

Cheung, T.H.C., Ding, Y.M., Zhuang, X.X. and Kang, U.J. (2023). Learning critically drives parkinsonian motor deficits through imbalanced striatal pathway recruitment. Proc Natl Acad Sci U S A. *120*, e2213093120.

Choe, J., Lin, S., Zhang, W., Liu, Q., Wang, L., Ramirez-Moya, J., Du, P., Kim, W., Tang, S., and Sliz, P et al. (2018). mRNA circularization by METTL3-eIF3h enhances translation and promotes oncogenesis. Nature *561*, 556-560.

Costa, R.M. et al. (2006). Rapid alterations in corticostriatal ensemble coordination during acute dopamine-dependent motor dysfunction. Neuron *52*, 359–369.

Cui, G., Jun, S., Jin, X. et al. (2013). Concurrent activation of striatal direct and indirect pathways during action initiation. Nature *494*, 238–242.

Cui, Q. et al. (2017). m^6A RNA Methylation Regulates the Self-Renewal and Tumorigenesis of Glioblastoma Stem Cells. Cell Rep. *18*, 2622–2634.

Day, J.J., Jones, J.L. and Carelli, R.M. (2011). Nucleus accumbens neurons encode predicted and ongoing reward costs in rats. Eur J Neurosci *33*, 308-21.

DeLong, M. R. (1990). Primate models of movement disorders of basal ganglia origin. Trends Neurosci. *13*, 281–285.

Desrosiers, R, Friderici, K and Rottman, F. (1974). Identification of methylated nucleosides in messenger RNA from Novikoff hepatoma cells. PNAS *71*:3971–75.

Devan, B.D., Hong, N.S. and McDonald, R.J. (2011). Parallel associative processing in the dorsal striatum: segregation of stimulus-response and cognitive control subregions. Neurobiol Learn Mem. *96*, 95-120.

Dominissini, D., Moshitch, M.S., Schwartz, S., Salmon, D.M., Ungar, L, Osenberg, S., Cesarkas, K., Jacob, H.J., Amariglio, N., Kupiec, M., Sorek, R., and Rechavi, G. (2012). Topology of the human and mouse m^6A RNA methylomes revealed by m^6A-seq. Nature. *485*, 201–6.

Doxtader, K. A., Wang, P., Scarborough, A. M., Seo, D., Conrad, N. K. and Nam, Y. (2018). Structural basis for regulation of METTL16, an S-adenosylmethionine homeostasis factor. Mol. Cell. *71*, 1001–1011.e4.

Dunnett, S. B. and Björklund, A. (2000). Dissecting embryonic neural tissues for transplantation. Neuromethods *36*: 3–25.

Engel, M., Eggert, C., Kaplick, P.M., Eder, M., Roh, S. et al. (2018). The role of m^6A/m-RNA methylation in stress response regulation. Neuron. *99*, 389-403.

Eom, T., Antar, L.N., Singer, R.H. and Bassell, G.J. (2003). Localization of a beta-actin messenger ribonucleoprotein complex with zipcode-binding protein modulates the density of dendritic filopodia and filopodial synapses. J Neurosci *23*, 10433-44

Evan, SD., and Oliver, H. (2014). Maintenance of postmitotic neuronal cell identity. Nature Neuroscience *17*, 899-907.

Fallon, J.H. and Moore, R.Y. (1978). Catecholamine innervation of the basal forebrain. IV. Topography of the dopamine projection to the basal forebrain and neostriatum. J Comp Neurol *180*, 545-80.

Feng, J., Zhou, Y., Campbell, S.L., Le, T., Li, E., Sweatt, J.D., Silva, A.J., and Fan, G. (2010). Dnmt1 and Dnmt3a maintain DNA methylation and regulate synaptic function in adult forebrain neurons. Nat Neurosci.*13* :423-30.

Franco, S.J. and Muller, U. (2013). Shaping our minds: stem and progenitor cell diversity in the mammalian neocortex. Neuron *77*, 19–34.

Frayling, T. M. et al. (2007). A common variant in the FTO gene is associated with body mass index and predisposes to childhood and adult obesity. Science *316*, 889–894.

Frye, M., Harada, B.T., Behm, M., and He, C. (2018). RNA modifications modulate gene expression during development. Science 361, 1346–1349.

Fu, Y, Dominissini, D, Rechavi, G, He, C. (2014). Gene expression regulation mediated through reversible m(6)A RNA methylation. Nature Reviews Genetics. *15*: 293-306.

Fu, Y and Zhuang, XW. (2020). m^6A-binding YTHDF proteins promote stress granule formation. Nat Chem Biol. *16*, 955–963

Gao, X., Shin, Y.H., Li, M. et al. (2010). The fat mass and obesity associated gene FTO functions in the brain to regulate postnatal growth in mice. PLoS One. *5*, e14005.

Gerfen, C.R. and Wilson, C.J. (2004). The Basal Ganglia. Amsterdam: Elsevier Science

Gerfen, C. R. and Surmeier, D. J. (2011). Modulation of striatal projection systems by dopamine. Annual review of neuroscience. *34*, 441-466.

Gerfen, C.R. and Wilson, C.J. (2004). The Basal Ganglia. Amsterdam: Elsevier Science.

Gerfen, C.R., Engber, T.M., Mahan, L.C., Susel, Z., Chase, T.N., Monsma, F.J. Jr. and Sibley, D.R. (1990). D1 and D2 dopamine receptor-regulated gene expression of striatonigral and striatopallidal neurons. Science *250*, 1429-32

Gerken, T. et al. (2007). The obesity-associated FTO gene encodes a 2-oxoglutarate-dependent nucleic acid demethylase. Science *318*, 1469–1472.

Geula, S., Moshitch-Moshkovitz, S., Dominissini, D., Mansour, A. A., Kol, N., Salmon-Divon, M. et al. (2015). Stem cells m^6A mRNA methylation facilitates resolution of naïve pluripotency toward differentiation. Science *347*, 1002–1006.

Glock, C., Heumuller, M. and Schuman, E.M. (2017). mRNA transport & local translation in neurons. Curr Opin Neurobiol *45*, 169-177.

Graefe, R.A. and Bonish, H. (1988). The transport of amines across the axonal membranes of noradrenergic and dopaminergic neurons. Handbook of experimental pharmacology (Trendelenburg U and Weiner N, eds). *Vol 90*, 193–245.

Graybiel, A.M., Aosaki, T., Flaherty, A.W. and Kimura, M. (1994). The basal ganglia and adaptive motor control. Science *265*, 1826–1831.

Hawes, S.L., Evans, R.C., Unruh, B.A., Benkert, E.E., Gillani, F., Dumas, T.C., and Blackwell, K.T. (2015) Multimodal plasticity in dorsal striatum while learning a lateralized navigation task. J Neurosci *35*:10535–10549.

Hernandez, P.J., Sadeghian, K., and Kelley, A.E. (2002). Early consolidation of instrumental learning requires protein synthesis in the nucleus accumbens. Nature Neuroscience. *5*, 1327-31.

Hess, M.E., Hess, S., Meyer, K.D. et al. (2013). The fat mass and obesity associated gene (fto) regulates activity of the dopaminergic midbrain circuitry. Nat Neurosci. *16*, 1042–1048.

Hintiryan, H., Foster, N. N., Bowman, I., Bay, M., Song, M. Y., Gou, L. et al. (2016). The mouse cortico-striatal projectome. Nat. Neurosci. *19*, 1100–1114.

Hobert O. and Kratsios P. (2019). Neuronal identity control by terminal selectors in worms, flies, and chordates. Curr Opin Neurobiol. *56*, 97-105.

Holmberg, J. and Perlmann, T. (2012). Maintaining differentiated cellular identity. Nat. Rev Genet. *13*, 429–439.

Holt, C. E., Martin, K. C. and Schuman, E. M. (2019). Local translation in neurons: visualization and function. Nat. Struct. Mol. Biol. *26*, 557–566.

Holt, C.E. and Schuman, E.M. (2013) The central dogma decentralized: new perspectives on RNA function and local translation in neurons. Neuron *80*, 648–657.

Hsu, P. J. et al. (2017). Ythdc2 is an N(6)-methyladenosine binding protein that regulates mammalian spermatogenesis. Cell Res. *27*, 1115–1127.

Hwang, F.-J., Roth, R. H., Wu, Y.-W., Sun, Y., Kwon, D. K., Liu, Y., & Ding, J. B. (2022). Motor learning selectively strengthens cortical and striatal synapses of motor engram neurons. Neuron, *110*, 2790-2801

Jedynak, J., Hearing, M., Ingebretson, A., Ebner, S.R., Kelly, M., Fischer RA, et al. (2016). Cocaine and Amphetamine Induce Overlapping but Distinct Patterns of AMPAR Plasticity in Nucleus Accumbens Medium Spiny Neurons. Neuropsychopharmacology. *41*, 464-76.

Jia, G., Fu, Y., Zhao, X., Dai, Q., Zheng, G., Yang, Y., Yi, C., Lindahl, T., Pan, T., Yang, Y.G. and He. C. (2011). N6-methyladenosine in nuclear RNA is a major substrate of the obesity-associated FTO. Nat. Chem. Biol. *7*, 885-887.

Jung, H., Gkogkas, C. G., Sonenberg, N. and Holt, C. E. (2014). Remote Control of Gene Function by Local Translation. Cell *157*, 26–40.
Kan, L., Ott, S., Joseph, B., Park, E.S., Dai, W., Kleiner, R.E. et al. (2021). A neural m^6A/Ythdf pathway is required for learning and memory in Drosophila. Nature Communications. *12*, 1458.

Kandel, E.R. (2001). Neuroscience - The molecular biology of memory storage: A dialogue between genes and synapses. Science. *294*, 1030-8.

Kandel, E.R. (2012). The molecular biology of memory: cAMP, PKA, CRE, CREB-1, CREB-2, and CPEB. Molecular Brain. *5*, 14.

Kelley, A.E. and Domesick, V.B. (1982). The distribution of the projection from the hippocampal formation to the nucleus accumbens in the rat: an anterograde- and retrograde-horseradish peroxidase study. Neuroscience *7*, 2321-35.

Knuckles, P., Carl, S.H., Musheev, M., Niehrs, C., Wenger, A. and Bühler, M. (2017). RNA fate determination through cotranscriptional adenosine methylation and microprocessor binding. Nat. Struct. Mol. Biol. *24*, 561-569.

Knuckles, P., Lence, T., Haussmann, I.U., Jacob, D., Kreim, N., Carl, S.H., Masiello, I., Hares, T., Villaseñor, R., Hess, D et al. (2018). Zc3h13/Flacc is required for adenosine methylation by bridging the mRNA-binding factor Rbm15/Spenito to the m^6A machinery component Wtap/Fl(2)d. Genes Dev. *32*, 415-429.

Koranda, J.L., Dore, L., Shi, H., Patel, M.J., Vaasjo, L.O., Rao, M.N. et al. (2018). Mettl14 Is Essential for Epitranscriptomic Regulation of Striatal Function and Learning. Neuron. *99*, 283-92.

Koranda, J.L., Krok, A.C., Xu, J., Contractor, A., McGehee, D.S. et al. (2016). Chronic Nicotine Mitigates Aberrant Inhibitory Motor Learning Induced by Motor Experience under Dopamine Deficiency. J Neurosci. *36*, 5228-40.

Kratsios, P. and Hobert, O. (2018) Nervous System Development: Flies and Worms Converging on Neuron Identity Control. Curr Biol. *28*, 1154-R1157.

Kravitz, A., Freeze, B., Parker, P. et al. (2010). Regulation of parkinsonian motor behaviours by optogenetic control of basal ganglia circuitry. Nature *466*, 622–626.

Lepelletier, L. et al. (2017). Sonic hedgehog guides axons via zipcode binding protein 1-mediated local translation. J. Neurosci. *37*, 1685–1695.

Li, H., Ren, Y., Mao, K., Hua, F., Yang, Y., Wei, N. et al. (2018). FTO is involved in Alzheimer's disease by targeting TSC1-mTOR-Tau signaling. Biochem. Biophys. Res. Commun. *498*, 234–239.

Li, L., Zang, L., Zhang, F., Chen, J., Shen, H., Shu, L. et al. (2017). Fat mass and obesity-associated (FTO) protein regulates adult neurogenesis. Hum. Mol. Genet. *26*, 2398–2411.

Li, M., Zhao, X., Wang, W., Shi, H., Pan, Q., Lu, Z., Perez, S.P., Suganthan, R., He, C., Bjoras, M. and Klungland, A. (2018). Ythdf2-mediated m(6)A mRNA clearance modulates neural development in mice. Genome Biol. *19*, 69.

Lin, S., Choe, J., Du, P., Triboulet, R. and Gregory R.I. (2016). The m(6)A Methyltransferase METTL3 Promotes Translation in Human Cancer Cells. Mol. Cell. *62*, 335-345.

Liu, J., Yue, Y., Han, D., Wang, X., Fu, Y., Zhang, L., Jia, G., Yu, M., Lu, Z., Deng, X et al. (2014). A METTL3-METTL14 complex mediates mammalian nuclear RNA N6-adenosine methylation. Nat. Chem. Biol. *10*, 93-95.

Liu, N., Dai, Q., Zheng, G., He, C.,Par isien, M. and Pan, T. (2015). N(6)-methyladenosine-dependent RNA structural switches regulate RNA-protein interactions. Nature. *518*, 560-564.

Liu, P., Li, F., Lin, J., Fukumoto, T., Nacarelli, T., Hao, X., et al. (2021). m^6A-independent Genome-wide METTL3 and METTL14 Redistribution Drives the Senescence-Associated Secretory phenotypeA-independent Genome-wide METTL3 and METTL14 Redistribution Drives the Senescence-Associated Secretory Phenotype. Nat. Cel Biol 23 (4), 355–365.

Liu, Y., Yue, D., Han, X., Wang, Y., Fu, L., Zhang, G., Jia, M., Yu, Z., Lu, X et al. (2014). A METTL3-METTL14 complex mediates mammalian nuclear RNA N6-adenosine methylation. Nat. Chem. Biol. *10*, 93-95.

Louloupi, A., Ntini, E., Conrad, T. and Ørom, U.A.V. (2018). Transient N-6-Methyladenosine Transcriptome Sequencing Reveals a Regulatory Role of m^6A in Splicing Efficiency. Cell Rep. *23*, 3429-3437

Luo, S. and Tong, L. (2014). Molecular basis for the recognition of methylated adenines in RNA by the eukaryotic YTH domain. Proc Natl Acad Sci USA. *111*, 13834–13839.

Lupo, G., Harris, W.A. and Lewis, K.E. (2006). Mechanisms of ventral patterning in the vertebrate nervous system. Nat Rev Neurosci *7*, 103–114.

Lutolf, S., Radtke, F., Aguet, M., Suter, U. and Taylor, V. (2002). Notch1 is required for neuronal and glial differentiation in the cerebellum. Development *129*, 373–385.

Lv, J., Xin, Y., Zhou, W., and Qiu, Z. (2013). The epigenetic switches for neural development and psychiatric disorders. Journal of genetics and genomics. *40*, 339-346.

Ma, C., Chang, M., Lv, H., Zhang, Z.W., Zhang, W., He, X., Wu, G., Zhao, S., Zhang, Y., Wang, D., Teng, X., Liu, C., Li, Q., Klungland, A., Niu, Y., Song, S. and Tong, W.M. (2018). RNA m(6)A methylation participates in regulation of postnatal development of the mouse cerebellum. Genome Biol. *19*, 68.

Ma, H., Wang, X., Cai, J., Dai, Q., Natchiar, S.K., Lv, R., Chen, K., Lu, Z., Chen, H., Shi, Y.G et al. (2019). N^{6-}Methyladenosine methyltransferase ZCCHC4 mediates ribosomal RNA methylation. Nat. Chem. Biol. *15*, pp. 88-94.

Marija, F. et al. (2015). How to make striatal projection neurons. Neurogenesis *2*:1 e1100227 1-6.

Martin, K.C. and Zukin, R.S. (2006). RNA trafficking and local protein synthesis in dendrites: an overview. J Neurosci *26*, 7131-7134.

Merkurjev, D., Hong, W.T., Iida, K., Oomoto, I., Goldie, B.J., Yamaguti, H. et al. (2018). Synaptic N6-methyladenosine (m^6A) epitranscriptome reveals functional partitioning of localized transcripts. Nature Neuroscience. *21*, 1004-14.

Meyer, K.D., Saletore, Y., Zumbo, P., Elemento, O., Mason, C.E., and Jaffrey, S.R. (2012). Comprehensive analysis of mRNA methylation reveals enrichment in 3' UTRs and near stop codons. Cell. *149*, 1635-46.

Meyer, K. and Jaffrey, S. (2014). The dynamic epitranscriptome: N^6-methyladenosine and gene expression control. Nat Rev Mol Cell Biol. *15*, 313–326.

Meyer, K.D., Patil, D.P., Zhou, J., Zinoviev, A., Skabkin, M.A., Elemento, O., Pestova, T.V., Qian, S.B., and Jaffrey, S.R. (2015). 5' UTR m(6)A Promotes Cap-Independent Translation. Cell. *163*, 999-1010.

Missale, C., Nash, S. R., Robinson, S. W., Jaber, M. and Caron, M. G. (1998). Dopamine receptors: from structure to function. Physiol. Rev. *78*, 189–225.

Neve, K.A., Seamans, J.K. and Trantham-Davidson, H. (2004). Dopamine receptor signaling. J Recept Signal Transduct. *24*, 165–205.

Nisenbaum, E.S., Mermelstein, P.G., Wilson, C.J. and Surmeier, D.J. (1998). Selective blockade of a slowly inactivating potassium current in striatal neurons by (±) 6-chloro-APB hydrobromide (SKF82958). Synapse *23*, 213–224.

Omori, Y., Kubo, S., Kon, T., Furuhashi, M., Narita, H., Kominami, T., Ueno, A., Tsutsumi, R., Chaya, T., Yamamoto, H., Suetake, I., Ueno, S., Koseki, H., Nakagawa, A., and Furukawa, T. (2017). Samd7 is a cell type- specific PRC1 component essential for establishing retinal rod photoreceptor identity. Proceedings of the National Academy of Sciences of the United States of America. *114*, E8264–E8273.

Panigrahi, B., Martin, K.A., Li, Y., Graves, A.R., Vollmer, A., Olson, L. et al. (2015). Dopamine is required for the neural representation and control of movement vigor. Cell. *162*, 1418–30.

Parker, J.G., Marshall, J.D., Ahanonu, B. et al. (2018). Diametric neural ensemble dynamics in parkinsonian and dyskinetic states. Nature *557*, 177–182.

Patil, D.P., Chen, C.K., Pickering, B.F., Chow, A., Jackson, C., Guttman, M., and Jaffrey S.R. (2016). m(6)A RNA methylation promotes XIST-mediated transcriptional repression. Nature, *537*, 369-373.

Pendleton, K.E., Chen, B., Liu, K., Hunter, O.V., Xie, Y., Tu, B.P. andConrad, N.K. (2017). The U6 snRNA m(6)A Methyltransferase METTL16 Regulates SAM Synthetase Intron Retention. Cell *169,* 824-835.

Pennartz, C. M., Berke, J. D., Graybiel, A. M., Ito, R., Lansink, C. S. et al. (2009). Corticostriatal interactions during learning, memory processing, and decision making. Journal of Neuroscience, *29*, 12831-12838.

Pereira, J. D., Sansom, S. N., Smith, J., Dobenecker, M. W., Tarakhovsky, A., & Livesey, F. J. (2010). Ezh2, the histone methyltransferase of PRC2, regulates the balance between self-renewal and differentiation in the cerebral cortex. Proceedings of the National Academy of Sciences. *107*, 15957-15962.

Perry, R.P. and Kelley, D.E. (1974). Existence of methylated messenger RNA in mouse L cells. Cell *1*:37–42.

Phillipson, O.T. and Griffiths, A.C. (1985). The topographic order of inputs to nucleus accumbens in the rat. Neuroscience *16*, 275-96.

Ping, X.L., Sun, B.F., Wang, L., Xiao, W., Yang, X et al. (2014). Mammalian WTAP is a regulatory subunit of the RNA N6-methyladenosine methyltransferase. Cell Res. *24*, 177-189.

Roundtree, I.A., Evans, M.E., Pan, T. and He, C. (2017). Dynamic RNA modifications in gene expression regulation. Cell. *169*, 1187–200.

Scheyer, A.F., Wolf, M.E. and Tseng, K.Y. (2014). A Protein Synthesis-Dependent Mechanism Sustains Calcium-Permeable AMPA Receptor Transmission in Nucleus Accumbens Synapses during Withdrawal from Cocaine Self-Administration. Journal of Neuroscience. *34*, 3095-100.

Schöller, E., Weichmann, F., Treiber, T., Ringle, S., Treiber, N., Flatley, A., Feederle, R., Bruckmann, A. and Meister, G. (2018). Interactions, localization, and phosphorylation of the m^6A generating METTL3-METTL14-WTAP complex. RNA *24*, 499-512.

Scuteri, A. et al. (2007).Genome-wide association scan shows genetic variants in the *FTO* gene are associated with obesity-related traits. PLoS Genet. *3*, e115.

Shafik, A.M., Zhang, F., Guo, Z. et al. (2021). N6-methyladenosine dynamics in neurodevelopment and aging, and its potential role in Alzheimer's disease. Genome Biol. 22: 17.

Shen, W., Flajolet, M., Greengard, P. and Surmeier, D. J. (2008). Dichotomous dopaminergic control of striatal synaptic plasticity. Science *321*, 848–851.

Shi, H., Wang, X., Lu, Z., Zhao, B.S., Ma, H., Hsu, P.J., Liu, C. and He, C. (2017). YTHDF3 facilitates translation and decay of N^6-methyladenosine-modified RNA. Cell Res. *27*, 315-328.

Shi, H., Wei, J., & He, C. (2019). Where, when, and how: context-dependent functions of RNA methylation writers, readers, and erasers. Molecular cell *74*, 640-650.

Shi, H., Zhang, X., Weng, Y.L., Lu, Z., Liu, Y., Lu, Z. et al. (2018). m^6A facilitates hippocampus-dependent learning and memory through YTHDF1. Nature. *563*, 249-53.

Shi, H.L., Wei, J.B. and He C. (2019). Where, When and How: Context-Dependent Functions of RNA Methylation Writers, Readers, and Erasers. Mol cell. *74*, 640-650.

Siciliano, S.A., Feriis, M.J. and Jones, S.R. (2015). Cocaine self-administration disrupts mesolimbic dopamine circuit function and attenuates dopaminergic responsiveness to cocaine. Eur J Neurosci. *42*, 2091-6.

Smith, Y., Bevan, M.D., Shink, E. and Bolam JP. (1998). Microcircuitry of the direct and indirect pathways of the basal ganglia. Neuroscience *86*, 353-87.

Steinberg, E. E. et al. (2014). Positive reinforcement mediated by midbrain dopamine neurons requires D1 and D2 receptor activation in the nucleus accumbens. PLoS ONE 9, e94771.

Sun, Y., Dong, D., Xia, Y., Hao, L., Wang, W., and Zhao, C. (2022). YTHDF1 Promotes Breast Cancer Cell Growth, DNA Damage Repair and Chemoresistance. Cel Death Dis 13 (3), 230.

Surmeier, D.J., Bargas, J., Hemmings, H.C., Nairn, A.C. and Greengard, P. (1995). Modulation of calcium currents by a D1 dopaminergic protein kinase/phosphatase cascade in rat neostriatal neurons. Neuron *14*, 385–397.

Tecuapetla, F., Jin, X., Lima, S.Q. and Costa, R.M. (2016). Complementary Contributions of Striatal Projection Pathways to Action Initiation and Execution. Cell *166*,703-715.

Tecuapetla, F., Matias, S., Dugue, G.P., Mainen, Z.F. and Costa, R.M. (2014). Balanced activity in basal ganglia projection pathways is critical for contraversive movements. Nat Commun. *5*, 4315.

Tecuapetla, F., Patel, J.C., Xenias, H., English, D., Tadros, I., Shah, F. et al. (2010). Glutamatergic signaling by mesolimbic dopamine neurons in the nucleus accumbens. J Neurosci. *30*, 7105–10.

Theler, D., Dominguez, C., Blatter, M., Boudet, J. and Allain., H.T. (2014). Solution structure of the YTH domain in complex with N6-methyladenosine RNA: a reader of methylated RNA. Nucleic Acids Res. *42*, 13911-13919.

Tritsch, N.X., Ding, J.B. and Sabatini, B.L. (2012). Dopaminergic neurons inhibit striatal output through non-canonical release of GABA. Nature. *490*, 262–6.

Van Tran, N., Ernst, F. G. M., Hawley, B. R., Zorbas, C., Ulryck, N., Hackert, P. et al. (2019). The Human 18S rRNA m^6A Methyltransferase METTL5 Is Stabilized by TRMT112. Nucleic Acids Res. *47*, 7719–7733.

Walsh, C.T., Garneau-Tsodikova, S., and Gatto, G.J., Jr. (2005). Protein posttranslational modifications: the chemistry of proteome diversifications. Angew Chem Int Ed Engl *44*, 7342-7372.

Wang, C. X., Cui, G. S., Liu, X., Xu, K., Wang, M., Zhang, X. X. et al. (2018). METTL3-mediated m^6A modification is required for cerebellar development. PLoS Biol. *16*, e2004880.

Wang, H. L., Qi, J., Zhang, S., Wang, H. & Morales, M. (2015). Rewarding effects of optical stimulation of ventral tegmental area glutamatergic neurons. J. Neurosci. *35*, 15948–15954.

Wang, P., Doxtader K.A., and Nam Y. (2016). Structural Basis for Cooperative Function of Mettl3 and Mettl14 Methyltransferases. Mol. Cell. *63*, 306-317.

Wang, X. and He, C. (2014). Reading RNA methylation codes through methyl-specific binding proteins. RNA Biol. *11*, 669-72.

Wang, X., Lu, Z., Gomez, A., Hon, G.C., Yue, Y., Han, D., Fu, Y., Parisien, M., Dai, Q., Jia, G., Ren, B., Pan, T., and He, C. (2014). N6-methyladenosine-dependent regulation of messenger RNA stability. Nature *505*, 117–120.

Wang, X., Zhao, B.S., Roundtree, I.A., Lu, Z., Han, D., Ma, H., Weng, X., Chen, K., Shi, H., He, C. (2015). N6-methyladenosine Modulates Messenger RNA Translation Efficiency. Cell. *161*, 1388-1399.

Wang, Y., Li, Y., Yue, M., Wang, J., Kumar, S., Wechsler-Reya, R.J., Zhang, Z., Ogawa, Y., Kellis, M., Duester, G. and Zhao, J.C. (2018). N(6)-methyladenosine RNA modification regulates embryonic neural stem cell self-renewal through histone modifications. Nat Neurosci. *21*, 195–206.

Wang, Z. et al. (2006). Dopaminergic control of corticostriatal long-term synaptic depression in medium spiny neurons is mediated by cholinergic interneurons. Neuron *50*, 443–452.

Warda, A. S., Kretschmer, J., Hackert, P., Lenz, C., Urlaub, H., Höbartner, C., et al. (2017). Human METTL16 Is a N6-methyladenosine (m^6A) Methyltransferase that Targets pre-mRNAs and Various Non-coding RNAs. EMBO Rep. *18*, 2004–2014.

Wei, C. M., Gershowitz, A. and Moss, B. (1975). Methylated nucleotides block 5′ terminus of HeLa-cell messenger-RNA. Cell *4*, 379–386.

Wen, J., Lv, R., Ma, H., Shen, H., He, C., Wang, J., Jiao, F., Liu, H., Yang, P., Tan, T et al. (2018). Zc3h13 Regulates Nuclear RNA m(6)A Methylation and Mouse Embryonic Stem Cell Self-Renewal Mol. Cell. *69*, 1028-1038.
Weng, Y. L., Wang, X., An, R., Cassin, J., Vissers, C., Liu, Y. et al. (2018). Epitranscriptomic m(6)A regulation of axon regeneration in the adult mammalian nervous system. Neuron *97*, 315-325.

Wilkinson, F. L. et al. (2003). Emerin interacts in vitro with the splicing-associated factor, YT521-B. Eur. J. Biochem. *270*, 2459–2466.

Wise, R.A. (2004). Dopamine, learning and motivation. Nat Rev Neurosci. *5*, 483-94.

Witten, I. B. et al. (2011). Recombinase-driver rat lines: tools, techniques, and optogenetic application to dopamine-mediated reinforcement. Neuron *72*, 721–733.

Worpenberg, L., Paolantoni, C., Longhi, S., Mulorz, M. M., Lence, T., Wessels, H. H. et al. (2021). Ythdf is a N6-methyladenosine reader that modulates Fmr1 target mRNA selection and restricts axonal growth in Drosophila. Embo J. *40*, e104975.

Wu, B., Su, S., Patil, D.P., Liu, H., Gan, J., Jaffrey, S.R. and Ma,J.(2018).Molecular basis for the specific and multivariant recognitions of RNA substrates by human hnRNP A2/B1. Nat. Commun. *9*, 420.

Wu, Z., Shi, Y., Lu, M., Song, M., Yu, Z., Wang, J., et al. (2020). METTL3 Counteracts Premature Aging via m^6A-dependent Stabilization of MIS12 mRNA. Nucleic Acids Res. *48*, 11083–11096.

Xiang, Y., Laurent, B., Hsu, C.H., Nachtergaele, S., Lu, Z., Sheng, W., Xu, C., Chen, H., Ouyang, J., Wang, S et al. (2017). RNA m^{6}A methylation regulates the ultraviolet-induced DNA damage response. Nature *543*, 573-576.

Xiao, W. et al. (2016). Nuclear m(6)A reader YTHDC1 regulates mRNA splicing. *Mol. Cell 61*, 507–519.

Yao, B., Christian, K.M., He, C., Jin, P., Ming, G.L. and Song, H. (2016). Epigenetic mechanisms in neurogenesis. Nat Rev Neurosci. *17*, 537-49.

Yin, H. H., Knowlton, B. J. and Balleine, B. W. (2005). Blockade of NMDA receptors in the dorsomedial striatum prevents action-outcome learning in instrumental conditioning. Eur. J. Neurosci. *22*, 505–512.

Yin, H.H. and Knowlton, B.J. (2006). The role of the basal ganglia in habit formation. Nat Rev Neurosci *7*:464–476.

Yin, H.H., Knowlton, B.J. and Balleine, B.W. (2004). Lesions of dorsolateral striatum preserve outcome expectancy but disrupt habit formation in instrumental learning. Eur J Neurosci *19*, 181-9.

Yin, H.H., Mulcare, S.P., Hilário, M.R.F., Clouse, E., Holloway, T., Davis, M.I., Hansson, A.C., Lovinger, D.M. and Costa, R.M. (2009). Dynamic reorganization of striatal circuits during the acquisition and consolidation of a skill. Nat Neurosci *12*:333–341.

Yoon, K.J., Ringeling, F.R., Vissers, C., Jacob, F., Pokrass, M., Jimenez-Cyrus, D., Su, Y., Kim, N.S., Zhu, Y., Zheng, L., Kim, S., Wang, X., Dore, L.C., Jin, P., Regot, S., Zhuang, X., Canzar, S., He, C., Ming, G.L. and Song, H. (2017). Temporal control of mammalian cortical neurogenesis by m(6)A methylation. Cell. *171*, 877-889.

Yu, J., Chen, M., Huang, H., Zhu, J., Song, H., Zhu, J. et al. (2018). Dynamic m^{6}A modification regulates local translation of mRNA in axons. Nucleic Acids Res. *46*, 1412–1423.

Yu, J., She, Y., Yang, L., Zhuang, M., Han, P., Liu, J. et al. (2021). The m(6) A readers YTHDF1 and YTHDF2 synergistically control cerebellar parallel fiber growth by regulating local translation of the key Wnt5a signaling components in axons. Adv. Sci. *8*, e2101329.

Yue, Y., Liu, J. and He, C. (2015). RNA N6-methyladenosine methylation in post-transcriptional gene expression regulation. Genes Dev. *29*, 1343–1355.

Yue, Y., Liu, J., Cui, X., Cao, J., Luo, G., Zhang, Z., Cheng, T., Gao, M., Shu, X., Ma, H *et al.* (2018). VIRMA mediates preferential m^{6}A mRNA methylation in 3'UTR and near stop codon and associates with alternative polyadenylation. Cell Discov. *4*, 10.

Zaccara, S. and Jaffrey, S.R. (2020).A unified model for the function of YTHDF proteins in regulating m(6)A-modified mRNA. Cell. *181*, 1582–1595 e18.

Zhang, C., Chen, Y., Sun, B., Wang, L., Yang, Y., Ma, D., Lv, J., Heng, J., Ding, Y., Xue, Y., Lu, X., Xiao, W., Yang, Y.G. and Liu, F. (2017). m^6A modulates hematopoietic stem and progenitor cell specification. *Nature* 549, 273–276 (2017).

Zhang, G., Neuber,t T.A. and Jordan, B.A. (2012). RNA binding proteins accumulate at the postsynaptic density with synaptic activity. J Neurosci *32*, 599-609.

Zhang, Z., Wang, M., Xie, D., Huang, Z., Zhang, L., Yang, Y. et al. (2018). METTL3-mediated N6-methyladenosine mRNA modification enhances long-term memory consolidation. Cell Research. *28*, 1050-61.

Zhao, B., Roundtree, I. and He, C. (2017). Post-transcriptional gene regulation by mRNA modifications. Nat Rev Mol Cell Biol. *18*, 31–42.

Zhao, B.S., Wang, X., Beadell, A.V., Lu, Z., Shi, H., Kuuspalu, A., Ho, R.K. and He, C. (2017). m^6A-dependent maternal mRNA clearance facilitates zebrafish maternal-to-zygotic transition. Nature. *542*, 475-478.

Zheng, G., Dahl, J.A., Niu, Y., Fedorcsak, P., Huang, C.M., Li, C.J., Vågbø, C.B., Shi, Y., Wang, W.L., Song, S.H et al. (2013). ALKBH5 is a mammalian RNA demethylase that impacts RNA metabolism and mouse fertility. Mol. Cell. *49*, 18-29.

Zhu, H., Sun, B., Zhu, L., Zou, G., and Shen, Q. (2021). N6-Methyladenosine Induced miR-34a-5p Promotes TNF-α-Induced Nucleus Pulposus Cell Senescence by Targeting SIRT1. Front. Cel Dev. Biol. 9, 642437.

Zhu, T.T., Roundtree, I.A., Wang, P., Wang, X., Wang, L., Sun, C. et al. (2014). Crystal structure of the YTH domain of YTHDF2 reveals mechanism for recognition of N6-methyladenosine. Cell Research. *24*, 1493-6

Zhuang, X., Belluscio, L. and Hen, R. (2000). G(olf)alpha mediates dopamine D1 receptor signaling. J Neurosci *20*, RC91.

Zou, Z.Y., Wei, J.B., Chen, Y.T., Kang, Y.H. Et al. (2022). FMRP phosphorylation modulates neuronal translation through YTHDF1. BioRxiv. https://www.biorxiv.org/content/10.1101/2022.11.29.518448v1.full